Institute of Hydrology
Faculty of Forest and Environmental Sciences
Albert-Ludwigs-University Freiburg

Reference Tracers to study Transport and Attenuation of Metolachlor in Constructed Wetlands

Steffi Schreiber

M.Sc. Thesis at the Institute of Hydrology Freiburg (IHF), Germany in cooperation with the Laboratory of Hydrology and Geochemistry of Strasbourg (LHyGeS), France

---

Supervisor: PD Dr. Jens Lange (IHF)

Co-Supervisor: Dr. Gwenaël Imfeld (LHyGeS)

November 2012

Institute of Hydrology
Faculty of Forest and Environmental Sciences
Albert-Ludwigs-University Freiburg

Reference Tracers to study Transport and Attenuation of Metolachlor in Constructed Wetlands

Steffi Schreiber

M.Sc. thesis at the Institute of Hydrology Freiburg (IHF), Germany in cooperation with the Laboratory of Hydrology and Geochemistry of Strasbourg (LHyGeS), France

---

Supervisor: PD Dr. Jens Lange (IHF)
Co-Supervisor: Dr. Gwenaël Imfeld (LHyGeS)

Freiburg, November 2012

Declaration of Authorship

I, Steffi Schreiber, hereby certify that the thesis I am submitting is entirely my own original work except where otherwise indicated. I am aware of the University's regulations concerning plagiarism, including those regulations concerning disciplinary actions that may result from plagiarism. Any use of the works of any other author, in any form, is properly acknowledged at their point of use.

Freiburg, 12.11.2012 Signature:

Acknowledgments

This dissertation would not have been possible without the guidance and the help of several individuals who in one way or another contributed and extended their valuable assistance in the preparation and completion of this study.

First and foremost I offer my gratitude and appreciation to my supervisors, Jens Lange at the Institute of Hydrology in Freiburg and Gwenaël Imfeld at the Institute of Hydrology and Geochemistry in Strasbourg for proposing this topic and for their advice throughout this joint project.

I want to express my warm and sincere thanks to Elodie Maillard for the collaborative work in the field, for sharing thoughts, literature and data and for answering many questions along the way. On this note, I also would like to thank Benoit Guyot, Jeanne Dollinger, and Yannis Risacher for their generous help in the field and for good company on many hot summer days in Colmar.

Many thanks to Nicolas Thevenin and Sylvain Pluchon from RITTMO, Colmar, for watching out for the equipment and providing tools when we needed to fix things on a fly.

Special thanks go to Emil Blattmann and Barbara Herbstritt who have been invaluable on the practical side of things.

In addition, many thanks to Ayse for her sense of style.

Most of all I am thankful to Stephen, who saw this project through with endless patience and clarity; and my mom, who always encouraged me to pursue my interests and who supported me unconditionally.

Contents

List of Abbreviations

BC	Breakthrough Curve
BMP	Best Management Practices
BR	Bromide
CDE	Convection-Dispersion Equation
CXTFIT	Program for estimating transport parameters (Toride et al, 1995)
DWD	European Union Drinking Water Directive
EDPM	Ethylene Propylene Diene Monomer
ENGEES	École National du Génie de l'Eau et de l'Environment de Strasbourg
ET	Evapotranspiration
EU	European Union
EWFD	European Water Framework Directive
FT	Fluorescence Tracer
GC-MS	Gas Chromatography coupled Mass Spectrometry
GWD	European Union Ground Water Directive
HRT	Hydraulic Retention Time
HSSFW	Horizontal Subsurface-Flow Wetland

IC	Ion Chromatograph
MC	Metolachlor
PE	Polyethylene
PVC	Polyvinyl Chloride
Ref-ET	Reference Evapotranspiration Calculation Software (Allen, 2011)
SFW	Surface-Flow Wetland
SRB	Sulphorhodamine B
SSFW	Subsurface-Flow Wetland
UR	Uranine

List of Symbols

Symbols

A_{Bed}	average bed surface area	7.2 m^2
C	concentration	μg/L, mg/L
C_{final}	final outflow concentration	μg/L, mg/L
C_{max}	peak outflow concentration	μg/L, mg/L
C_{inj}	injection concentration	μg/L, mg/L
C_{P-In}	concentration measured in inlet piezometer	μg/L
C_{P-Out}	concentration measured in outlet piezometer	μg/L
c_p	specific heat of the air	MJ $kg^{-1}{}^{\circ}C^{-1}$
D	hydrodynamic dispersion coefficient	cm^2/h, m^2/h
DT_{50}	degradation half-life of parent compound	h
e_a	actual vapor pressure of the air	KPa
e_s	saturation vapor pressure of the air	KPa
ET_0	reference evapotranspiration	mm/unit time
ET_a	actual evapotranspiration	mm/unit time
G	soil heat flux	MJ m^2 h^{-1}
h	water level height	m, cm
INT_{Tracer}	fluorescence intensity of tracer	intensity counts
K_d	partitioning coefficient liquid-solid phase	cm^3/g
K_{time}	time unit conversion	3600 h^{-1}
K_{OC}	organic carbon adsorption coefficient	ml/g

K_{OW}	partitioning coefficient octanol / water	(-)
M_{inj}	total mass of injected compound	mg, g
P	pressure probe readout	mW
Q_{in}	average inflow pump rate	L/h
Q	discharge	L/h
R	target compound percent recovery	%
Rd	retardation factor	(-)
R_f	retardation factor	(-)
R_{Load}	recovered mass of target compound	mg, g
R_n	net radiation	MJ m^2 h^{-1}
R^2	coefficient of determination	(-)
r	radius	m
r_a	aerodynamic resistance	s/m
r_s	bulk surface resistance	s/m
V	volume	L, m^3
V(t)	pressure readout to water volume conversion function	(-)
V_{In}	inflow volume	L, m^3
V_{Out}	total outflow volume	L, m^3
V_{Res}	residual water volume in Bed II and III	L, m^3
v	pore water velocity	m/s
v_{max}	maximum flow velocity	m/s
v_{mean}	average flow velocity	m/s
t_1	time of first target compound detection in outflow	h
t_{50}	time when 50% of target compound has passed the outlet	h
t_N	nominal residence time	h
t_p	time of target compound peak concentration in outflow	h
W_{Piezo}	water level in the piezometer	m
x	transport distance	m

Greek Symbols

β	partitioning coefficient in non-equilibrium transport	(-)
γ	zero-order production coefficient for equilibrium transport	(-)
γ_{psych}	psychrometric constant	KPa $°C^{-1}$

λ	hydraulic efficiency	(-)
λ_H	latent heat of vaporization	MJ kg^{-1}
μ	first-order decay coefficient	h^{-1}
μ_1	first-order decay coefficient for equilibrium sites	(-)
μ_2	first-order decay coefficient non-equilibrium sites	(-)
ω	mass transfer coefficient	(-)
ϕ	soil porosity	%
ρ_a	mean air density at constant pressure	kg/m^3
σ	standard deviation	(-)
θ_S	saturated volumetric water content	L, m^3
Δ	difference operator	(-)

List of Figures

List of Tables

Abstract

Pesticides are among the most relevant and persistent chemicals found in worldwide surface runoff and groundwater due to intensified agriculture and poorly managed agricultural operations. Wetland systems are actively capable of reducing pesticide transfer to natural water bodies. The contaminant removal efficiency of wetlands has been linked to vegetation type and density, climate, flow conditions and hydraulic retention time. Knowledge about the effect of different flow regimes on pesticide mitigation is rather limited. The presented study focused on the transfer and attenuation of the widely used pesticide metolachlor in constructed, vegetated subsurface flow wetlands operating under continuous flow and batch flow regimes with step injection and batch injection contamination patterns, respectively. Two fluorescence tracers (FT), the photosensitive uranine (UR) and the sorptive sulphorhodamine B (SRB) served as reference tracer for the transport behavior of metolachlor under the different flow regimes. The conservative salt tracer bromide (BR) was used to assess general system hydraulics. Both flow regimes facilitated contaminant removal in the wetlands, but metolachlor removal was higher in the batch flow operated system (≈90%) than in the wetland bed operating under continuous flow conditions (≈40%). The applied reference tracers displayed non-conservative behavior under both flow regimes. The suitability of UR and SRB as proxies for metolachlor behavior under continuous flow conditions could not be ascertained because FT recoveries diverged from metolachlor recoveries after two consecutive step injections. However in the batch flow wetland, similar tracer and pesticide recoveries showed that UR and SRB might serve as proxies for metolachlor transport. SRB was found to correlate strongly with the metolachlor concentration measured in the wetland bed piezometers. Tracer and pesticide losses were attributed to irreversible sorption, possible

photodegradation and potential plant uptake. High resolution tracer concentration, outflow and turbidity data from the batch mode wetland indicated different removal efficiencies in the sand and gravel layers. This study emphasizes the importance and the need for expansion of comparative reference tracer investigations to model pesticide transport in order to identify the attenuation processes, such as sorption kinetics and degradation pathways, in wetlands operating under different flow regimes.

Keywords: constructed wetlands, flow regimes, batch flow, step injection, removal efficiency, pesticides, reference tracer, metolachlor, bromide, uranine, sulphorhodamine B

Zusammenfassung

Pestizide gehören nachweislich zu schwer abbaubaren Stoffen, welche auf Grund ihres intensiven Einsatzes in der Landwirtschaft und der oft nicht fachgerechten Applikation durch Abdrift, Erosion, Abschwemmung und Verflüchtigung in ober-und unterirdische Fließsysteme eingetragen werden. Feuchtflächen können den Eintrag von Pestiziden in Oberflächengewässer und ins Grundwasser effektiv vermindern. Die Schadstoffretention in Feuchtflächen hängt maßgeblich von der Vegetation, den klimatischen Bedingungen, den Durchströmungsverhältnissen und der hydraulischen Verweilzeit ab. Veränderungen des hydraulischen Regimes in Feuchtflächen wirken sich auf Schlüsselparameter aus, die mit dem Schadstoffabbau in Zusammenhang stehen (z.B. Redoxpotential, pH-Wert, organischer Kohlenstoffgehalt). Hingegen ist bisher ist wenig bekannt über den Einfluss verschiedener hydraulischer Regime auf den effektiven Rückhalt von Pestiziden in Feuchtflächen.

In der vorliegenden Studie wurde der Transport und Rückhalt des Pestizides Metolachlor unter kontinuierlichen Durchflussbedingungen, sowie unter Batch Flow Bedingungen in künstlich angelegten, bepflanzten, unterirdisch fließenden Feuchtflächen untersucht. Die gleichzeitig mit dem Pestizid eingespeisten Fluoreszenztracer (FT), Uranin (UR) und Sulphorhodamin B (SRB), dienten dabei als Referenztracer und sollten den photolytischen Abbau und den sorptiven Charakter von Metolachlor simulieren. Zusätzlich wurde der konservative Salztracer Natriumbromid (BR) zur Charakterisierung der hydraulischen Eigenschaften der kontinuierlich durchflossenen Feuchtfläche eingesetzt.

In der Feuchtfläche mit kontinuierlichem Durchfluss erfolgte die Schadstoffeinspeisung erfolgte über zwei Wochen, gefolgt von einer vierwöchigen Spülung mit klarem Wasser ("Step Injection"). Die Feuchtfläche im "Batch Flow" Modus wurde mit Schadstofflösung aufgesät-

tigt, für zwei Wochen unter stagnierenden Bedingungen belassen und im Anschluss künstlich drainiert. Zwei Step Injections und vier Batch Flow-Versuche wurden über einen Zeitraum von drei Monaten durchgeführt.

Beide hydraulischen Regime begünstigten den Rückhalt des Schadstoffes, aber der Metolachlor Rückhalt in der Batch Flow Feuchtfläche war größer (90%) als in der kontinuierlich durchflossenen Feuchtfläche (40%). Alle Tracer wiesen in beiden Systemen ein nichtkonservatives Verhalten auf. Aufgrund verschiedener Rückerhalte von Fluoreszenztracern und Metolachlor nach der zweiten Step Injection in der Feuchtfläche mit kontinuierlichem Durchfluss, konnte die Eignung von UR und SRB als Referenztracer für den Transport von Metolachlor unter kontinuierlichen Fließbedingungen nicht sicher festgestellt werden. Dagegen lagen die Rückerhalte von SRB, UR und Metolachlor im Batch Flow System durchgängig unter 10%, was auf paralleles Verhalten der Fluoreszenztracer und Metolachlor unter Batch Flow Bedingungen deutet. Die starke Korrelation zwischen den Piezometer Proben von Metolachlor und SRB ($R^2 = 0.93$) in der Batch Flow Feuchtfläche stützt diese Beobachtung. Allgemein bestimmen wahrscheinlich irreversible Sorptionsprozesse, Aufnahme und Umbau durch Pflanzen, sowie mikrobiologischer Abbau den Rückhalt von Metolachlor und Tracern in den Batch Flow Feuchtflächen. Tracer-, Abfluss- und Trübungsdaten von den Drainagen des Batch Flow Systems deuten auf verschiedene Schadstoffrückhaltekapazitäten im Sand- und Kiesfilter hin.

Die Ergebnisse dieser Studie zeigen, dass das hydraulische Regime großen Einfluss auf den Rückhalt von Metolachlor in Feuchflächen hat, und dass UR und SRB den relativen Rückhalt von Metolachlor unter Batch Flow Bedingungen gut simulieren. Mehr Forschungsbedarf besteht im Hinblick auf die Sorptionskinetik und den mikriobiologischen Abbau von Fluoreszenztracern und Pestiziden innerhalb der Feuchtflächen, damit die Anwendbarkeit von Tracern zur Pestizidtransportmodellierung ausgebaut werden kann.

Schlüsselworte: künstliche Feuchtflächen, hydraulische Regime, batch flow, step injection, Schadstoffrückhalt, Pestizide, Referenztracer, Metolachlor, Bromid, Uranin, Sulphorhodamin B

1

Introduction

Agricultural Pesticides as an Environmental Hazard Pesticides are chemicals commonly applied at the soil surface to control pests and weeds in agricultural activities. As such, pesticides are often discharged into aquatic environments through surface runoff and atmospheric deposition, but they may also be conveyed by meteoric water through the soil and vadose zone to reach the groundwater (Carter, 2000; Gutierrez and Baran, 2009). In light of continuous growth of the world population and the increasing global demand for food, further worldwide expansion and intensification of agriculture is projected through 2050 (Tilman et al., 2001). As a result of poorly managed agricultural operations, pesticides are among the most relevant and important chemicals found in European surface runoff and groundwater samples (Barth et al., 2009; Gonçalves et al., 2007; Hildebrandt et al., 2008; Loos et al., 2010; Stehle et al., 2011). The presence of pesticides in water intended for human consumption is linked to high treatment costs, possible toxicological incidences and can result in prohibition of water use (Hildebrandt et al., 2008). Traditionally, the quality of groundwater and drinking water with regard to pesticide contents has been assessed in the European Union (EU) according to the Ground Water Directives (GWD) and the Drinking Water Directives (DWD) (European Commission, 2006, 1998). Both directives set out criteria for the assessment of the chemical status of the water and established quality criteria of water intended for human consumption. The DWD sets a maximum concentration of 0.1 μg/L for individual pesticides and their degradation products and 0.5 μg/L for total pesticides present in a sample (European Commission, 2006). Despite these directive guidelines and bans of certain compound

applications, the maximum allowable residue levels for pesticides have still been exceeded in the groundwater of many European countries (Gonçalves et al., 2007; Gutierrez and Baran, 2009; Hanke et al., 2007). Moreover, pesticides and their metabolites have been found in the groundwater many years after their application, suggesting environmental persistence and slow transport in the subsurface (Barth et al., 2009; Gutierrez and Baran, 2009). In a pan-european effort to monitor flux, turnover and accumulation of various pollutants including pesticides in soils, water and biomass, the European Water Framework Directive (EWFD) was initiated in the year 2000. The goal of the directive is to achieve a good qualitative status of all european water bodies by 2015. Other EU-integrated monitoring projects, like AquaTerra (Barth et al., 2009) and the Interreg IV PhytoRet project (Maillard et al., 2011), have since been created to stimulate cooperation in the investigation of longterm cumulative effects of pesticides in the environment as well as mitigation practices.

Pesticide Input Paths Pesticides enter surface and groundwater via diffuse or point-source input. Diffuse input from treated agricultural fields occurs via tile drain outflow, baseflow seepage, surface and subsurface runoff, soil erosion, leaching through the soil and unsaturated zone, and infiltration through river banks and beds. Furthermore, spray drift at application and deposition after volatilization cause a certain portion of the applied pesticide to be deposited outside the target area (Carter, 2000; Reichenberger et al., 2007; Schulz, 2004). Point sources for pesticides include mainly farmyard runoff, sewage plants, sewer overflows, and accidental spills (Reichenberger et al., 2007).

Pesticide Mitigation Potential via Constructed Wetlands More than a decade ago, the EU implemented best management practices (BMP) by equipping farmers with the knowledge and the technical know-how needed in order to reduce pesticide-related deterioration of agricultural surface waters. However, BPMs alone are not sufficient to address the ubiquity of pesticides in environmental waters and soils. Reichenberger et al. (2007) and Schulz (2004) discussed additional pesticide risk mitigation strategies in their reviews, including soil conservation schemes, implementation of no-spray buffer strips, as well as artificial or constructed wetlands located in the receiving agricultural surface water systems. Stehle et al. (2011) stated that the advantage of these wetland systems is their applicability as a risk management option, particularly in intensive agricultural cropping systems with high-quality crops in which solutions like buffer strips may require too much space. Typical designs for constructed wetlands fall into one of two categories, namely subsurface-flow (SSFW) and

surface-flow wetlands (SFW). In the subsurface flow wetlands, water flows either horizontally (i.e. parallel to the surface) or vertically through the matrix and out of the system, whereas in surface flow wetlands the water moves above the substrate. Many studies have since shown that such wetland buffer zones are actively capable of reducing pesticide transfer to natural water bodies (Lange et al., 2011; Maillard et al., 2011; Moore et al., 2001; Passeport et al., 2010).

The pesticide removal processes actively occurring within constructed wetlands, which depend on the physio-chemical properties of the compound and substrate characteristics, include sorption, photolysis, hydrolysis, volatilization and biodegradation (Imfeld et al., 2009; Kadlec, 1992; Mitsch et al., 2009; Moore et al., 2001; Passeport et al., 2010). The mobility and pollution potential of pesticides is usually assessed by the sorption coefficient (K_d), the hydrophobicity (K_{ow}) and the degradation half-life (DT_{50}) of the compound in question, and many laboratory sorption studies have contributed to the understanding of these complex processes (Crisanto et al., 1995; Seybold et al., 2001; Mersie et al., 2004). Indeed, the above-mentioned removal mechanisms are often not constant over space or time, and subsequent desorption and pesticide remobilization may occur when organic carbon content and quality of the substrate, or electrochemical characteristics change (Crisanto et al., 1995; Weber et al., 2007; Zhu and Selim, 2000). Furthermore, substrate characteristics are strongly influenced by vegetation type and density, climate, flow conditions and hydraulic retention time (HRT) (Gregoire et al., 2008; Lange et al., 2011; Persson et al., 1999; George et al., 2003; Trang et al., 2010). Removal efficiencies with respect to certain nutrients have been found to increase during batch flow conditions in SSF constructed wetlands because of enhanced contact between nutrients and reactive compartments (Burgoon et al., 1995; Stein et al., 2003). However, far more research has been conducted on nutrient retention within constructed wetlands than on pesticide mitigation (Stehle et al., 2011). While shifts in the hydraulic regime impact key parameters (e.g., redox potential, organic carbon content, pH), which may control the fate of contaminants in wetlands, knowledge about an effective pesticide concentration reduction in constructed wetlands operating under different flow conditions is rather limited (Gregoire et al., 2008; Schulz, 2004; Stehle et al., 2011). Keeping in mind that the ultimate scientific goal behind the ecological risk assessment of pesticides is to understand and assess potential effects under field conditions, the present study focused on the transfer and attenuation of the widely used herbicide metolachlor in constructed wetland mesocosms operating under different hydraulic regimes and contamination patterns.

Target Pesticide Metolachlor The racemic compound metolachlor ([(RS)-2-Chloro-N-(2-ethyl-6-methyl-phenyl)-N-(1-methoxypropan-2-yl)acetamide]) is a chloroacetanilide herbicide that has been used since 1980 to control annual grasses and broad leaf weeds in soybean, corn and many other crops (Crisanto et al., 1995; Si et al., 2009). Originally, metolachlor (MC) was applied as a 1:1 racemic mixture of the S- and R-stereoisomers. However, the R-stereoisomer was determined to be inactive as an herbicide and modern application mixes are now made up of approximately 80% S-metolachlor (Ma et al., 2006; Shaner et al., 2006).

Because metolachlor has a wide range of applications, the parent herbicide and its metabolites have been detected in surface and groundwater (Barra Caracciolo et al., 2005; Kalkhoff et al., 1998; Wauchope, 1978). Flury (1996) and Carter (2000) estimated that approximately 1% to 9% of the field-applied herbicides are removed by direct surface runoff, indirectly by sorption to clay and silt particles (which erode), or by leaching. Metolachlor has been found to be moderately mobile in 79% and mobile in 21% of the 33 soils studied by Crisanto et al. (1995). Krutz et al. (2004) and Crisanto et al. (1995) found that the mobility of metolachlor is inversely related to the contents in organic matter, as well as silt and clay portions of the soils. Wetlands and vegetated buffer zones have been shown to facilitate organic matter accumulation, which increases adsorption capacity and microbial activity for herbicide degradation, thus reducing the amount of herbicide in surface runoff and leaching (Krutz et al., 2004; Vianello et al., 2005). Several studies have shown that metolachlor degradation is mostly affected by soil type, moisture content, soil temperature, microbial activity and the presence of vegetation (Accinelli et al., 2001; Mersie et al., 2004; Vianello et al., 2005). Staddon et al. (2001) found evidence of phytoremediation in the degradation of metolachlor. Photodegradation might be another process which aids in the immobilization of metolachlor, as Lin et al. (1999) found that metolachlor toxicity in fresh and salt water decreased with increasing light intensity. In terms of environmental persistence, Zhu and Selim (2000) reported that numerous field and laboratory studies indicate that metolachlor half-life values are highly dependent on the experimental conditions and the investigated phase (sediment or water), with reported half-lives ranging from as low as 11 days and as high as 440 days.

The wide range of parameters affecting metolachlor degradation and the complexity of possible contaminant interactions make it difficult to make inferences between mitigation systems. An approach that focuses on a narrow subset of these parameters, such as the hydraulic regime or the contamination pattern, is needed in order to assess the performance of a specific mitigation system in terms of pesticide transfer, removal, and the major degradation

processes involved. The reactive solute transport and attenuation of metolachlor can be characterized using conservative reference tracers, which are an important tool to assess flow pathways, flow velocities and other general system hydraulics (Flury and Wai, 2003; Lange et al., 2011; Leibundgut et al., 2009).

Modeling Pesticide Transport with Tracers Tracer tests provide a convenient method of assessing system hydraulics in the field-scale characterization of wetland hydrological properties (Kadlec, 1994; Lange et al., 2011; Leibundgut et al., 2009). A tracer is a substance that is experimentally measured in a system of interest for the purpose of deducing process information from the tracer signal (Flury and Wai, 2003). Tracers are especially useful when the system of interest is inaccessible by direct measurements, such as the subsurface environment of wetlands. Usually, tracers are used to describe the movement of water. Thus, an ideal tracer should be non-reactive in terms of sorption to the studied matrix, degradation, changes in pH, alkalinity and the ionic strength of the aqueous solution. Furthermore, the tracer signal should be clearly discernible from the background of the system, so that it is easily detectable by chemical analysis. Finally, the tracer should have little or nor toxicological impact on the environment (Flury and Wai, 2003; Leibundgut et al., 2009).

Salt tracers are considered almost ideal conservative tracers for water movement. Among them, the bromide ion (BR) is considered the most suitable human-applied tracer in field studies because of its low toxicity and low background signal in the environment (Flury and Wai, 2003; Käss, 2004; Leibundgut et al., 2009). However, bromide will not behave conservatively if the soil possesses a dominant positive charge and electrostatic adsorption occurs (Seaman et al., 1995). Additionally, Xu et al. (2004) found bromide accumulation in root and leaf tissues of *Phragmites australis* and *Typha latifolia* as well as a concentration of dissolved bromide in the sediment due to plant transpiration.

Fluorescent dye tracers (FT) are also commonly used to track the movement of water, even though these compounds are to some degree retarded by the subsurface medium because they consist of relatively large organic molecules (Flury and Wai, 2003). Precisely this characteristic makes them suitable to serve as a proxy for the non-conservative behavior of a target compound (i.e. pesticides). Fluorescent dye tracers have low ecotoxicity and can be applied in very small quantities, which is advantageous because, unlike salt tracers, they usually do not affect water density or flow patterns (Leibundgut et al., 2009). Uranine (UR) plays a dominant role among the fluorescent tracers, due to its much higher fluorescence intensity and its general conservative behavior compared to other FTs. However, the fluorescence of UR is

pH-dependent because the functional group of UR can protonate and deprotonate at varying pH, thereby changing the net charge of the molecule. At a pH below 7, the less fluorescent UR cation dominates the solution, which is also more prone to sorption (Gerke et al., 2008; Kasnavia et al., 1999; Sabatini, 2000). Furthermore, UR shows photolytic dependency, so exposure to light has an irreversible effect on UR fluorescence (DT_{50}= 11 h). Thus, UR can only be used as a conservative FT in the absence of daylight (Leibundgut et al., 2009). Another widely used but non-conservative FT is sulphorhodamine B (SRB). Sulphorhodamine B displays highly sorptive behavior, especially onto positively charged inorganic surfaces due to its two strongly electronegative sulfonic groups (Kasnavia et al., 1999; Sabatini, 2000; Smart and Laidlaw, 1977). Sabatini (2000) also found that sorption of SRB decreased with increasing sediment particle diameter, which he interpreted as a sign of diffusion-limited intraparticle sorption. Little is known about microbial degradation of fluorescence tracers. The University Lüneburg, a partner in the Interreg IV PhytoRet project, currently is conducting "closed bottle tests" to assess the biodegradation of hydrological tracers.

In the presented study, bromide was used as a conservative tracer in order to obtain a baseline tracer breakthrough curve, a mass recovery and hydraulic parameters, to which the non-conservative behavior of the reference tracers uranine and sulphorhodamine B as well as the pesticide metolachlor could be compared. Uranine and SRB have been successfully applied as a pesticide surrogates, mimicking sorption and photolytic decay, to investigate the pesticide peak attenuation and retention capacities of surface flow wetlands in a study by Lange et al. (2011). However, to the best of our knowledge, the impact of different hydraulic regimes and contamination patterns on the transport, attenuation and pesticide removal efficiencies in constructed wetlands using these tracers has not been investigated before.

2

Study Objectives

The overall goal of this study was to evaluate and compare the influence of different hydraulic regimes and contamination patterns on the transport and attenuation of the pesticide metolachlor and the reference tracers UR and SRB in constructed wetland mesocosms. Particular focus was placed on:

1) the influence of flow regimes on tracer/pesticide removal efficiency

2) the influence of contamination patterns on tracer/pesticide removal efficiency

3) the suitability of UR and SRB as proxies for metolachlor behavior

4) the role of plant development in tracer/pesticide removal efficiency

Three vegetated SSF wetlands were set up in Colmar, France. Two beds operated under batch flow mode, the third bed operated under continuous flow mode. In the continuous flow bed, hydraulic parameters from two step injections were evaluated and compared using tracer breakthrough curves. BR was expected to behave as a conservative tracer. SRB and UR recoveries were anticipated to be lower than BR but similar to metolachlor recoveries. After the second step injection, different hydrological system parameters were expected due to plant maturation. Effects of plant development (density, height, transpiration, uptake) were expected to increase tracer-pesticide removal efficiencies. Plant maturation was expected to proceed faster in the continuous flow bed. In the continuously contaminated batch flow bed, decreasing removal efficiencies were anticipated for each treatment cycle, as leaching would increase due to occupied sorption sites. The feasibility of UR and SRB for pesticide transport modeling was evaluated based on the tracer/pesticide recovery data from all beds.

3

Materials and Methods

3.1 Study Site

The study site is located on the grounds of the RITTMO agro-environment center for applied research in Colmar, France (48° 4′ 54″ N, 7° 21′ 20″ E). Colmar lies in the rainshadow of the Vosges Mountains and a dry microclimate prevails. The average annual rainfall in Colmar is only 607 mm, yet from April through September, monthly rainfall may be as high as 100 mm. The most intense precipitation events occur typically during convective storms in the summer. Average minimum and maximum temperatures are 6.1°C and 15.7°C respectively for the last standard reference period (Meteo France Online, 2012). Colmar receives on average 1799 hours of sunshine annually. In the summer, daily maximum temperatures may exceed 40°C. Thus, from April through September the precipitation-evapotranspiration balance is often negative (Bernhard et al., 1992).

3.2 Wetland Design

Experimental wetlands with holding volumes ranging from 40 L to 2500 L have been the subject of many studies investigating contaminant transport and fate (Bowmer, 1987; Gregoire et al., 2008; Hench et al., 2003; Maillard et al., 2011; Page et al., 2010). Because their design, function and degree of sophistication can be controlled, experimental wetlands are suited to answer specific questions regarding the movement of contaminants through the sed-

iment. The goal of this study was to compare three different hydraulic and contamination regimes in mesoscale experimental wetlands. Three wetland beds were constructed: Bed I was designated for continuous flow - continuous contamination step injection experiments, Bed II for intermittent flow - continuous contamination batch experiments and Bed III for intermittent flow - intermittent contamination batch experiments.

3.2.1 Wetland Dimensions and Characteristics

The construction of the three wetlands started in November 2011 and lasted through March 2012. The wetlands were designed as horizontal subsurface-flow wetlands (HSSFW) . The average dimensions of a wetland bed were 4 m by 1.80 m by 0.52 m (see Figure 3.1). The average surface area of the beds was 7.2 m^2. The beds lay adjacent to each other and were separated by concrete walls of approximately 2 cm thickness. To prevent seepage, the beds were completely lined with impermeable ethylene propylene diene monomer (EPDM) rubber tarp. The bottoms of the beds were filled with an average of 0.12 m of gravel (diameter 4-8 mm) to enhance drainage and were topped with 0.40 m of sand (diameter 0-4 mm). Sand and gravel came from the company Waibel, Gernsheim, Germany. The saturated volumetric water content (θ_S) was experimentally determined by slowly filling the dry beds with site water until excess water pooled up above the sediment surface. An average of 600 L fit into each bed, corresponding to a porosity of 16%. To monitor the water level within the bed and for sampling purposes, three piezometers were embedded in the sediment layer along the center line of each bed (see Figure 3.1). The piezometer length was 1.05 m and the diameter 5.50 cm. In December of 2011 and March of 2012, *Phragmites australis* (20 plants per m^2), *Phalaris arundinacea* (3 plants per m^2) and *Glyceria maxima* (2 plants per m^2) were planted in each bed. All three plant species are perennial reed grasses which show high tolerance against pH fluctuations, salinity and anaerobic conditions (Herbst and Kappen, 1999; Moro et al., 2004). *P. australis* and *P. arundinacea* are commonly found near lakes, streams and in natural wetlands, but they also have been planted in artificial wetlands because of their phytoremediation potential (Stearman et al., 2003; Verhoeven and Meuleman, 1999).

3.2.2 Inlet Design

Bed I The water in Bed I was to be injected at a constant rate to maintain continuous flow and facilitate a homogeneous dispersion of tracers and pesticide. This was achieved by installing an inlet pump (see Table 3.6). Pesticide and tracers had to be applied at a point

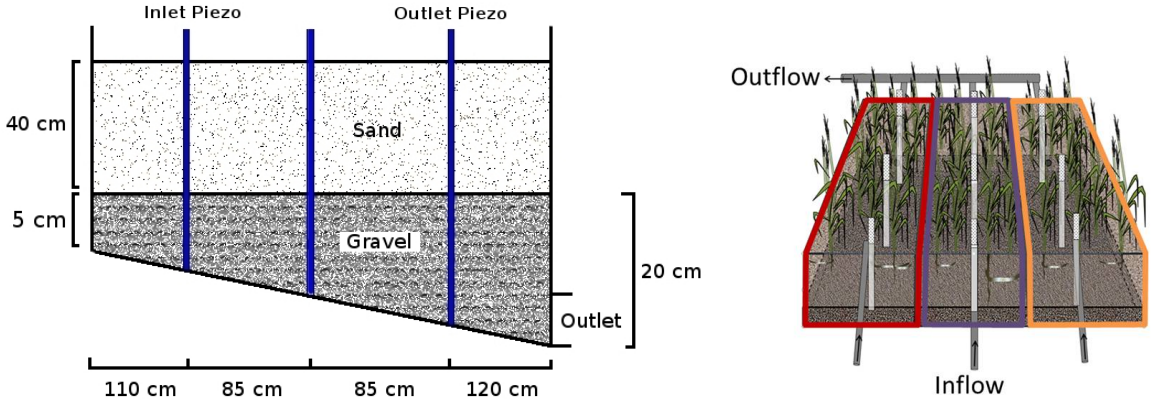

Figure 3.1: **Left:** Layout of the wetland bed dimensions (not to scale). **Right:** Layout of the three beds (not to scale).

source to facilitate horizontal flow from inlet to outlet as well as the registration of a tracer breakthrough curve and the calculation of hydraulic parameters. Because the application was stretched over a two week period, the tracer-pesticide-mix needed to be protected from UV radiation and heat. A 1000 L black tank made of polyethylene (PE) served as tracer-pesticide-mix storage. The tank was additionally covered with a space blanket to prevent uranine losses due to photolytic decay. To secure infiltration near the inlet, a section of 25 cm length was closed off using a wooden board, which was pushed 3 cm into the sediment (see Figure 3.2). The inlet pump rate was always low enough to prevent erosion from underneath the separation board.

Bed II and Bed III The injection setup of wetland Bed II and Bed III consisted of a perforated garden hose system connected to a 1000 L tank. There were eight tanks in total on site lined up along the inlet side of the beds. The tanks were made of weather resistant, inert PE material, which is known not to interact with any of the chemicals used in this experiment. The water was drained into the beds via gravity feed. Flow could only be controlled manually by means of a valve.

3.2.3 Outlet Design

The bottoms of all three beds were slightly slanted from inlet to outlet at an angle of approximately 2.5° (see Figure 3.1). The outlet of each bed was covered with a mesh filter to prevent sediment outwash, and was then connected to a T-shaped polyvinyl chloride (PVC) pipe (⌀10 cm). To cease flow, the base of the T-pipe was plugged with a rubber stopper.

Figure 3.2: From left to right: 1) Bed I inlet with isolated inlet section. 2) Bed II perforated inlet hose during filling on 24.05.12. 3) Aerial view of a bed outlet drain. 4) Man hole with outflow tub and sampling equipment.

The T-pipe essentially functioned as an access point for sampling and was covered with a lid to eliminate evapotranspiration and rainwater intrusion. Figure 3.3 illustrates the complete outlet design of each bed. Each bed outlet drained into a single main pipe that channeled bed water into an outflow tub containing measuring and sampling equipment, located in the outlet man hole (see Figures 3.2 and 3.4). When the outflow tub was full, a pump was triggered and the tub was purged. The water was pumped into an on-site waste water tank for disposal.

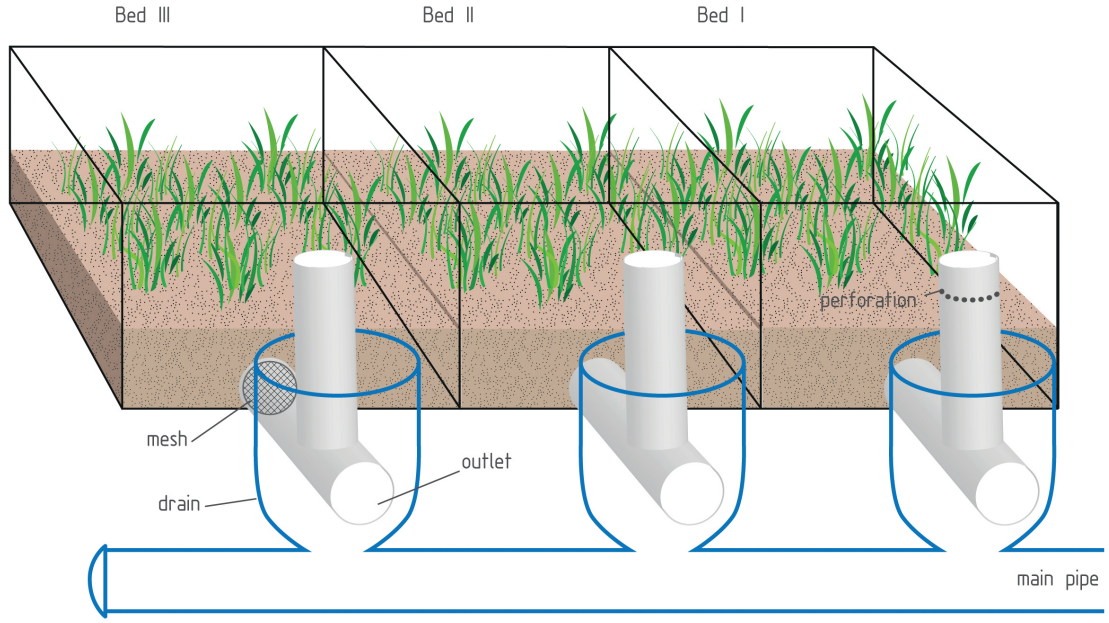

Figure 3.3: Experimental set up of the beds and the drainage outlets (not to scale).

Bed I The T-pipe of the Bed I outlet was perforated at the sediment level to ensure constant outflow and prevent gravitational draining effects (Figure 3.3). The outflowing water passed

through the main pipe and entered the outflow tub in the man hole via a pipe diameter reducing spout. This spout emptied into a tipping gauge device of 0.1 L holding capacity. From there the water ran into a rubber beaker (0.4 L volume), which served as sampling container for the autosampler (Figure 3.4).

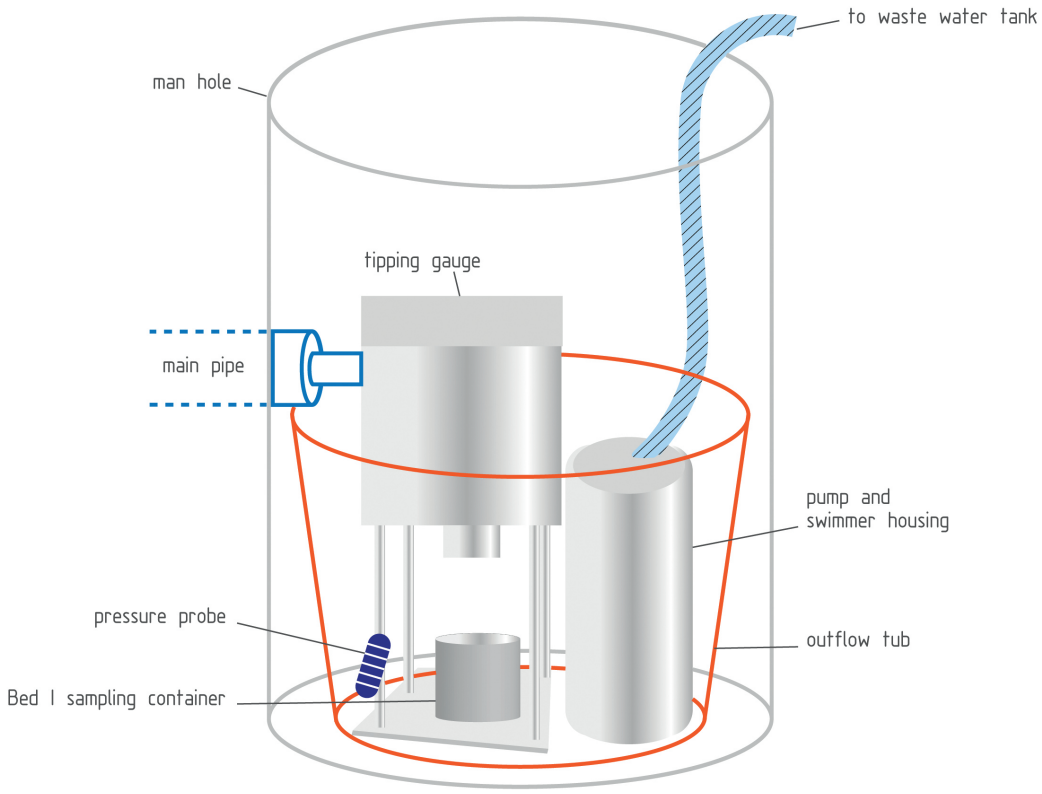

Figure 3.4: Experimental set up of the shared drain located in the man hole (not to scale).

Bed II and Bed III The outlet pipe of bed II and III was blocked by a rubber stopper, which was only removed for draining events (see Figure 3.2). The diameter reducing spout in the main pipe of the man hole outlet was removed to speed up the draining process of Bed II and Bed III. To prevent any rainwater from entering the main pipe via the individual outlet drain, a rubber mat was skirted around the outlet T-pipe and weighed down with rocks.

3.3 Experimental Design

3.3.1 System Operation Overview

Once the continuous flow and the two batch wetland systems were set up, each bed was treated with tracer-pesticide-mix on different schedules to simulate three contamination regimes,

which are described below. The contamination pattern for the batch flow beds simulated a point source pollution via injection of a high concentrated tracer-pesticide mix. The continuous flow bed received a lower concentrated injection mix than the batch flow beds, which was supposed to imitate a more diffuse contaminant input. The schedule for each treatment is listed in Table 3.1.

- **Bed I: Continuous flow - intermittent contamination** Tracer-pesticide-mix was continuously applied for two weeks (step injection) followed by four weeks of clean site water flushing.
- **Bed II: Intermittent flow - continuous contamination** The bed was saturated with tracer-pesticide-mix (pulse injection). The mix was allowed to react with the beds matrix for two weeks while the outlet was plugged. After two weeks the bed was drained. Then, the outlet was plugged again and a one week pause was interposed before the next pulse injection with tracer-pesticide-mix began.
- **Bed III: Intermittent flow - intermittent contamination***: The experimental procedure was the same as in Bed II. But, instead of repeatedly injecting a tracer-pesticide-mix, the injections alternated between tracer-pesticide pulse injection and pulse injection of clean site water.

* note: Bed III system operation had to be modified due to leaking (see Results Section 4.6).

Table 3.1: Treatment schedule for each wetland bed.

Date	Week	Bed I	Bed II	Bed III	
24.5.-31.5.	1	**1st step injection**	**pulse injection**	**pulse injection**	Batch 1
31.5.-7.6.	2		draining on 7.6.	draining on 7.6.	
7.6.-14.6.	3	flushing	pause	pause	
14.6.-21.6.	4	with	**pulse injection**	**site water injection**	Batch 2
21.6.-28.6.	5	clean	draining on 28.6.	draining on 28.6.	
28.6.-5.7.	6	site water	pause	pause	
5.7.-12.7.	7	**2nd step injection**	**pulse injection**	**pulse injection**	Batch 3
12.7.-19.7.	8		draining on 19.7.	draining on 19.7.	
19.7.-26.7.	9	flushing	pause	pause	
26.7.-2.8.	10	with	**pulse injection**	**site water injection**	Batch 4
2.8.-9.8.	11	clean	draining on 9.8.	draining on 9.8.	
9.8.-16.8.	12	site water	-	-	

3.3.2 Applied Tracers and Pesticide

Physio-chemical Properties The tracers bromide (BR, in form of NaBr), uranine (UR, fluorescein sodium, $C_{20}H_{10}O_5Na_2$) and sulphorhodamine B (SRB, $C_{27}H_{29}N_2NaO_7S_2$) were chosen to model the transport and fate of the pesticide metolachlor ($C_{15}H_{22}ClNO_2$) through the wetland matrix. Metolachlor (MC), a chiral, hydrophobic compound, is a herbicide from the chloroacetanilide group. The salt tracer bromide was to act as a conservative tracer and was designated to be the baseline for recovery calculations.

The fluorescent dye tracers SRB and UR were selected to model the physio-chemical transformation of metolachlor due to sorption and photolytic degradation, respectively. Uranine undergoes photolytic decay, but under alkaline conditions it is assumed to be a more conservative tracer than SRB, which has a high sorption potential (Käss, 2004; Leibundgut et al., 2009). Table 3.2 summarizes the physio-chemical properties of metolachlor, BR, UR and SRB.

Table 3.2: Physio-chemical properties (20°C-25°C) of applied tracers and pesticide. K_d = distribution coefficient between liquid and solid phase at equilibrium , K_{OC} = organic carbon adsorption coefficient.

Property	**BR**	**UR**	**SRB**	**Metolachlor**
Chemical Family	Salt Tracer	Fluorescence Tracer	Fluorescence Tracer	Acetamide
Aqueous Solubility [g/L]	850[a]	25[a]	70[a]	0.48[d]
Ionizability (pKa)	ionizable[a]	ionizable[a]	ionizable[a]	nonionizable[d]
Photolytic Stability (DT_{50})	stable[a]	11 h[a]	820 h[a]	70 d[c]
Hydrolytic Stability (DT_{50})	stable[a]	stable[a]	stable[a]	12 d[d]
Soil Retention (K_d) [ml/g]	-	0-0.4[b]	1.2-3.2[b]	0.1-2.1[d]
Sorptivity (K_{OC}) [mg/L]	-	-	-	369[d]

[a] Leibundgut et al. (2009), [b] Sabatini (2000), [c] Weber et al. (2007), [d] Agritox Online (2012)

Tracer Target Concentration In order to calculate the appropriate tracer injection mass and the target concentration, the following aspects were taken into account: detection limit of the analyzing instruments, natural background concentration, favored mean concentration to avoid time-intensive sample dilution during lab analysis, and losses due to photolytic decay and sorption. To compare the effects of different hydrological and contamination regimes, the tracer and pesticide load was held constant for all wetland treatments. However, because of the varying hydrological regimes, the tracer concentration in Bed I was necessarily different than in Bed II and Bed III. During step injection in Bed I, a target concentration of tracers

and pesticide was injected over a period of two weeks to generate a concentration plateau in the system outflow (steady state). The position and shape of the resulting breakthrough curve (BC) and the plateau give information about the transport behavior of the injected substances as well as processes involved like sorption or degradation (Käss, 2004; Leibundgut et al., 2009). In Bed II and III, batch operations consisted of applying the tracer-pesticide-mix as a pulse injection and letting it react with the bed's matrix for two weeks. The beds were subsequently drained, replugged and allowed to rest for one week, before the next batch operation started. The tracer loads satisfying all the above mentioned aspects for the three beds are listed in Table 3.3 along with the target injection volumes.

Table 3.3: Tracer load, injection type and target injection volume for the three wetland systems.

Bed	**Tracer**	**Injection Type**	**Injection mass** [mg]	**Target Injection Volume** [L]
I	NaBr	two-week	10^5	2 x 950
	SRB	step injection	100	
	UR	(5.9 L/h flow rate)	50	
II and III	NaBr	pulse injection	10^5	600
	SRB		100	
	UR		50	

Laboratory Preparation of Tracers Eight portions of the desired amount of each tracer were weighed out prior to the beginning of the experimental phase. Sodium bromide portions were weighed into 250 ml Nalgene® bottles and stored as solid until application. Just before tracer injection, 200 ml of site water was added and the bottle was shaken until complete dissolution of the salt tracer. The UR (50 mg) and SRB (100 mg) portions were combined in a 50 ml Nalgene® bottle and dissolved in 25 ml of distilled water. The eight bottles of fluorescence tracer solution were stored in a dark, cool place until application.

On site Preparation of Injection Solution Due to tracer-pesticide-mix holding capacity constraints, the step injection in Bed I was split into two consecutive application periods, each period lasting one week. Shortly before injection, the black inlet tank was filled with 950 L of site water and spiked with half of the tracer load prepared in the lab. The pesticide was added as metolachlor in the commercial product Mercantor Gold®, which which is composed of 80% S-metolachlor and 20% R-metolachlor. The mix was diluted in methanol at 1.7 ‰. Methanol acted as surfactant and facilitated complete emulsion of the hydrophobic compound. The

injection solution was stirred vigorously using an aluminum rod to ensure complete mixing of all added components. After one week of injection, the black tank was refilled with 950 L of site water and the remaining half of the tracer-pesticide-load was mixed in for the second week of step injection. In Bed II and III, tracers and pesticide were added to the inlet tank filled with 600 L of site water or less, depending on the residual water volume in each bed, just prior to pulse injection (see Section 3.3.4.2). The mix was stirred to assure complete dispersion using an aluminum rod. During injection, the inlet tank was covered with brown tarp to prevent photolytic degradation.

3.3.3 Sampling Procedures

Sampling for Tracers and Pesticide Water samples for tracer laboratory analysis were taken from the inlet tank, the piezometers and the outlet. Depending on the desired sampling frequency, outflow sampling was done manually or using an autosampler. Samples from the bed piezometers were taken at least once a week. All tracer samples were stored in 100 ml brown glass bottles in a cool, dark place until lab analysis. The analysis for UR and SRB was done within five to seven days after sample collection. Bromide analysis was delayed by several weeks due to problems with the analysis equipment.

Inlet tank tracer samples were always taken during tracer-pesticide injection to check the initial injection concentration. In order to characterize the flow path of tracers and pesticide in Bed I, individual samples were taken from each piezometer. In the other two beds, tracer samples were taken only from the inlet and outlet piezometer. Prior to sampling the piezometers were purged using an SDEC pump (Reignac sur Indre, France) and allowed to refill. This assured the extraction of a sample representing the conditions within the bed, not within the piezometer.

Outlet tracer samples in Bed I were taken by an autosampler from the outflow tub sampling container every hour up to 3.5 days after tracer injection and after beginning of flushing with clean site water. This way, the data resolution was high for the breakthrough curve during the increase and decrease of concentration measured in the outflow. When the tracer concentration plateau was expected to have established, the sampling interval was increased to two hours. After Bed I had been flushed with clean site water for more than two weeks, the sampling interval was incrementally increased from four to twelve hours.

In Bed II and III, manual outlet samples were taken for tracer analysis at fixed intervals prior to and during the course of draining. Composite 10 L pesticide samples were taken

by the French group during draining (1 L every 10 min). Tables 3.4 and 3.5 summarize the location and frequency of water sampling in the beds. Additionally, continuous measurements of fluorescence tracer concentrations were taken during each draining of Bed II and III using a flow-through filter fluorometer, which was placed in the outlet T-pipe (see Table 3.5). The fluorometer also recorded changes in the turbidity of the outflow during draining events. An overview of all the instruments used for sampling and other field measurements during the experiment is given in Table 3.6.

Table 3.4: Sampling schedule and number of samples taken for tracers and pesticide in Bed I. If not indicated otherwise the same sampling interval for tracers (^{T}) and pesticide (^{P}) applied. All pesticide samples were taken and analyzed by the French group.

Sampling Location	**Number of samples taken in Bed I during:**					
	Week 1	Week 2	Week 3	Week 4	Week 5	Week 6
	(Tracer-Pesticide Injection)		(Flushing with clean site water)			
Inlet	3	3	-	-	-	-
In/Center/Out Piezo	1	1	1	1	1	1
Outlet^T *	1 per 1-1.5 h	1 per 2 h	1 per 1-1.5 h	1 per 2 h	1 per 6 h	1 per 12 h
Outlet^P	1	1	1	1	1	1

*samples taken by autosampler

Table 3.5: Sampling schedule for tracers and pesticide in Bed II and III. If not indicated otherwise, the same sampling interval for tracers (^{T}) and pesticide (^{P}) applied. All pesticide samples were analyzed by the French group.

Sampling Location	**Number of samples taken in Bed II and Bed III during:**			
	Pulse Injection	Batch Operation	Draining	Pause
Inlet	3	-	-	-
Inlet and Outlet Piezo^T	-	1/week[a]	-	1/week[a]
Inlet, Center and Outlet Piezo^P	-	1 pooled/week[a]	-	1 pooled/week[a]
Outlet^T	-	-	1/1-30 min[a]	-
	-	-	1/10 sec[b]	-
Outlet^P	-	-	1/10 min[a]	-

[a]samples taken manually [b]samples taken by flow-through fluorometer

Sampling for Hydrochemistry and Water Quality Water samples for hydrochemical analysis (TOC, DOC, P_{tot}, PO_4^{3-}, NO_2^-, NO_3^{2-}, SO_4^{2-}, SO_3^{2-}, K^+, NH_4^+) were taken weekly from the piezometers and each outlet T-pipe. In Bed I, all three piezometers were sampled, whereas in Bed II and III a water sample composite of all three piezometers was taken. The lab analysis for hydrochemistry was carried out by the French group. Water quality parameters (pH, redox, dissolved oxygen, conductivity and water temperature) were monitored using different probes, which were placed in the bed's piezometers (see Table 3.6).

Soil Sampling At the end of the batch experiments on August 9^{th}, bulk soil samples for sorption and microbiology analysis were taken from each bed at three different depths (0 to 10 cm, 20 to 30 cm and 40 to 50 cm) using a stainless steel spoon. The zones located 0.5 m from the inlet and the outlet of the beds were sampled that way. In total six bulk soil samples were extracted from each bed. The samples were stored in 1 L plastic bags and placed in a cooler for transport. All bulk soil samples were stored at -20°C until analysis by the French group. On August 16^{th} two soil core cutter samples were taken from the in- and outlet zones of each bed for pF-curve analysis and determination of soil porosity.

3.3.4 Field Measurements

In order to calculate hydraulic parameters and achieve a tracer mass balance for each bed, it was crucial to quantify all water balance entities: inflow volume, precipitation, evapotranspiration and outflow volume. Additionally, several instruments were installed on-site to measure in- and outflow volumes (see Table 3.6).

3.3.4.1 Climate Data and Precipitation

Precipitation was measured using a weighing pluviometer, which was set up on the lawn 20 m away from the inlet side of the beds. The pluviometer was read out, emptied and cleaned once a week. Climate data was available from a nearby weather station maintained by the Institute of Hydrology, Freiburg. The station is located in Eichstetten, Germany, approximately 30 km away from the study site. The recorded data is listed in Table 3.6.

3.3.4.2 Inflow

Bed I: The inflow of Bed I was measured using three methods: 1) multiplying the hours of pump operation by the pump rate, 2) measuring the remaining volume in the tank after one

experimental week and 3) measuring while refilling the tank. The first method is a simple, but crude approach and rests on the assumption that the pump rate remained constant over time. This measurement method can be viewed as expressing the maximum of water that entered Bed I. The second method was applied when the tracer-pesticide-mix tank needed to be emptied. It required the complete draining of the tank and the quantification of the volume drained. This was achieved by emptying the tank incrementally via the inlet hose into a 10 L HDPE bottle, which was then drained into the waste water tank on site. The third method was applied during flushing cycles with clean site water. Usually, the Bed I inlet tank was filled to the maximum with water (i.e. 1000 L) before the start of another flushing cycle. A week later, the tank was refilled to its initial volume using a flow meter (Chierici Tito s.r.l, Rubiera, Italy). Thus, the water volume needed to refill the tank was roughly equal to the volume which had been pumped into Bed I.

Bed II and Bed III: Before filling the inlet tanks with water using a flow meter, the water level in the bed piezometers was checked using a measuring tape. The residual water in the bed was calculated using Equation 3.1 where V_{res} is the residual water, W_{Piezo} is the water level in the center piezometer, A_{Bed} is the average surface area of the bed and ϕ is the porosity (i.e. 16 %). The injection volume was calculated by subtracting V_{res} from the bed's saturated volumetric water content (θ_S=600 L). The tanks were then always completely drained into the beds.

$$V_{res} = W_{Piezo} \cdot A_{Bed} \cdot \phi \tag{3.1}$$

3.3.4.3 Outflow

Bed I: The outflow was measured using three different methods:

1. A tipping gauge located underneath the outlet spout in the outflow tub tipped at a fill volume of 0.1 L. The tipping gauge was connected to a data logger, which recorded every tipping event and the time of occurrence (see Figure 3.4).

2. A pressure probe placed on the bottom of the main outflow tub recorded the change in water pressure over time (see Figure 3.4).

3. The water level in the waste water tank was measured at least once a week as well as before and after draining using a folding meter stick.

Method three was a back-up in case the other two instruments should fail. For detailed information on the devices used see Table 3.6.

Table 3.6: Instruments used for field measurements.

Instrument	**Measurement Purpose**	**Parameters**	**Units**
Ott Pluviometer	precipitation	precipitation	mm
Climate Station Eichstetten	evapotranspiration	relative humidity	%
		wind speed	m/s
		mean air temperature	°C
		solar radiation	W/m^2
Flow Meter	tank fill volume	-	L
Seepex Pump	inflow Bed I	-	L/h
Tipping Gauge with Hobo Logger	outflow quantification	outflow	0.1 L/tipping
Pressure Probe with Mikromec Logger		water pressure	Δ mW per min
Filter Fluorometer GGUN-FL30	field fluorometry	UR and SRB conc.	ppb
		turbidity	NTU
SDEC Pump	sample collection	-	-
Hanna Instrument Multi Parameter Probe (HI 9828)	water quality monitoring	pH	-
		redox potential	mV
		dissolved oxygen	mg/L
		conductivity	μS/cm
		water temperature	°C
Odyssey Capacitative Water Level Logger	piezometer water level	water level	mm/10 min
APEG Autosampler	Bed I outflow sampling	-	capacity for 42 samples

Bed II and Bed III: The outflow in Bed II and III was only measured during draining events the pressure probe (Method 2, above). The tipping gauge was not designed for high outflow rates and was removed from the outflow tub. While draining Bed II, the continuous injection in Bed I was paused to avoid cross contamination of Bed I and II outflow. The end of a draining event was determined when the field fluorometer took in air. At that time, the Bed II outlet was plugged, so no Bed II drain water would mix with the Bed I continuous outflow. The water level in the wastewater tank was measured before and after draining each bed as a substitute in case the pressure probe failed (Method 3, above).

3.3.4.4 Monitoring of Plant Development

Plant growth and density in each bed were measured weekly and monthly. The growth was evaluated by measuring the height of five individual plants marked with tape. These plants were randomly chosen at the beginning of the experiment in May. Each week, minimum, mean and maximum plant height were noted. No differentiations between plant species were made. Every three weeks, an inventory of plant density was taken by counting all live plant stems found within 25% of the bed's area near the outlet side ($\approx$ 1.8 m^2). Furthermore, pictures taken from within each bed and from above were used to document the progress of plant maturation.

3.4 Data Analysis

All calculations were done using the program R (The R Foundation for Statistical Computing, Version 2.15.2) if not stated otherwise. The data analysis components are detailed in the sections below.

3.4.1 Fluorescence Tracer Analysis

Fluorescence intensity of the collected water samples was measured in the lab using a fluorescence spectrometer (LS-50B, Perkin-Elmer). The accuracy of fluorescence spectrometry is a result of the instrument's detection limit (1%) and the ability to reproduce measurements (UR = $\pm$0.62% and SRB = $\pm$2.64%). The total accuracy of the fluorescence spectrometry for each tracer was:
UR = $\pm$1.62% and SRB = $\pm$3.64%
The light source for spectrometry was a pulsed Xenon emission lamp. The excitation wavelength for UR and SRB was 488 nm and 561 nm, respectively. The emission wavelength was measured at 512 nm for UR and at 583 nm for SRB. The difference between the excitation and the emission wavelength is nearly equivalent for UR and SRB ($\Delta\lambda \approx 22$ nm). Thus, a double scan method was applied, where a wavelength range from 400 nm to 600 nm was scanned at 100 nm/s. Fluorescence intensity was related to the fluorescence tracer concentration via a linear calibration curve. Standards of known concentration were prepared for UR and SRB using site water for dilution. This made corrections due to background fluorescence of dissolved organic matter unnecessary. The concentration range of the standards covered the expected concentration in the samples (UR range from 0.5 ppb to 15 ppb, SRB range

from 0.5 ppb to 50 ppb). The standards were analyzed on the spectrometer for fluorescence intensity (INT_{Tracer}). Subsequently, a calibration curve was fitted. Site water background intensity for UR was on average 17.05 ($\sigma = 0.63$) and 2.37 for SRB ($\sigma = 0.27$). However, background intensities were subject to change over time due to variation in the dissolved organic matter contents of the samples. The calibration curves can be found in the Appendix (Figure A.1). The R^2 value for regression was 0.99 for UR and 1 for SRB. Equations 3.2 and 3.3 were used to calculate tracer concentration from fluorescence intensity.

$$C_{UR} = \frac{(INT_{UR} \cdot \text{Dilution Factor}) - 19.47}{56.59} \tag{3.2}$$

$$C_{SRB} = \frac{(INT_{SRB} \cdot \text{Dilution Factor}) - 2.40}{3.50} \tag{3.3}$$

The pH of the water samples was checked randomly before spectrometry analysis and was usually between 7.2 and 7.9. Uranine fluorescence intensity is known to decrease at a pH below eight (Käss 2004). In order to account for intensity losses due to low pH the sample pH was brought up to nine by adding five drops of NaEDTA buffer solution to 20 ml of sample. The UR fluorescence intensity was measured before and after addition of NaEDTA. In this experiment no significant change in fluorescence intensity was found. High concentration samples ($\mathrm{C}_{UR} \geq$ 17ppb and $\mathrm{C}_{SRB} \geq$ 285ppb) were diluted with clean site water to stay within the linear concentration range. The dilution factor was accounted for in Equations 3.2 and 3.3.

Initial tracer concentration for Bed I step injection and Bed II pulse injection were derived by averaging the UR and SRB concentrations measured in samples from the first and second inlet tank as well as from the inlet hose. Deviation from target concentrations was mostly due to uncertainties in the fill volume of the tank using the water meter. In order to calculate tracer mass balance, the tracer load was determined by multiplying the initial tracer concentration by the total inflow volume of injection mix.

3.4.2 Bromide Analysis

Bromide analysis was done using an ion chromatograph (IC, Dionex-DX 500) . The Dionex can analyze bromide concentrations ranging from 140 ppb to 100 ppm with an accuracy of 8% (Dionex, 1993). Samples were filtered with a 0.45 μm filter and diluted for sharper peak results when expected concentration exceeded 30 ppm. The prepared samples were filled into analysis vials and stored in the fridge at 4°C until analysis. Calibration standards from

0.1 mg/L to 10 mg/L were used by the machine for internal calibration and concentration calculation. Due to time constraints and technical problems with the IC, only the first step injection samples from Bed I and the Bed II draining samples from batch numbers three and four were analyzed.

Some difficulties arose due to high bromide concentration in the batch draining samples. Even though the samples were diluted, the concentration was too high to stay within the range of the internal calibration. Thus, additional standards were prepared spanning from 10 mg/L to 100 mg/L and the existing calibration curve was extended accordingly. Even with this adjustment, the true concentration of the samples was underestimated, which was confirmed by comparing the results of a sample from the inlet with known injection concentration. Depending on the bromide concentration, the underestimation ranged from 20% (samples with 50 mg/L to 100 mg/L BR) to nearly 40% (samples with more than 100 mg/L BR). The bromide injection load for batch three and four was adjusted to the injection tank concentration measured by the IC, even though the actual injection concentration was probably higher. This way at least some of the batch draining samples could be used for comparing bromide and fluorescence tracer mobility as well as mass recovery calculations. Still, the batch drain analysis can only be viewed as a proxy for bromide transport and fate in Bed II. Due to the complications listed above, the results from the Bed II bromide analysis only qualify for relative solute transport comparisons, not absolute ones.

3.4.3 Metolachlor Analysis

Pesticide water samples were collected by the French group and analyzed for metolachlor contents in the ENGEES laboratory in Strasbourg, France. The distinction between S- and R-stereoisomers in the metolachlor samples was still pending at the time this study was printed. Analysis methods for the quantification of metolachlor included solid-phase extraction followed by coupled gas chromatography and mass spectrometry (GC-MS) .

3.4.4 Evapotranspiration Computation

Reference evapotranspiration (ET_0) was calculated using the Ref-ET (Reference Evapotranspiration Calculation) software version 3.1 from the University of Idaho (Allen, 2011). The Ref-ET program provides standardized calculations of reference evapotranspiration by fifteen of the more common methods compatible with United Nations Food and Agriculture Organization Irrigation Paper No. 56 by Allen et al. (2006) and with the standardized forms of

the ASCE Penman-Monteith equation and components. The minimum required input data includes: air temperature, relative humidity, solar radiation and wind speed. All remaining input data (see Equation 3.4) is calculated by the program. Furthermore, geographic reference coordinates of the climate station, its elevation and the height of equipment need to be entered. The program calculates reference evapotranspiration using alfalfa and grass vegetation at 0.12 m and 0.5 m height respectively. The evapotranspiration (ET) in this study was computed using the full ASCE Penman-Monteith with resistance reference evapotranspiration for grass used by Allen et al. (2006):

$$ET_0 = \frac{\Delta(R_n - G) + K_{time} \cdot \rho_a \cdot c_p \cdot \frac{e_s - e_a}{r_a}}{\lambda_H \Big(\Delta + \gamma_{psych}(1 + \frac{r_s}{r_a})\Big)} \tag{3.4}$$

Whereby R_n corresponds to net Radiation, G is the soil heat flux, e_s is the saturation vapor pressure of the air, e_a is the actual vapor pressure of the air, $(e_s - e_a)$ is the vapor pressure deficit, ρ_a is the mean air density at constant pressure, c_p is the specific heat of the air, Δ is the slope of the saturation vapor pressure temperature relationship, γ_{psych} is the psychrometric constant, r_s is the bulk surface resistance, r_a is the aerodynamic resistance, λ_H is the latent heat of vaporization and K_{time} is a time unit conversion.

The calculated ET_0 represents a maximum of the actual evapotranspiration (ET_a) from the wetland beds. Because Bed I was always saturated it can be assumed that no water stress occurred and ET_a was equal to ET_0. However, in Bed II and III soil saturation only occurred after injection of the spiked inlet solution or clean site water. Thus, ET_a was much lower than ET_0 for most of the batch operation time.

3.4.5 Computing Outflow from Pressure Probe Data

Coaxing a nuanced outflow from the pressure-probe data was a process complicated by several factors inherent to the style of volume measurement employed. A description of each of these factors along with corresponding the methods used to coerce the data into increasingly more useful forms is detailed below.

3.4.5.1 Correlating Pressure with Volume:

Firstly, the shape of the tank and the presence of instruments resting within the tank itself necessitated the use of a correlation curve between pressure readouts and outflow tub water volume. This curve was generated by a running a linear regression over data obtained by recording pressure readouts while incrementally adding 500 mL of water to a recently flushed

tub. The water volume V (in L) in the tub at pressure probe readout P (in mW) at time t were given by the function:

$$V(t) = 165.310 \cdot \mathrm{P(t)} - 14.319 \tag{3.5}$$

The linear regression R^2 value for this equation was 0.999. The average outflow tub volume before the swimmer in the pump initiated a pumping cycle, was determined to be 14 L. The detection limit of the pressure probe was at 0.001 mW, which is equivalent to 0.167 L.

3.4.5.2 Overwriting measurements taken during pumping:

Additionally, short intervals of measurement and relatively long tank flushing times led to many occurrences of pressure measurements being taken during periods of tank pumping. All such nuisance measurements were removed and replaced with an estimate calculated using the average flowrate in a neighborhood around each removed data point. The specific algorithms used for each bed are detailed below.

Bed I: Here the logging interval (1 min) was significantly longer than one pumping cycle (≈20 sec). As such, all nuisance measurements were isolated and a two sided differential approximation was used. Specifically, for each such nuisance point $(t, V(t))$ the following computation was executed in R:

$$V(t) \leftarrow V(t-1) + \frac{\overbrace{\Delta V(t-1) + \Delta V(t+1)}^{\text{average volume differential near t}}}{2} \tag{3.6}$$

whereby the two differentials in the correction term are given by the left and right discrete differentials, respectively. The R-pseudocode is given by Algorithm 1.

Algorithm 1 : Replace Bed I nuisance measurements with an approximation.

for $i = 2 \rightarrow$ Length $(V) - 2$ **do**
  if $V[i-1] > V[i] > V[i+1]$ **then**
    $V[i] \leftarrow V[i-1] + \big(V[i-1] - V[i-2] + V[i+2] - V[i+1]\big)/2$
  end if
end for

Bed II: Due to the extremely high outflow rate observed while flushing Bed II, a shortened sampling interval (10 sec) was eventually used during week 11 to ensure no fill-flush cycles

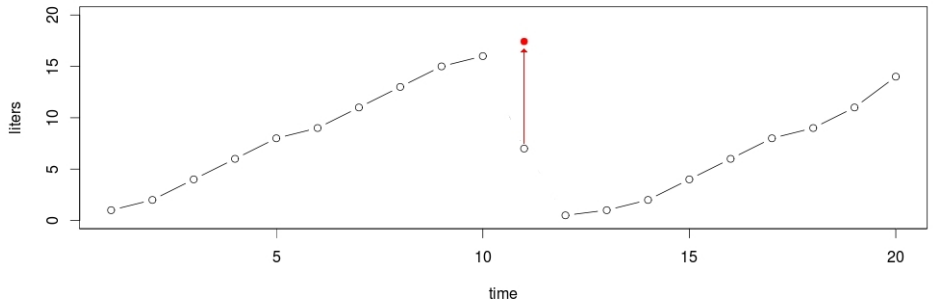

Figure 3.5: Graphic example of Algorithm 1 replacing Bed I pressure probe measurements taken during outflow tub pumping.

were omitted. At this sampling rate, nuisance pumping measurements were no longer strictly isolated, so a left-sided differential approximation was used.

$$V(t) \leftarrow V(t-1) + \overbrace{\Delta V(t-1)}^{\text{left volume differential}} \tag{3.7}$$

This correction is given in R-pseudocode by Algorithm 2.

Algorithm 2 : Replace Bed-2 nuisance measurements with an approximation.

for $i = 2 \rightarrow \text{Length}\ (V) - 2$ **do**
  if $V[i-1] > V[i] > V[i+1]$ **then**
    $V[i] \leftarrow V[i-1] + (V[i-1] - V[i-2])$
  end if
end for

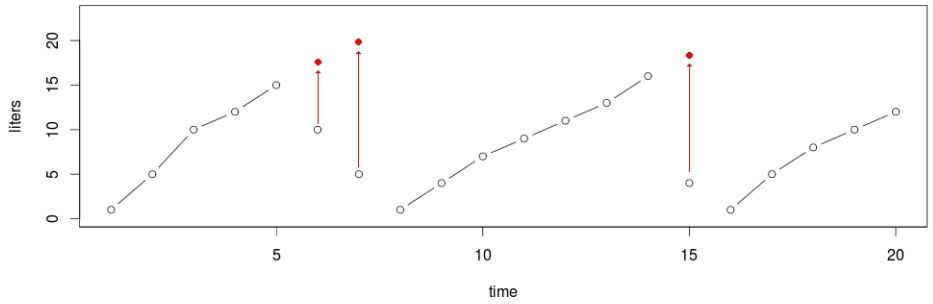

Figure 3.6: Graphic example of Algorithm 2 replacing Bed II pressure probe measurements taken during outflow tub pumping.

3.4.5.3 Converting Sawtooth Monotonicity into Regular Monotonicity

The sawtooth-wave nature of the volume function at this stage prohibited one from calculating the outflow rate in a consistent manner because all left and right endpoints of continuous segments failed to have meaningful left and right derivatives, respectively. This issue was resolved by algorithmically shifting all continuous blocks of data upward by a correction term. The precise vertical shift after each break in continuity was estimated by the same method of differentials used in Algorithm 1, and an accumulator was employed to record the sum of all previous shifts. This is given by the following R-pseudocode.

Algorithm 3 : Convert "sawtooth-wave" pressure probe data into regular monotonic increasing data, estimating vertical shifts via two-sided differentials

```
end ← Length(V)
for i = 1 → end do
    afterflush[i] ← FALSE                          ▷ Initialize a boolean vector
end for
for i = 2 → (end − 1) do
    if (V[i − 1] − V[i]) > 1 then                  ▷ Locate all continuity breaks
        afterflush[i] ← TRUE
    end if
end for
acc ← 0                                            ▷ Initialize the accumulator
for i = 1 → end do                                 ▷ If a break occurs, adjust the accumulator
    if afterflush[i] == TRUE then
        acc ← (V[i − 1] − V[i]) + (V[i − 1] − V[i − 2] + V[i + 1] − V[i + 2])/2
    end if
    V[i] ← V[i] + acc                              ▷ adjust value by the current accumulator amount
end for
```

Bed II Adjustment: The resulting monotonically increasing curve represented the cumulative outflow of Bed I and each draining of Bed II. However, due to some loss of information during pumping events while draining Bed II, Algorithm 3 potentially underestimates the total outflow volume. To resolve this, the number of pumping events (i.e. "sawtooth-waves") during Bed II draining were counted and the result multiplied by 14 L. Then, the accumulated outflow after the very last recorded pumping event was added and coupled with the

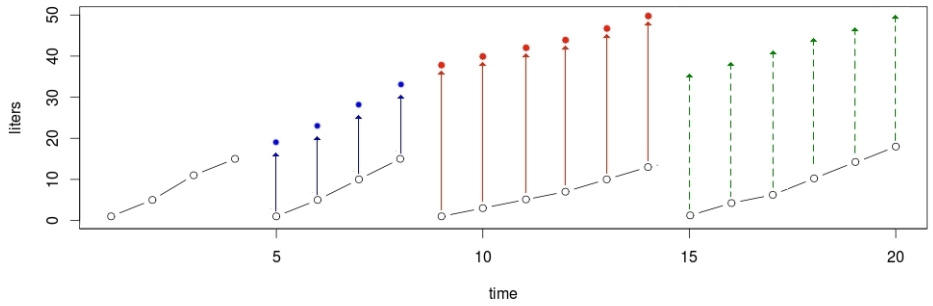

Figure 3.7: Graphic example of Algorithm 3 converting "sawtooth-wave" pressure probe data into regular monotonic increasing data, estimating vertical shifts via two-sided differentials.

accuracy due do the detection limit of the pressure probe for each pumping event. The total difference between applying Algorithm 3 and counting pumping events was approximately 10 L.

3.4.5.4 Calculating Outflow Rate:

With the previous adjustments having been implemented, the outflow was obtained by simply taking the discrete derivative, which was calculated with a timestep of two minutes. Outflow per minute was defined as:

$$Q(t) := \frac{\Delta V}{\Delta t}\Big|_{\Delta t=2} = \frac{V(t+1) - V(t-1)}{2} \tag{3.8}$$

3.4.6 Outflow from Tipping Gauge Data

The tipping gauge data (in tips per unit time) from Bed I was converted to outflow data using R. The irregular tipping events, each accounting for 0.1 L of outflow, were merged with a regular time series. Subsequently, the data was aggregated to minute and hourly outflow data. Unfortunately, the tipping gauge data logger failed to record on June 6^{th} and could not be repaired. The outflow data measured by the the pressure probe was used as substitute. Tipping gauge and pressure probe data showed a strong correlation for the outflow data period when both devices were recording. Figure 3.8 shows the outflow time series recorded by each device.

The outflow measured for the period from 28.05.2012 1 am to 06.06.2012 12 am by the tipping gauge and the pressure probe was 798.60 L and 847.09 L, respectively. The difference of 48.49 L is due to a general underestimation of outflow by the tipping gauge during high flow

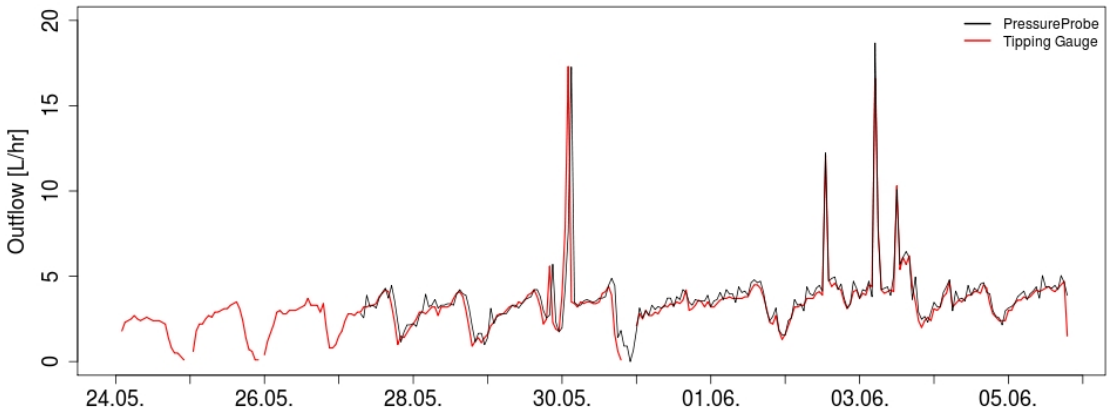

Figure 3.8: Tipping gauge and pressure probe outflow data from 27.05.2012 - 06.06.2012.

periods. This phenomenon was observed during test draining of Bed II, where overflowing tipping compartments caused some of the outflow not to be accounted for.

3.4.7 Outflow from Dip Stick Method

The water level in the wastewater tank was measured before and after each draining of Bed II and III. The total outflow volume was then determined using the following equation:

$$V_{out} = \Pi \cdot r^2 \cdot \Delta h \tag{3.9}$$

Where V_{out} is the total draining volume, r is the radius of the wastewater tank (1.5 m), and Δh is the water level increase in the tank after draining. An approximated error of 14 L was associated with this method for each reading due to the uncertainty inherent in the measurement style (i.e. 2 mm error range on the dip stick reading).

3.4.8 Hydraulic Parameters and Recovery Computations

Hydraulic system parameters were evaluated on the basis of the two tracer breakthrough curves in Bed I. The parameter definition and computation methods are based on the paper published by Kadlec (1994) with modifications according to Lange et al. (2011). Table 3.7 gives an overview of the assessed parameters.

Table 3.7: Hydraulic parameters calculated from the breakthrough curves after bromide, UR and SRB step injection in Bed I.

Parameter	Description
HRT	(theoretical) hydraulic retention time [h]
v_{max}	maximum flow velocity [$m\ s^{-1}$]
v_{mean}	average flow velocity [$m\ s^{-1}$]
t_1	time of first tracer detection in outflow [h]
t_p	time of tracer peak concentration in outflow [h]
t_{50}	time when 50% of the injected tracer has passed the outlet [h]
t_N	nominal residence time [h]
C_{max}	peak outflow concentration [$mg\ L^{-1}$]
R_f	retardation factor
λ	hydraulic efficiency
R	tracer recovery [%]

The theoretical hydraulic retention time for Bed I was calculated using the volumetric water content of the bed at saturation (i.e. $\theta_S = 600$ L) and the average inflow pump rate (Q_{in} in L/h):

$$HRT = \frac{\theta_S}{Q_{in}} \tag{3.10}$$

The maximum flow velocity was calculated using the flow distance between injection and tracer sampling (x in m) and the time of first tracer appearance after injection:

$$v_{max} = \frac{x}{t_1} \tag{3.11}$$

The mean flow velocity was determined using the time when 50% of the injected tracer mass had passed the outlet via the following equation:

$$v_{mean} = \frac{x}{t_{50}} \tag{3.12}$$

The retardation factor was calculated by dividing the mean flow velocity of the ideal (conservative) tracer bromide by the mean flow velocity of each non-conservative fluorescence tracers:

$$R_f = \frac{v_{mean}BR}{v_{mean}FT} \tag{3.13}$$

The nominal residence time is a parameter that takes wetland geometry and average outflow rate (Q_{mean} in L) into account:

$$t_N = \frac{V}{Q_{mean}} \tag{3.14}$$

Finally, the hydraulic efficiency can be determined by the time of peak outflow concentration and the nominal residence time as proposed by Persson et al. (1999):

$$\lambda = \frac{t_{peak}}{t_N} \tag{3.15}$$

Persson et al. (1999) described three categories for hydraulic efficiency: good hydraulic efficiency ($\lambda > 0.75$), satisfactory hydraulic efficiency ($0.5 \leq \lambda < 0.75$) and poor hydraulic efficiency ($\lambda < 0.5$).

Tracer mass recovery expressed in percent of the injected tracer mass (M_{inj}) was calculated for both Bed I step injections as well as each draining of the batch experiment in Bed II according to the following equation:

$$R = \frac{\int_0^\infty C(t) \cdot Q(t) dt}{M_{inj}} \cdot 100 \tag{3.16}$$

It is important to note that the actual bromide content in a sodium bromide (NaBr) injection solution is only 76.6 %. However, all initial bromide injection mass values used in the recovery calculations were based on the IC injection solution concentration measurements multiplied by the total injection solution volume. This made the sodium bromide to bromide conversion unnecessary.

3.4.9 Modeling Tracer Transport

The quantification of solute transport parameters is essential to the evaluation of the fate of tracers and pesticide. These crucial transport parameters include: pore-water velocity, retardation factors, dispersion coefficients, as well as degradation and production parameters. However, the experimental determination of such transport parameters over sufficiently long distances and/or time periods is usually not feasible. The program CXTFIT 2.0 , originally developed by Parker and van Genuchten in 1984 and expanded by Toride et al. (1995), was used to estimate transport parameters during steady one-dimensional flow by fitting the parameters to observed field data. The inverse problem of estimating solute transport parameters from empirical observations is solved by minimizing an objective function, which consists of the sum of the squared differences between observed and fitted concentrations. The objective function is minimized using a non-linear least-squares inversion method (Marquart 1963 in Toride et al. (1995)). CXTFIT provides three different transport models: (1) equilibrium transport according to the convection-dispersion equation (CDE) , (2) nonequilibrium CDE transport and (3) a stochastic stream tube model for a simple conceptualization of solute transport in heterogeneous fields.

3.4.9.1 Equilibrium Convection-Dispersion Equation

In this project, the equilibrium CDE was applied for modeling non-reactive solute transport and obtaining transport parameters based on the observed bromide breakthrough curve from the first step injection in Bed I. Bromide acts as a conservative tracer, and thus it is expected not to be subject to kinetic adsorption. Ideally, a non-reactive tracer like bromide allows the measurement of the pore velocity (v) and the hydrodynamic dispersion coefficient (D) without altering the fluid properties of the surface chemical and the transmissive properties of the soil matrix (Seaman et al., 1995). The pore velocity and hydrodynamic dispersion coefficient approximated by the model were subsequently used to determine transport parameters for non-conservative transport of SRB and UR. The equilibrium solute transport is based on the following CDE for one-dimensional transport:

$$Rd\frac{\partial C_r}{\partial T} = D\frac{\partial^2 C_r}{\partial x^2} - v\frac{\partial C_r}{\partial x} - \mu C_r + \gamma(x) \tag{3.17}$$

where C_r is the reduced volume-averaged solute concentration, D is the hydrodynamic dispersion coefficient, v is the average pore-water velocity, μ is a first-order decay coefficient, γ is a zero-order production coefficient for equilibrium transport and x is the transport distance. The retardation factor Rd is directly proportional to the empirical distribution constant K_d, which describes solute adsorption to the solid phase (Toride et al., 1995).

3.4.9.2 Nonequilibrium Convection-Dispersion Equation

Solute transport can be affected by several chemical and physical nonequilibrium processes such as kinetic adsorption and heterogeneous flow regimes. Adsorption to sites in the soil matrix may occur instantaneously upon first contact with reactive solute. However, as exposure time progresses, adsorption to the remaining sites is controlled by first-order kinetics (Lal and Shukla, 2004; Toride et al., 1995). Physical nonequilibrium processes are modeled using a two-region approach where the medium consists of a distinct mobile (flowing) and an immobile (stagnant) liquid region (Toride et al., 1995). Both chemical two-site and physical two-region nonequilibrium processes are combined in CXTFIT under the dimensionless nonequilibrium CDEs:

$$\beta Rd\frac{\partial C_1}{\partial T} = P^{-1}\frac{\partial^2 C_1}{\partial Z^2} - \frac{\partial C_1}{\partial Z} - \omega(C_1 - C_2) - \mu_1 C_1 + \gamma_1(Z) \tag{3.18}$$

$$(1-\beta)Rd\frac{\partial C_2}{\partial T} = \omega(C_1 - C_2) - \mu_2 C_2 + \gamma_2(Z) \tag{3.19}$$

The subscripts 1 and 2 refer to the equilibrium and nonequilibrium sites, P is the Peclet number, β is a partitioning coefficient, ω is a dimensionless mass transfer coefficient and T and Z are dimensionless time and space variables. In this study, the input parameters v and D were taken from the equilibrium CDE model for bromide. The remaining parameters μ, β and ω were fitted by the model based upon the breakthrough curve concentration for UR and SRB. For both models (equilibrium and nonequilibrium CDE), a flux-averaged concentration, no constant production term, and a multiple pulse input condition was used for a series of two successive solute pulse applications. The first pulse accounted for the tracer-pesticide step injection for two weeks, followed by the second pulse flushing with clean site water for four weeks.

4

Results

4.1 Bed I: First Step Injection

The first step injection in Bed I began on May 24^{th} and lasted six weeks until July 5^{th}. On May 24^{th} at 7 pm constant tracer-pesticide injection began and ran for a total of 324 hours ending on June 7^{th} at 10 am. A total of 1749 L tracer-pesticide mix was injected. Subsequently, from June 7^{th} until July 5^{th}, the bed was flushed with clean site water. The average inflow pump rate during the six week step injection was 5.9 L/h.

4.1.1 Water Balance

The first outflow was recorded after one hour of pump operation. Figure 4.1 shows the precipitation, reference evapotranspiration and outflow data for the entire six week period. The apparent diurnal fluctuation in the outflow (see Figure 4.1) was governed by evapotranspiration, which reached a maximum in the early afternoon. During the night, evapotranspiration was negligibly low and the outflow rate was nearly equal to the inflow pumping rate. Precipitation events were usually short and intense, marking the convective storm character typical of Colmar summers. The highest precipitation intensity during tracer application was measured at 5:40 am on June 8^{th} with 0.3 mm/min. The most intense rainfall of the entire period occurred around 22:00 on June 30^{th} with more than 0.4 mm/min lasting for three minutes. The outflow rate response during precipitation events shows hardly any time lag because the bed was always nearly saturated. Table 4.1 summarizes the water balance data and lists

the maximum inflow and outflow events. The weekly water balances were not compensated during the first step injection and from week two through week six the balances were negative.

Table 4.1: Weekly water balances and high intensity events for the first step injection cycle in Bed I. Evapotranspiration values are based on reference evapotranspiration (ET_0). For the sake of easy comparison, all water balance components are presented in liters. Precipitation and ET_0 refer to the entire bed surface area.

	Tracer-Pesticide Injection		Flushing with Clean Site Water			
	Week 1	Week 2	Week 3	Week 4	Week 5	Week 6
Inflow $[L]$	923	826	837	865	1221	1243
Precip. $[L]$	16	30	273	45	50	283
ET_0 $[L]$	373	243	236	318	354	279
Outflow $[L]$	430*	662	1072	747	757	1820
Balance $[L]$	136	-49	-198	-156	-202	-573
$Precip._{max}$ $[L/h]$	10 (8pm 30.5.)	9 (11pm 3.6.)	28 (3am 11.6.)	14 (11pm 16.6.)	25 (6pm 21.6.)	28 (11pm 30.6.)
$Outflow_{max}$ $[L/h]$	17 (9pm 30.5.)	19 (11pm 3.6.)	38 (2am 11.6.)	24 (11pm 16.6.)	31 (6pm 21.6.)	45 (1pm 1.7.)

*data from Tipping Gauge

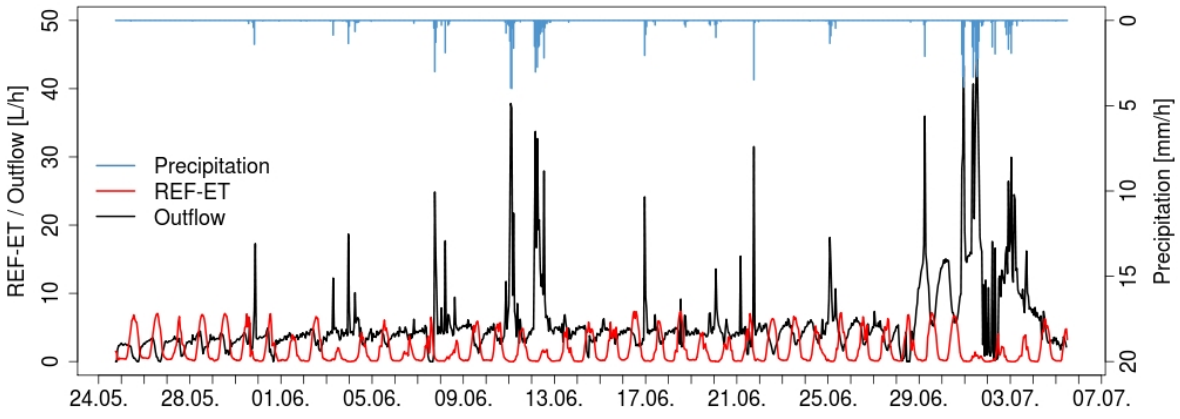

Figure 4.1: Precipitation, outflow and reference evapotranspiration data from the first step injection in Bed I. (Date-axis marks correspond to midnight.)

The water level measured in the Bed I piezometers fluctuated on a diurnal basis in accordance with changing evapotranspiration rates. Continuous data collected by the Odyssey capacitative water level loggers is plotted in Figure 4.2 and illustrates this daily fluctuation.

Some uncertainty in the data collection with the Odyssey probe seemed to occur during high precipitation events, as evidenced by the high variability of the probe's reading on July 2^{nd}.

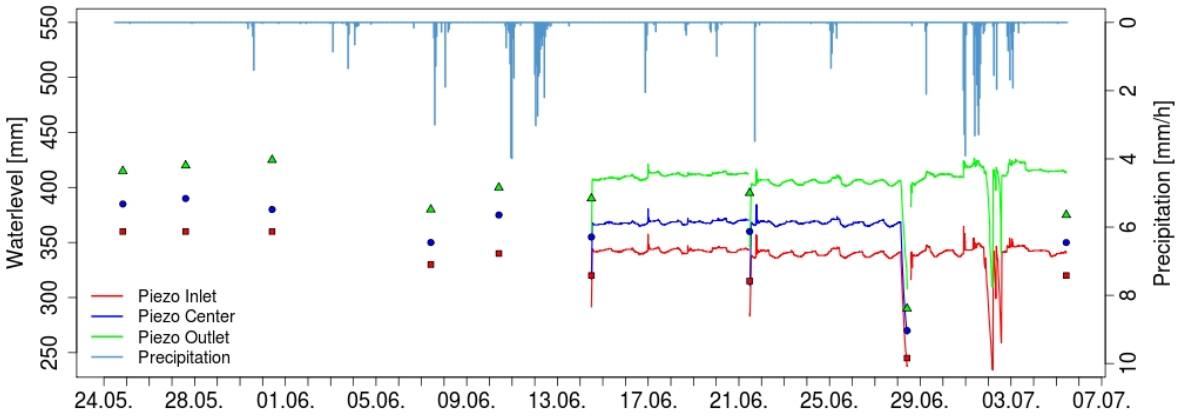

Figure 4.2: Bed I piezometer capacitative water level logger data for the first step injection. Individual data points represent the manual water level measurements taken every week using a measuring tape. The first two weeks of data are missing due to logger malfunction.

4.1.2 Tracer Breakthrough Curve and Recovery

The breakthrough curves (BC) for BR, UR and SRB are illustrated in Figure 4.3. Table 4.2 summarizes the important hydraulic parameters from the first step injection experiment. The first tracer measured in Bed I outflow was BR after 19 hours, followed by UR after 37 hours and SRB after 44 hours. Bromide reached the average plateau concentration of 35 mg/L after 129 hours. The theoretical hydraulic retention time was 102 hours. Thus, BR showed some retardation in terms of conservative transport through the bed's matrix. Plateau concentrations of UR (18 μg/L) and SRB (36 μg/L) were reached after 221 and 223 hours, respectively. However, the increase of UR concentration to the plateau concentration level proceeded much faster than in the case of SRB.

Maximum tracer concentration measured in the outflow never reached injection concentration level for any of the tracers. Plateau concentration was maintained for at least 4.5 days for all tracers before flushing with clean site water began. Once the tracer injection was stopped, BR showed the fastest response with a steep decline in effluent BR concentration, followed by UR and SRB. On the evening of June 7^{th}, high precipitation caused outflow sample dilution (see Figure 4.3), which obfuscated the beginning of the concentration decline in the BC.

As of June 10^{th}, BR recovery lagged behind UR recovery. Consecutive precipitation events between June 10^{th} and June 13^{th} appear to have caused tracer plug outflow. Outflow samples

taken after the event show higher concentrations than before the event (see Figure 4.3). The tracer tailing is most pronounced for SRB. None of the tracers fully returned to background level outflow concentration during the experiment, but tailing concentration of UR was very low (0.08 μg/L) in comparison to SRB (1.69 μg/L) and BR (0.77 mg/L). After four weeks of flushing, 78% of BR and 67% of SRB were recovered. In contrast, only 60% of UR were recovered. The ratio of UR to SRB recovery was 0.89. The overall SRB retardation factor with respect to BR was slightly greater than the UR retardation factor with 1.3 and 1.2, respectively. Figure 4.4 shows the tracer load recovery graphs for the first step injection.

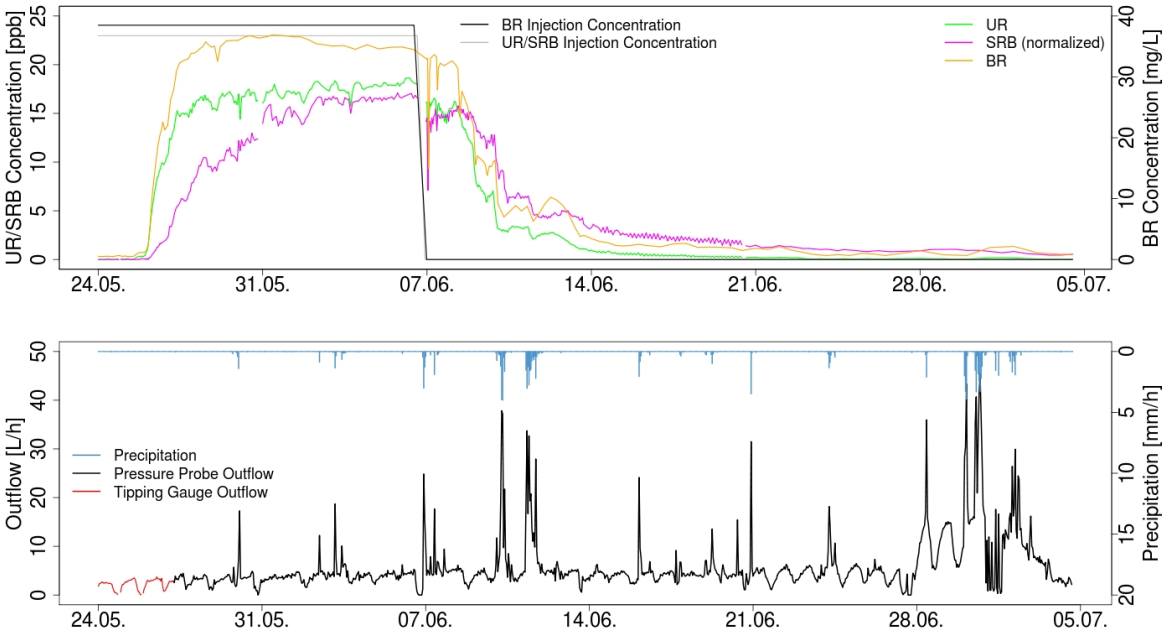

Figure 4.3: First tracer-pesticide-mix step injection in Bed I. **Top:** Tracer breakthrough curves. SRB concentration is normalized to UR concentration (SRB/UR = 2.15). Initial concentrations of tracers injected were: BR = 38.48 mg/L, UR = 22.97 ppb, SRB = 49.35 ppb. **Bottom:** Precipitation and outflow time series.

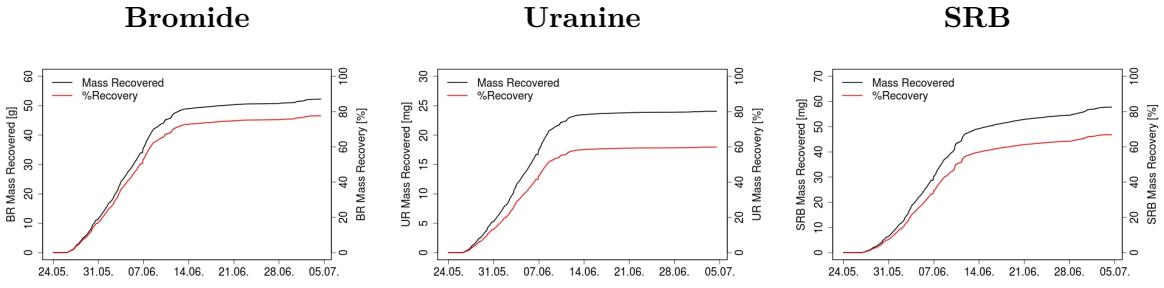

Figure 4.4: Tracer recovery for the first step injection in Bed I.

Table 4.2: Bed I first step injection recovery data: total mass injected (M_{inj}), time of first tracer detection in the outflow (t_1), maximum flow velocity (v_{max}), detection time of peak concentration (t_{peak}), peak concentration (C_{max}), time when 50% of the injected tracer has passed the outlet (t_{50}), mean flow velocity (v_{mean}), nominal residence time (t_N), hydraulic efficiency (λ), recovered tracer load (R_{Load}), % recovery (R) and retardation factor (R_f).

Tracer	M_{inj} $[mg]/^*[g]$	t_1 $[h]$	v_{max} $[m/h]$	t_{peak} $[h]$	C_{max} $[mg/L]$	t_{50} $[h]$	v_{mean} $[m/h]$	t_N $[h]$	λ	R_{Load} $[mg]/^*[g]$	R %	R_f
BR	67.31*	19	0.218	178	36.38	324	0.013	109	1.63	52.24*	78	-
UR	40.18	37	0.109	319	0.019	367	0.011	109	2.93	24.06	60	1.2
SRB	86.31	44	0.104	307	0.037	419	0.010	109	2.82	57.77	67	1.3

$\sigma_{UR} = 0.26$ μg/L, $\sigma_{SRB} = 0.43$ μg/L, $\sigma_{BR} = 0.85$ mg/L

Tracer and Metolachlor Concentration in the Piezometers Weekly water samples were taken from the three piezometers located in Bed I to provide information about the horizontal transport of tracers and metolachlor (MC) through the bed. Due to problems with the IC and time constraints, the samples could not be analyzed for BR. However, fluorescence tracer and pesticide analysis revealed a succession of concentration increases from the inlet to the outlet piezometer after tracer-pesticide injection had started. Figure 4.5 shows the tracer and pesticide concentrations measured in the piezometer samples. As expected, the inlet piezometer had the highest and the outlet piezometer the lowest tracer and pesticide concentration after three days of tracer injection. The difference between the inlet, center and outlet piezometer concentration never exceeded 3 μg/L for the tracers. The tracer peak concentration was measured on June 7^{th} with 28 μg/L UR and 56 μg/L SRB. Metolachlor maximum concentration was measured on May 31^{st} (148 μg/L). The peak concentrations of the piezometer samples were for both fluorescence tracers and pesticide higher than the peak concentration measured in the outflow samples (see Table 4.2). Upon flushing with clean site water, the concentration decreased first at the inlet piezometer and last at the outlet piezometer. The SRB piezometer samples converged slower to a constant concentration than the UR piezometer samples, indicating SRB retardation due to sorptive processes. Pre-injection background levels were not reached in any of the piezometers for tracers and metolachlor. For a table of the Bed I piezometer waterlevel, as well as tracer and pesticide concentrations see the Appendix (Tables A.1 and A.6).

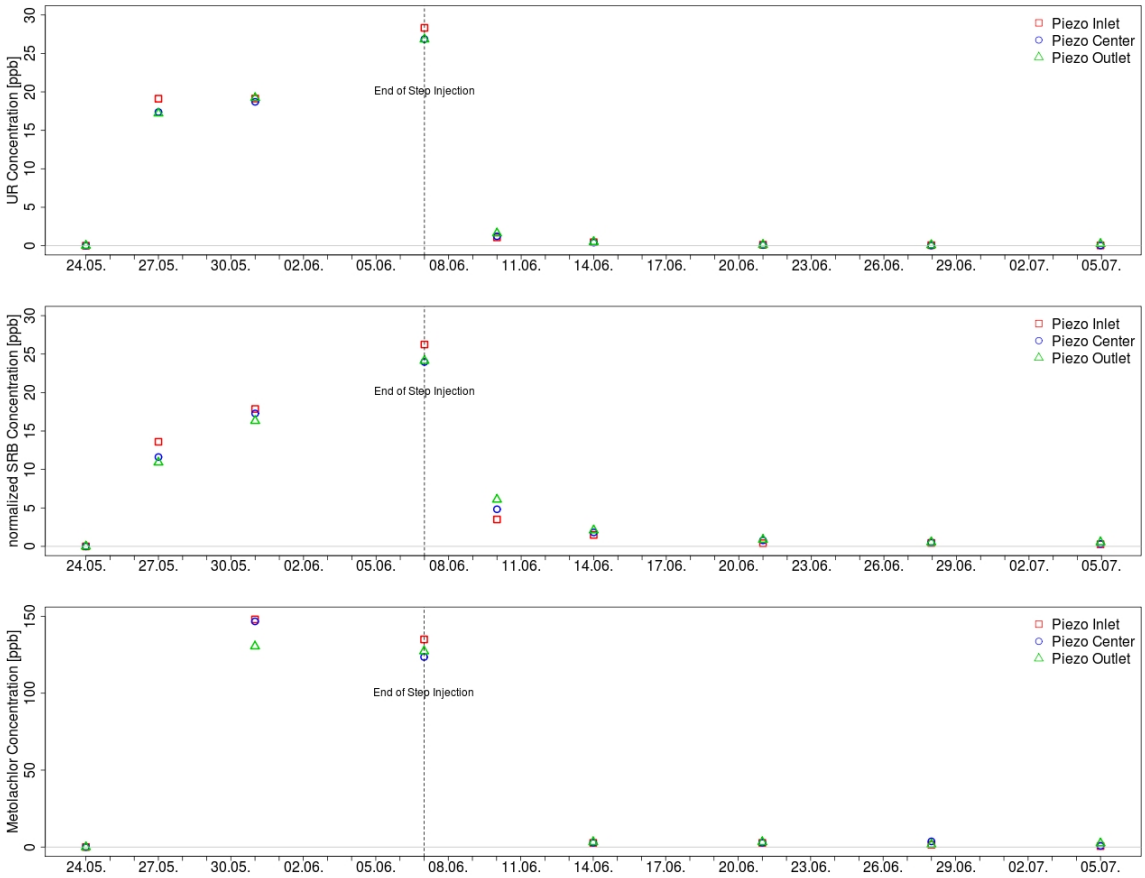

Figure 4.5: Uranine (top), SRB (center) and metolachlor (bottom) concentrations measured in water samples taken weekly from each piezometer in Bed I during the first step injection experiment. Initial concentrations of tracers and pesticide injected were: UR = 22.97 ppb, SRB = 49.35 ppb and metolachlor = 146.88 ppb. SRB is normalized to UR.

Uranine and SRB concentrations from all three piezometers were averaged, normalized to metolachlor and correlated with the averaged metolachlor concentration. The linear correlation was inconclusive for SRB and UR despite high R^2 values because of point clusters at low concentrations (see Appendix Figure A.2).

4.2 Bed I: Second Step Injection

The second step injection in Bed I began on July 5^{th} and lasted six weeks until August 16^{th}. Constant tracer-pesticide injection started on July 5^{th} at 5 pm and ran for an estimated 248 hours (taking the hours of pump failure into account) until 10 am on July 19^{th}. In total, 2222 L of tracer-pesticide mix were injected. However, the tracer-pesticide mix was not injected at the intended constant rate of 5.9 L/h because the original pump failed to

work on July 7^{th}. A replacement pump operating at 7.1 L/h was installed on July 10^{th}. The replacement pump rate was faster than the old pump, which meant that more tracer-pesticide mix had to be prepared. In order to keep the overall tracer-pesticide load the same, the tracer-pesticide mix was diluted. From June 19 th until August 16^{th}, the bed was flushed with clean site water. Due to recurrent pump malfunctioning, 1000 L of clean site water were pumped into Bed I from July 23^{rd} until July 26^{th}. A check valve was installed on July 26^{th} to prevent any more water from simply passing through the pump. The pump rate was then set to 6.9 L/h. One week later, on August 2^{nd}, the pump rate was down to 2.2 L/h. Only 400 L had been pumped into Bed I during July 26^{th} and August 2^{nd}. The same pattern repeated itself for the last two weeks of the flushing cycle.

4.2.1 Water Balance

The calculation of the water balance was complicated by several problems with the inlet pump, which failed to work reliably during the second step injection. Figure 4.6 shows the precipitation, reference evapotranspiration and outflow graph for the six week period. The most intense rainfall event during tracer application was measured on July 6^{th} at 8 pm with 0.07 mm/min lasting for ten minutes. The maximum precipitation rate for the entire six week period was logged on August 5^{th} with more than 0.4 mm/min lasting for five minutes. Table 4.3 summarizes the water balance parameters as well as weekly maximum events during second step injection. The extreme water level variation in Bed I caused by pump malfunctioning is illustrated in Figure 4.7. The water level volatility even masked the diurnal cycle caused by evapotranspiration, which could be detected during the first step injection (see Figure 4.2).

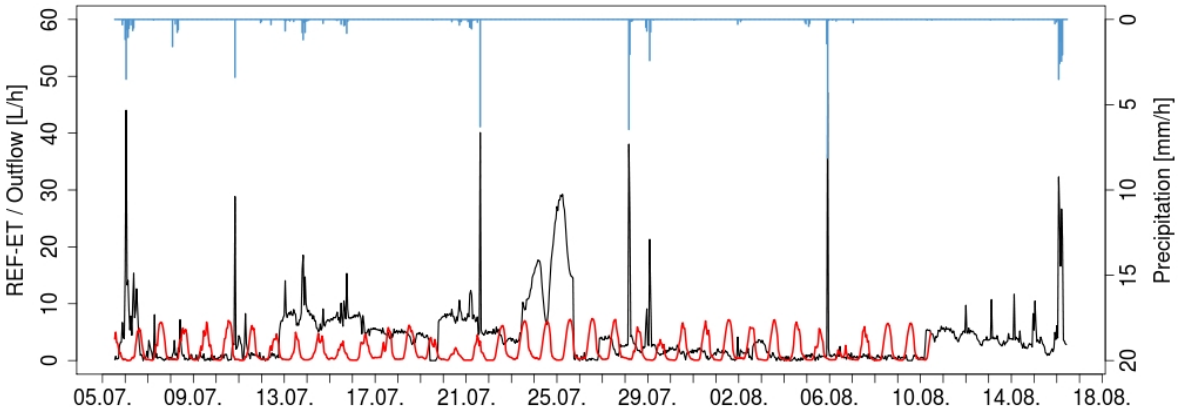

Figure 4.6: Bed I second step injection precipitation, outflow and reference evapotranspiration data.

Table 4.3: Weekly water balances and high intensity events for the second step injection in Bed I. Evapotranspiration values are based on reference evapotranspiration (ET_0). For the sake of easy comparison, all water balance components are presented in liters. Precipitation and ET_0 refer to the entire bed surface area.

	Tracer-Pesticide Injection		Flushing with clean site water			
	Week 1	Week 2	Week 3	Week 4	Week 5	Week 6
Inflow $[L]$	194	1014	1300	400	474	773
Precip. $[L]$	114	46	65	98	79	90
ET_0 $[L]$	327	283	309	354	312	-
Outflow $[L]$	387	1050	1495	402	187	721
Balance $[L]$	-406	-273	-439	-259	54	-
$Precip._{max}$ $[L/h]$	25 (1am 6.7.)	9 (8pm 13.7.)	29 (3pm 21.7.)	46 (4am 28.7.)	58 (10pm 5.8.)	25 (2am 16.8.)
$Outflow_{max}$ $[L/h]$	44 (1am 6.7.)	19 (8pm 13.7.)	38 (3pm 21.7.)	38 (4am 28.7.)	47 (10pm 5.8.)	32 (2am 16.8.)

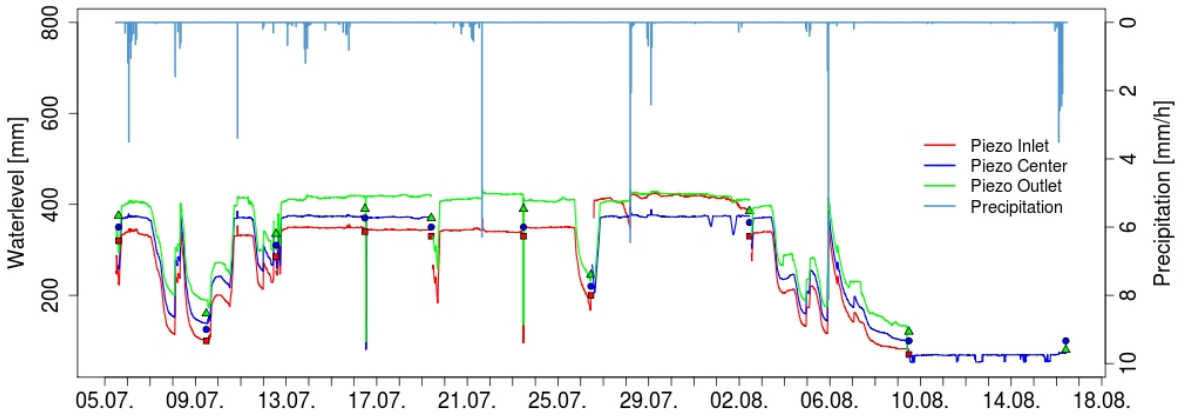

Figure 4.7: Bed I piezometer capacitative water level logger data. Individual data points represent the manual measurements taken every week using a measuring tape.

4.2.2 Tracer Breakthrough Curve and Recovery

The problems with the inflow pump introduced extreme variations in the injection rate and concentration during the second step injection. The replacement pump required a higher inflow rate, thus the second injection tank was filled with 1400 L of tracer-pesticide-mix at a lower concentration than the first tank, which was filled with 950 L of the mix. Figure 4.8

shows the effects this concentration switch had on the fluorescence tracer breakthrough curve. Some data was missing because of the inlet pump failure on July 7^{th}, which caused a complete outflow stop. Furthermore, no bromide data analysis could be performed due to malfunctioning of the IC and resulting time constraints. Tail-end concentrations of UR and SRB from the first step injection were still detected in Bed I outflow on July 5^{th}. Therefore, residual concentrations of 0.087 μg/L UR and 1.688 μg/L SRB were subtracted from all outflow tracer concentrations of the second step injection. The first tracer signals in the outflow were distinguished from background variation by taking the calculated standard deviation of the background fluctuation ($\sigma_{UR} = 0.053$ μg/L and $\sigma_{SRB} = 0.443$ μg/L) into account.

The first UR signal in the outflow was detected after 35 hours, followed by SRB after 134 hours. Table 4.4 contains relevant tracer recovery data for the second step injection. Uranine maximum flow velocity (v_{max}) did not differ much from v_{max} during first step injection, but SRB v_{max} was only one third of the velocity calculated for the first step injection. Uranine reached the average plateau concentration of 12 μg/L after 223 hours. SRB reached the average plateau concentration of 22 μg/L after 303 hours. Similar to the first step injection, the plateau and maximum measured concentrations never reached the injection concentration. The rising limb of the SRB breakthrough curve was delayed compared to UR (see Figure 4.8). Table 4.4 shows that the average flow velocity (v_{mean}) increased by 30% for UR and SRB as compared to the first step injection. Plateau concentration was maintained for one day by SRB and for more than four days by UR before flushing with clean site water began and the levels dropped. During the second step injection experiment, less SRB mass (85%) was recovered than UR (90%). The UR to SRB mass recovery ratio was 1.05. Figure 4.9 illustrates the tracer recovery for UR and SRB.

Table 4.4: Bed I second step injection recovery data: total mass injected (M_{inj}), time of first tracer detection in the outflow (t_1), maximum flow velocity (v_{max}), detection time of peak concentration (t_{peak}), peak concentration (C_{max}), time when 50% of the injected tracer has passed the outlet (t_{50}), mean flow velocity (v_{mean}), nominal residence time (t_N), hydraulic efficiency (λ), recovered tracer load (R_{Load}) and % recovery (R).

Tracer	M_{inj} [mg]	t_1 [h]	v_{max} [m/h]	t_{peak} [h]	C_{max} [mg/L]	t_{50} [h]	v_{mean} [m/h]	t_N [h]	λ	R_{Load} [mg]	R %
UR	18.56	35	0.118	289	0.013	271	0.015	137	2.17	16.64	90
SRB	37.75	134	0.031	351	0.023	319	0.013	137	2.56	32.09	85

$\sigma_{UR} = 0.17\mu$g/L, $\sigma_{SRB} = 0.67\mu$g/L

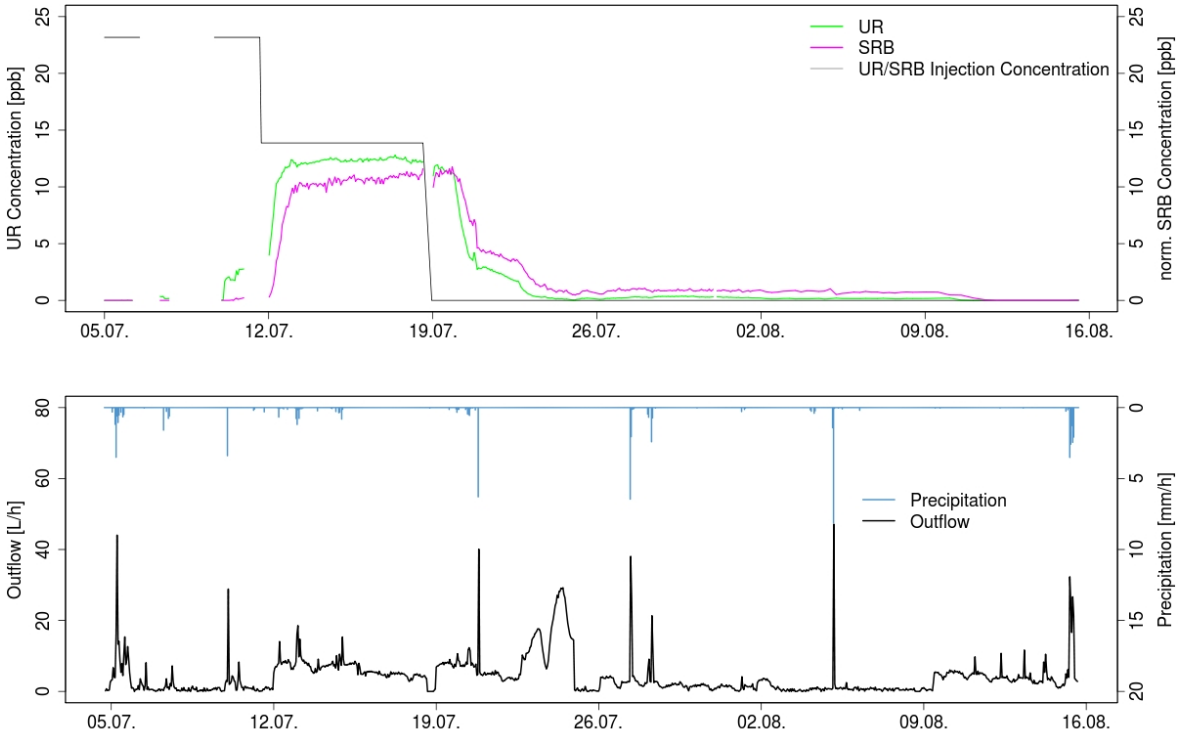

Figure 4.8: **Top:** Tracer breakthrough curves for the second step injection in Bed I. SRB concentration is normalized to UR concentration (SRB/UR = 1.99). Total tracer-pesticide-mix injection volume was 1208 L (194 L at UR = 23.17 ppb and SRB = 43.89 ppb followed by 1014 L at UR = 13.87 ppb and SRB = 28.83 ppb). **Bottom:** Precipitation and outflow time series.

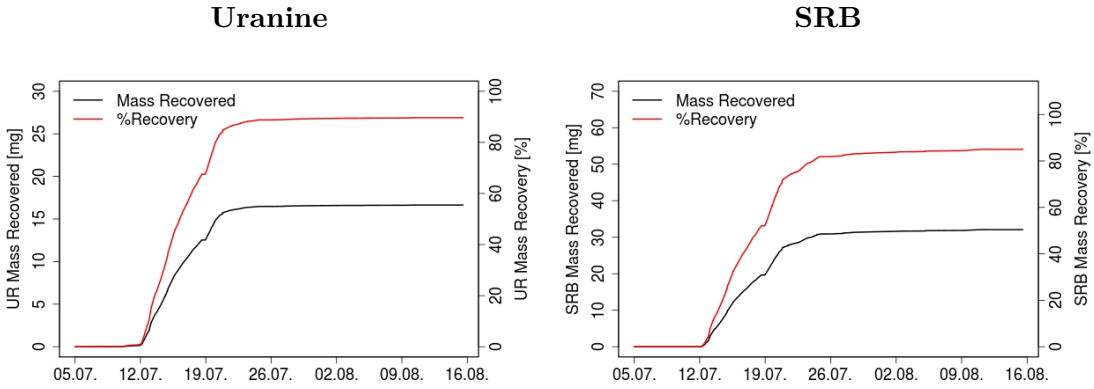

Figure 4.9: Fluorescence tracer recovery for the second step injection in Bed I.

Tracer and Metolachlor Concentration in the Piezometers Similar to the first step injection, the tracer concentration in the inlet piezometer samples was higher than the concentration measured in the center and outlet piezometer samples, and furthermore this differential was greater for SRB than for UR. Figure 4.10 presents the variation of tracer and

metolachlor concentration measured in the piezometer samples over time. After the first week of tracer injection, the concentration difference between the inlet and outlet piezometer samples was 12 μg/L for SRB and for UR 10 μg/L. Because of the low pump rate, this difference in concentration was more pronounced than during the first step injection (compare Figure 4.5). The UR piezometer peak concentration of 15 μg/L was measured on July 9^{th} and the SRB piezometer peak concentration of 31 μg/L was measured on July 12^{th}. Both peak concentrations were detected in the inlet piezometer, and they exceeded the peak concentration measured in the outflow samples (see Table 4.4). By the end of the two week tracer injection period, the tracer concentrations in the three piezometers had converged to nearly the same concentration, as was already observed during first step injection. When flushing with clean site water began, the decrease in piezometer tracer concentration was first detected in the inlet piezometer. One week after flushing, all piezometer tracer concentrations had almost converged, with SRB showing a slight delay.

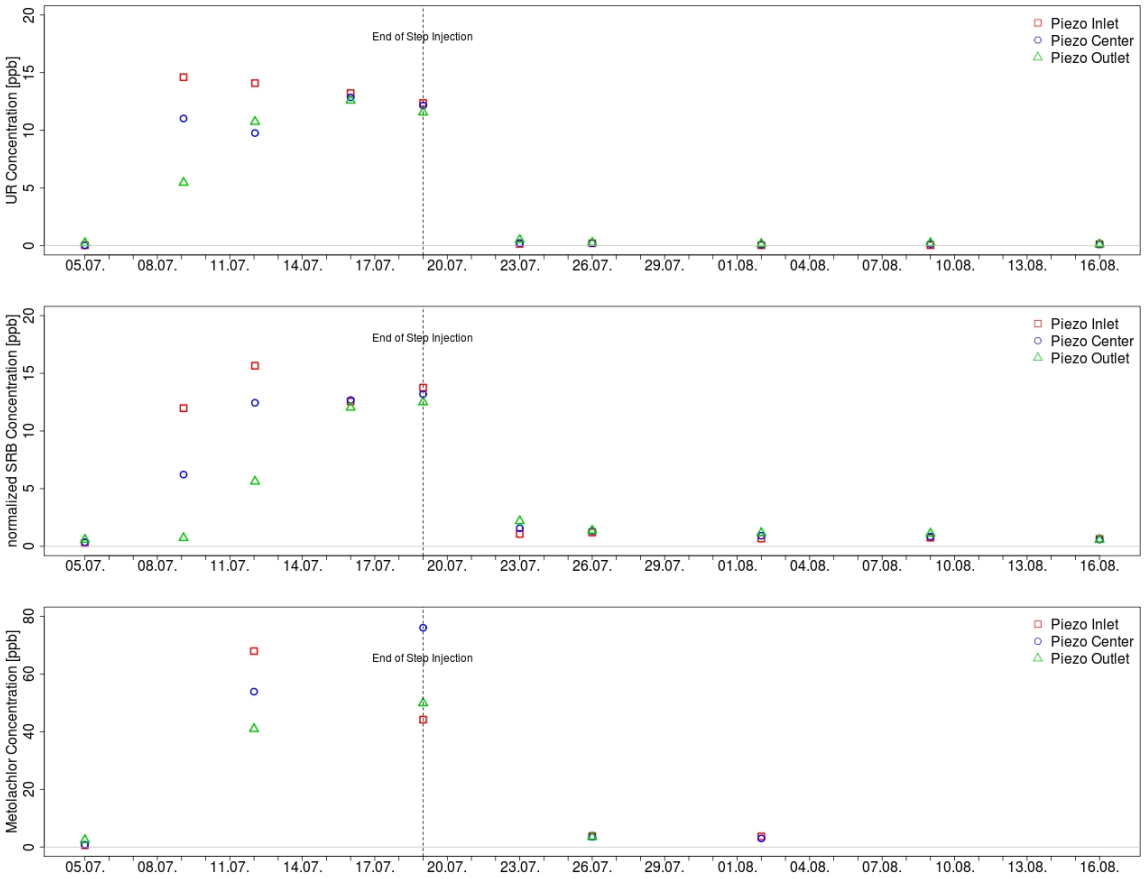

Figure 4.10: Uranine (top), SRB (center) and metolachlor (bottom) concentrations measured in water samples taken weekly from each piezometer in Bed I during the second step injection. SRB is normalized to UR.

The metolachlor piezometer concentrations still varied after two weeks of constant tracer-pesticide injection and did not converge like the FT tracers. During the first week of the step injection, the inlet piezometer had the highest metolachlor concentration, followed by the center and outlet piezometer. But two weeks later, on July 12^{th}, the maximum piezometer metolachlor concentration of 76 μg/L was measured in the center piezometer. It exceeded the concentration measured in the other two piezometers by more than 20 μg/L. After the first week of flushing with clean site water, the metolachlor concentration in the three piezometers had converged to approximately 3.5 μg/L. A table containing all tracer and pesticide piezometer concentrations measured in Bed I can be found in the Appendix (see Table A.1).

4.3 Bed I Metolachlor Recovery

The metolachlor mass recovery did not differ greatly between first and second step injection experiments. Nearly 60% of the injected mass was recovered. In both cases, the metolachlor outflow concentration measured never reached injection concentration levels. Tail-end metolachlor concentration for the first step injection experiment was 1.1 μg/L. The tail-end concentration for the second step injection experiment was not available yet. Analysis effort and expenditure limited metolachlor sampling frequency to weekly sampling campaigns, thus no time series of metolachlor recovery in the outflow were available. The sampling and laboratory analysis were done by the French group. Table 4.5 shows the results of metolachlor recovery for the first and second step injection.

Table 4.5: Metolachlor recovery data for the first and second step injection in Bed I: injection concentration (C_{inj}), total injection mass (M_{inj}), peak outflow concentration (C_{max}), final outflow concentration (C_{final}), recovered load (R_{Load}) and % recovery (R).

Step Injection	$\mathbf{C}_{inj}$ [μg/L]	$\mathbf{M}_{inj}$ [mg]	$\mathbf{C}_{max}$ [μg/L]	$\mathbf{C}_{final}$ [μg/L]	$\mathbf{R}_{Load}$ [mg]	**R** %
1	176.55	259.77	140.97	1.11	155.69	59.93
2	91.65/77.62*	96.49	40.83	-	56.36	58.41

*concentration from first/ and second injection tank

4.4 Bed I: CXTFIT Modeling

4.4.1 Bromide

The breakthrough curve for the BR step injection was modeled assuming macroscopic steady state water flow, constant soil-moisture content, and no interactions between the conservative tracer and the soil matrix (Toride et al., 1995). Thus, applying the equilibrium convection-dispersion equation (CDE) in CXTFIT was permissible. There were four parameters that needed to be entered either as a fixed value, or as value to be fitted, namely: pore water velocity (v), the hydrodynamic dispersion coefficient (D), the retardation factor (Rd) and the first order degradation coefficient (μ). Because BR is a conservative tracer, Rd was fixed at 1, which assumes no interactions between solute and soil. The remaining hydraulic parameters v and D were calculated by CXTFIT by iteratively approximating the solution to the equilibrium CDE. Table 4.6 shows the results of this approximation. Model quality and breakthrough curve plateau simulation were improved when μ was also fitted, which is evidenced by Figure 4.11. Implementing a fitted μ was adequate, taking the observed BR recovery losses into account. However, despite satisfactory modeling of the plateau, the observed breakthrough curve peak shape and the tailing were never reproduced by the model (see Figure 4.11). The resulting values for v and D were treated as specific to the system and were subsequently used to model UR and SRB breakthrough curves as well as hydraulic parameters.

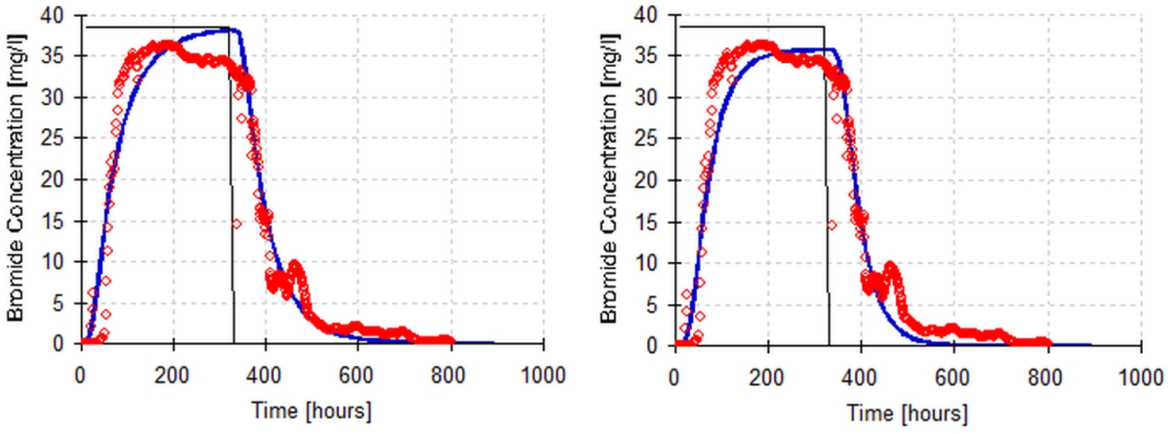

Figure 4.11: CXTFIT results for equilibrium CDE application. Before fitting μ (left) and after fitting μ (right). The step injection concentration and duration is represented by the black line. Red dots correspond to the observed bromide breakthrough curve and the blue line represents the modeled curve.

Table 4.6: CXTFIT modeling results for specific hydraulic parameters to the bromide breakthrough curve from the first step injection in Bed I. Model quality was estimated based on R^2 values and mean square error (MSE).

Model	v [m/h]	**D** [m^2/h]	**Rd** [-]	μ [h^{-1}]	R^2	**MSE**
Equ. CDE	$6.47 \cdot 10^{-2}$	$7.41 \cdot 10^{-2}$	1*	0*	0.965	7.802
Equ. CDE	$7.04 \cdot 10^{-2}$	$3.69 \cdot 10^{-2}$	1*	$1.15 \cdot 10^{-3}$	0.972	6.120

*fixed value for model analysis

4.4.2 Uranine

The equilibrium CDE application for UR breakthrough curve modeling did not produce any adequate breakthrough curve simulation. Thus, the two-site non-equilibrium CDE was implemented. This model included additional parameters like the mobile-immobile phase partitioning coefficients β and ω, which describe the mass transfer between those two phases. Furthermore, μ_1 and μ_2 are mobile and immobile phase degradation coefficients, respectively. The model yielded the best fit ($R^2 = 0.99$) when Rd, β, ω and μ_1 were fitted. Figure 4.12 (left) shows that the UR breakthrough curve was simulated adequately, though plateau and tailing concentrations were globally underestimated by the model.

Table 4.7: CXTFIT modeling results for a step-wise fitting of specific hydraulic parameters to the UR breakthrough curve from the first step injection in Bed I. The input parameters pore water velocity ($v = 7.04 \cdot 10^{-2}$ m/h) and dispersion coefficient ($D = 3.69 \cdot 10^{-2}$ m^2/h) were taken from BR modeling results (Table 4.6). Model quality was estimated based on R^2 values and mean square error (MSE).

Model	**Rd** [-]	β [-]	ω [-]	μ_1 [h^{-1}]	μ_2 [h^{-1}]	R^2	**MSE**
Non-Equ. CDE	1*	$2.98 \cdot 10^{-1}$	$2.11 \cdot 10^{-2}$	0*	0*	0.964	1.997
Non-Equ. CDE	1*	$3.16 \cdot 10^{-1}$	$1.09 \cdot 10^{-2}$	$1.12 \cdot 10^{-2}$	0*	0.987	0.721
Non-Equ. CDE	0.39	$7.77 \cdot 10^{-1}$	$1.31 \cdot 10^{-2}$	$1.70 \cdot 10^{-2}$	0*	0.990	0.531

*fixed value for model analysis

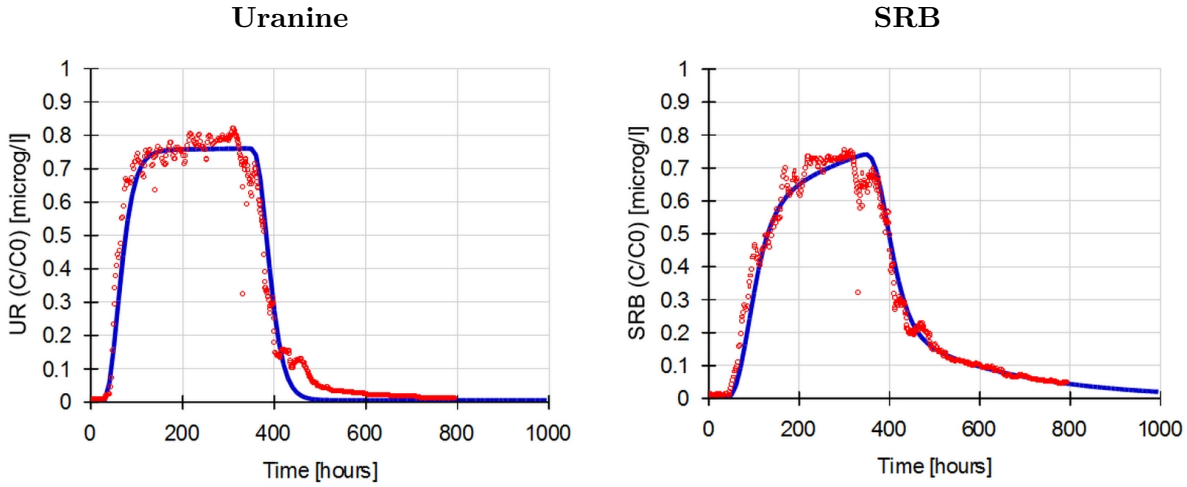

Figure 4.12: CXTFIT results for non-equilibrium CDE application for UR and SRB. Red dots correspond to the observed tracer breakthrough curve and the blue line represents the modeled curve.

4.4.3 Sulphorhodamine B

In the case of modeling the SRB breakthrough curve for the first Bed I step injection experiment, the two-site non-equilibrium CDE gave the best results in terms of tracer transport simulation as well as model quality. Table 4.8 summarizes the values for the fitted transport parameters and the model quality. Again, optimum modeling results were achieved when Rd, β, ω and μ_1 were fitted. In contrast to UR, the fitted Rd for SRB was greater than 1. Additionally, a higher μ_1 value was modeled for SRB than for UR transport. The general concentration distribution of the SRB breakthrough curve is asymmetrical (see Figure 4.12). The tail of the modeled and observed breakthrough curve diverged from the x-axis. Overall, the modeled shape of the breakthrough curve was in accordance with the peak and tail shape of the observed data.

Table 4.8: CXTFIT modeling results for a step-wise fitting of specific hydraulic parameters to the SRB breakthrough curve from the first step injection in Bed I. The input parameters pore water velocity ($v = 7.04{\cdot}10^{-2}$ m/h) and dispersion coefficient (D = $3.69{\cdot}10^{-2}$ m^2/h) were taken from BR modeling results (Table 4.6). Model quality was estimated based on R^2 values and mean square error (MSE).

Model	**Rd** [-]	$\boldsymbol{\beta}$ [-]	$\boldsymbol{\omega}$ [-]	$\boldsymbol{\mu_1}$ [h^{-1}]	$\boldsymbol{\mu_2}$ [h^{-1}]	$\mathbf{R^2}$	**MSE**
Non-Equ. CDE	1*	$1.05{\cdot}10^{-1}$	$2.76{\cdot}10^{-2}$	$5.98{\cdot}10^{-2}$	0*	0.675	54.980
Non-Equ. CDE	2.92	$5.79{\cdot}10^{-1}$	$6.33{\cdot}10^{-2}$	$3.32{\cdot}10^{-2}$	0*	0.986	2.403

*fixed value for model analysis

4.5 Bed II: Intermittent Flow - Continuous Contamination

The target tracer-pesticide-mix volume of 600 L was only applied during batch one, and injection volumes for all following batches were lower than the target amount, as residual water from previous drains and precipitation had saturated the bed. Nevertheless, the same tracer-pesticide load was injected into Bed II for each batch, and the injection concentrations varied accordingly (see Table 4.10). In particular, only 100 L of injection mix were applied during batches two and three. The week after the third drain had low precipitation, so 350 L of injection solution was used for batch four. On all occasions, excess injection mix pooled up near the outlet area of Bed II.

4.5.1 Water Balance

The water balances listed in Table 4.9 were mostly negative due to overestimation of evapotranspiration (ET). The determination of the correct injection volume to avoid excess tracer-pesticide-mix pooling at the surface of the bed was difficult. Before injection, the water level in the piezometers was measured and the residual water volume in the bed was estimated using Equation 3.1. The water content of the bed varied greatly depending on the precipitation input during batch pauses, which resulted in inconsistent batch injection volumes. Despite the careful assessment of the projected injection volume, excess injection mix pooled up in the bed. Especially after the second and third application it was observed that excess injection mix pooled near the outlet zone.

There were also uncertainties about the outflow quantification that affected water balance calculations. First of all, Bed II was never completely drained. At the end of each draining, a slow outflow rate was observed. Because of time constraints and parallel operation of continuous injection in Bed I, the draining was stopped by plugging the Bed II outlet. Thus, any additional outflow was trapped inside the bed and potentially concentrated near the outlet because of the slanted bed bottom. Secondly, the logging interval of the pressure probe was set to minute measurements during the first, second and third draining. This logging interval was too coarse, especially during the initial draining phase where the outflow rate was approximately 10 L/h. Before the fourth draining, the logging interval was set to 10 seconds, which enabled better outflow quantification. The ramifications of the logger settings are discussed in Section 5.2.1.3. Table 4.9 summarizes the water balance parameters for the Bed II batch experiments.

Table 4.9: Water balance for each batch experiment in Bed II. W_{Piezo} is the average piezometer water level before injection, V_{Res} is the calculated residual water volume in the bed before injection, V_{In} is the injected volume and V_{Out} is the volume drained from the bed.

	1^{st} Batch	**Pause**	**2^{nd} Batch**	**Pause**	**3^{rd} Batch**	**Pause**	**4^{th} Batch**
	24.5-7.6	7.6-14.6	14.6-28.6	28.6-5.7	5.7-19.7	19.7-26.7	26.7-9.8
W_{Piezo} $[m]$	-	-	0.26	-	0.23	-	0.07
V_{Res}* $[L]$	-	-	304	-	270	-	80
V_{In} $[L]$	600	-	110	-	105	-	350
Precip. $[L]$	46	273	95	283	160	64	176
ET_0 $[L]$	616	236	672	279	610	309	666
V_{Out} $[L]$	175	-	164	-	195	-	248
Balance	-145	37	-327	4	-270	-245	-308

Piezometer Water Level The water level dynamics in the Bed II piezometers illustrated by Figure 4.13 result from the influence of ET and precipitation. Piezometer data from the first batch operation is missing due to logger failure. The response of the piezometer water level to precipitation events varied greatly depending on the preceding state of saturation of the soil. After some periods of sustained dryness, the water level barely responded to a rainfall event (for instance on July 21^{st}). This contrasts with the dramatic increase in water level in response to the rainfall on July 1^{st}, which is attributable to the difference in magnitude of precipitation. In particular, during the July 21^{st} event, 9 mm of rain fell, whereas during the July 1^{st} event 37 mm of rain fell over the course of two days. Similarly, the water level response to rainfall when the bed was fully saturated was also minimal, approaching a one-to-one increase with respect to the amount of precipitation. This manifested as subtle bumps on the plateaus seen in Figure 4.13. Piezometer readouts were the most dynamic when the water level indicated moderate saturation. During such times, even small precipitation amounts resulted in quick and dramatic water level increases. This behavior can be seen in Figure 4.13 on June 25^{th} and on August 5^{th}.

The dynamics of water level decreases, presumably occurring due to ET, displayed the same behavior described above. In general, water level fluctuations due to ET were not noticeable during times of full saturation. However, water level drops below a certain threshold (≈40 cm in the inlet piezometer) were always followed by dramatic declines. Naturally, when the water level had bottomed out, effects of ET were no longer detected by the piezometers loggers.

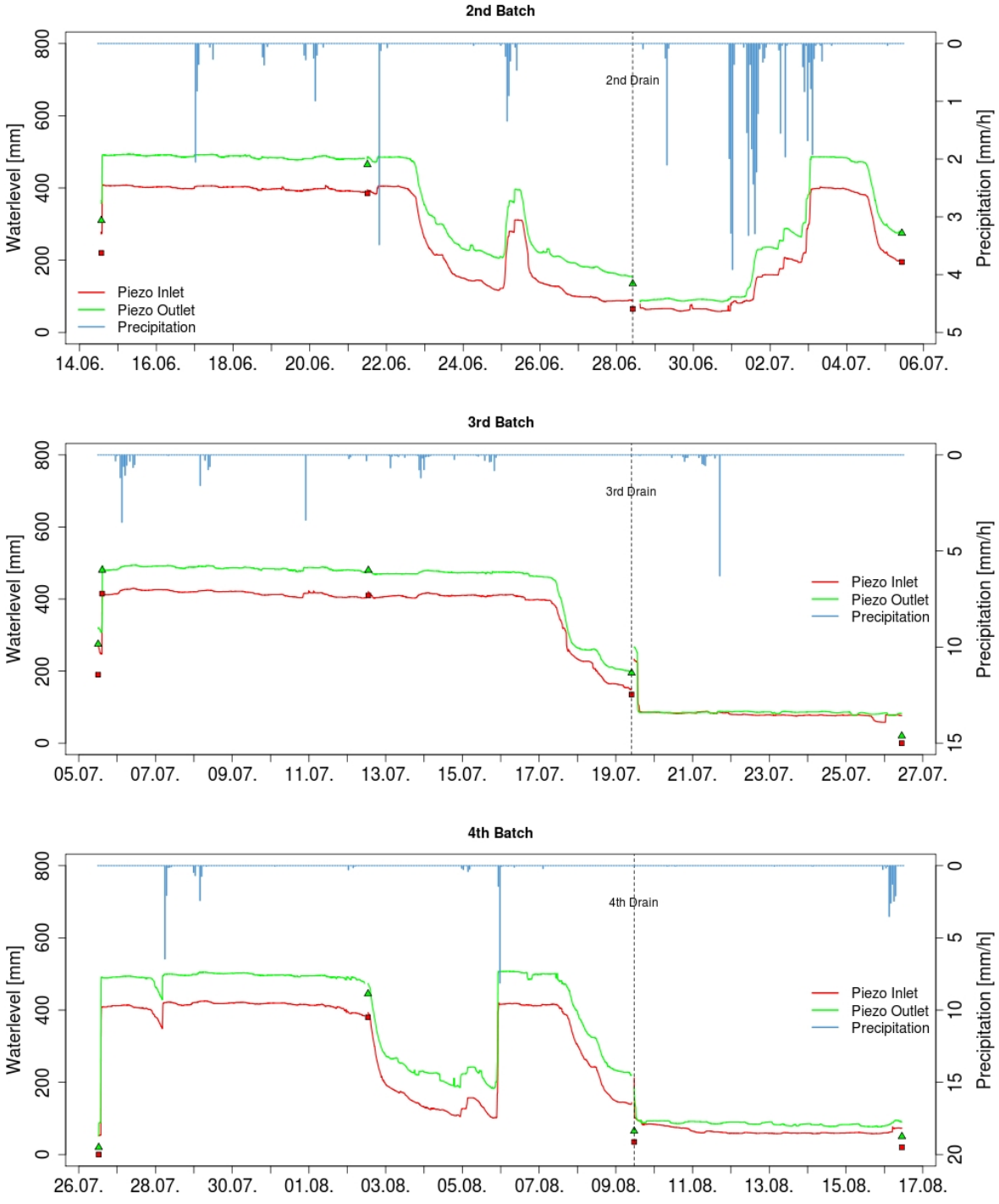

Figure 4.13: Fluctuation of the piezometer water level in Bed II for the 2^{nd}, 3^{rd} and 4^{th} batch operation. Manually measured water level data is added (red square = inlet piezometer, green triangle = outlet piezometer). The inlet-outlet water level differential reflects piezometer placement depths.

4.5.2 Tracer and Metolachlor Concentration in the Piezometers

The tracer concentration dynamics resulting from the varying batch injection concentrations were apparent in the weekly piezometer water samples. Each injected tracer showed a different concentration pattern. Figure 4.15 illustrates the fluctuation of tracers and pesticide concentration over time. The UR inlet piezometer concentration was initially lower than the outlet piezometer concentration, but concentrations converged during the second and third batch. After the fourth batch injection, the UR inlet piezometer concentration exceeded the outlet piezometer concentration by a factor of five. The SRB concentrations measured in the inlet and outlet piezometers were nearly the same during the first batch. After the second batch application at very high injection concentration, the SRB outlet piezometer concentration exceeded the concentration measured in the inlet piezometer by a factor of four. During the third and fourth batch applications, the SRB piezometer concentrations converged again. Bromide piezometer samples were not analyzed due to laboratory equipment failure. The metolachlor piezometer concentration showed a response to the batch treatments that was similar to SRB. Tables containing all tracer and pesticide piezometer concentrations and the waterlevel measured in Bed II can be found in the Appendix (see Tables A.2 and A.5). On July 26^{th} no samples were taken due to insufficient water level in the piezometers.

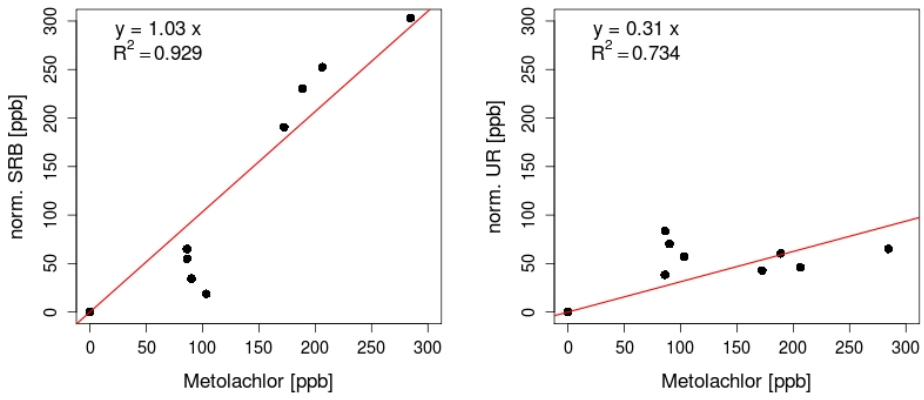

Figure 4.14: Linear regression for SRB (left) and UR (right) concentrations with metolachlor concentrations from Bed II piezometer samples. SRB and UR concentrations were normalized to metolachlor and averaged from weekly inlet and outlet piezometer samples in Bed II. Metolachlor samples were taken weekly as pooled samples from all three piezometers.

Uranine and SRB inlet and outlet piezometer concentrations for each sampling event were averaged and plotted against the pooled metolachlor concentration. The linear correlation

revealed an R^2 value of 0.93 for SRB and metolachlor (see Figure 4.14). At low concentrations the fit between SRB and metolachlor is weaker than at higher concentrations. In particular, at low metolachlor concentrations the SRB concentration appears to be underrepresented, which is indicated by the cluster of points below the fitted line in Figure 4.14 (left). The data correlated especially well at higher concentrations. The linear correlation between UR and metolachlor was poor with an R^2 value of 0.73.

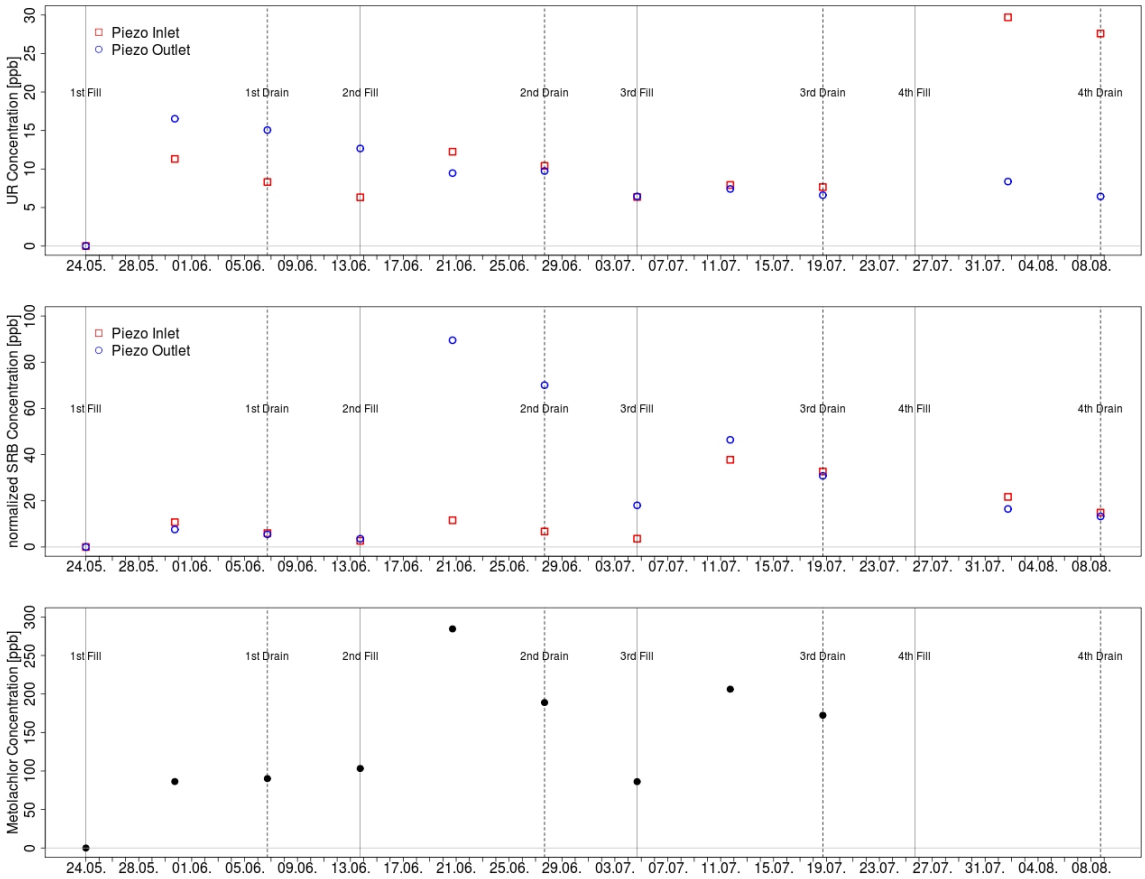

Figure 4.15: Uranine (top), SRB (center) and metolachlor (bottom) concentrations from the Bed II piezometers. Metolachlor samples were taken as pooled samples from all three piezometers. SRB concentrations were normalized to UR. Samples were always taken before filling and draining of Bed II.

4.5.3 Draining Dynamics

The fluorometry samples taken during draining events reflect varying batch injection concentrations and potentially even effects of residual batch tracer accumulation, and the different signatures of the gravel and sand filters. The upper graphs of Figures 4.16, 4.17 and 4.18 show the fluorescence tracer concentrations measured manually and those measured by the

field fluorometer during each draining. Bromide results from manual samples are only available for the third and fourth draining. The lower graphs of Figures 4.16, 4.17 and 4.18 show the outflow dynamics and the turbidity measured by the field fluorometer. Draining Bed II after each batch operation took on average two hours. During the first five minutes of draining, the maximum outflow rate was approximately 10 L/min. For the last ninety minutes of draining the outflow rate never exceeded 0.5 L/min. Bed II was never completely drained to the point where no more outflow was observed. Consequently, old water from the previous batch containing tracers and pesticides still resided within the Bed II matrix.

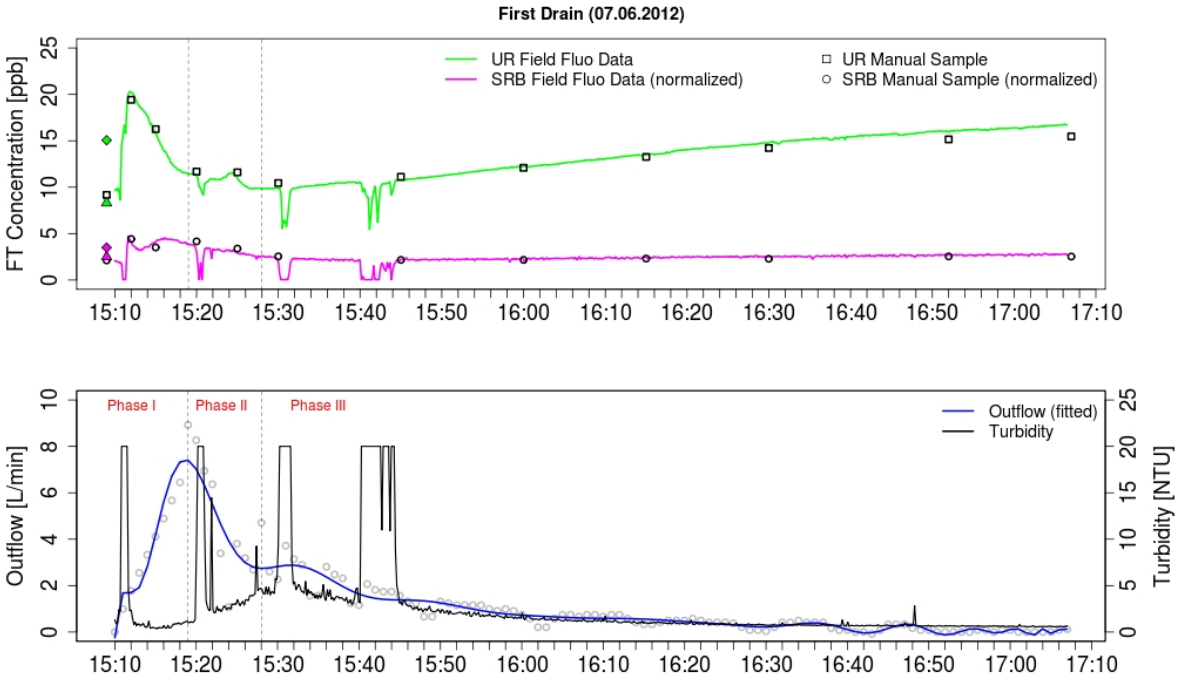

Figure 4.16: First draining of Bed II. The first manual samples were taken before draining from the outlet T-pipe. The inlet (triangle) and outlet (diamond) piezometer tracer concentrations before draining are added (UR = green and SRB = magenta). SRB concentrations were normalized to UR concentrations. Turbidity spikes were due to manipulations during manual sampling, thus data greater than 20 NTU was omitted from the plot. The three phases marked in the outflow-turbidity plot roughly correspond to the draining of the immediate outlet zone, the gravel filter and the sand filter, respectively.

In general, the concentration of each fluorescence tracer exhibited a unique dynamic during draining. Uranine concentration demonstrated a short-lived spike within the first few minutes of draining corresponding to a spike in turbidity. At the tail-end of the first and fourth draining, UR concentration showed a gradual increase, whereas on the second and third draining the tail-end concentration stabilized near a constant value.

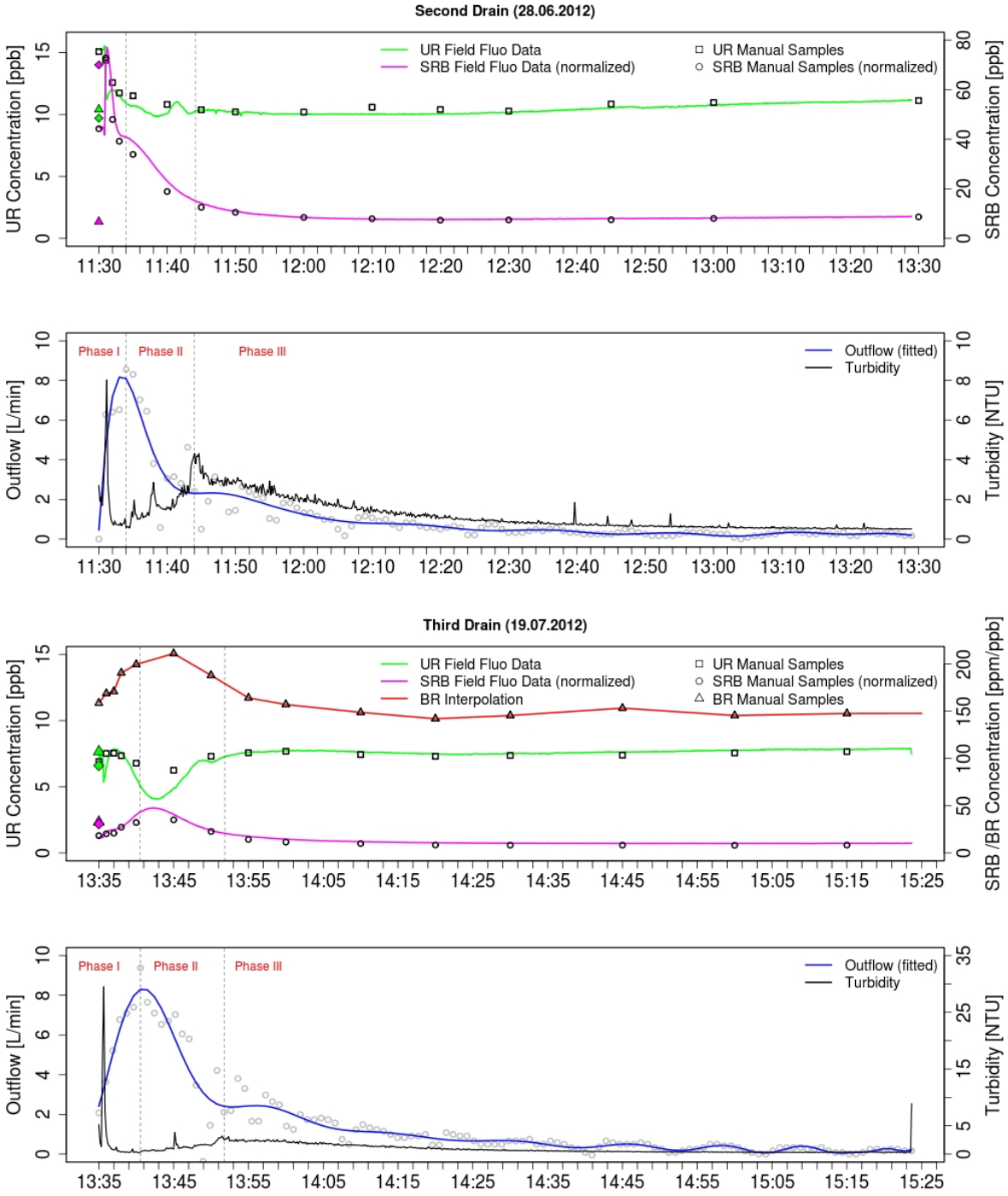

Figure 4.17: Second and third draining of Bed II. The first manual samples were taken before draining from the outlet T-pipe. The inlet (triangle) and outlet (diamond) piezometer tracer concentrations before draining are added (UR = green and SRB = magenta). SRB concentrations were normalized to UR concentrations. The three phases marked in the outflow-turbidity plot roughly correspond to the draining of the immediate outlet zone, the gravel filter and the sand filter, respectively.

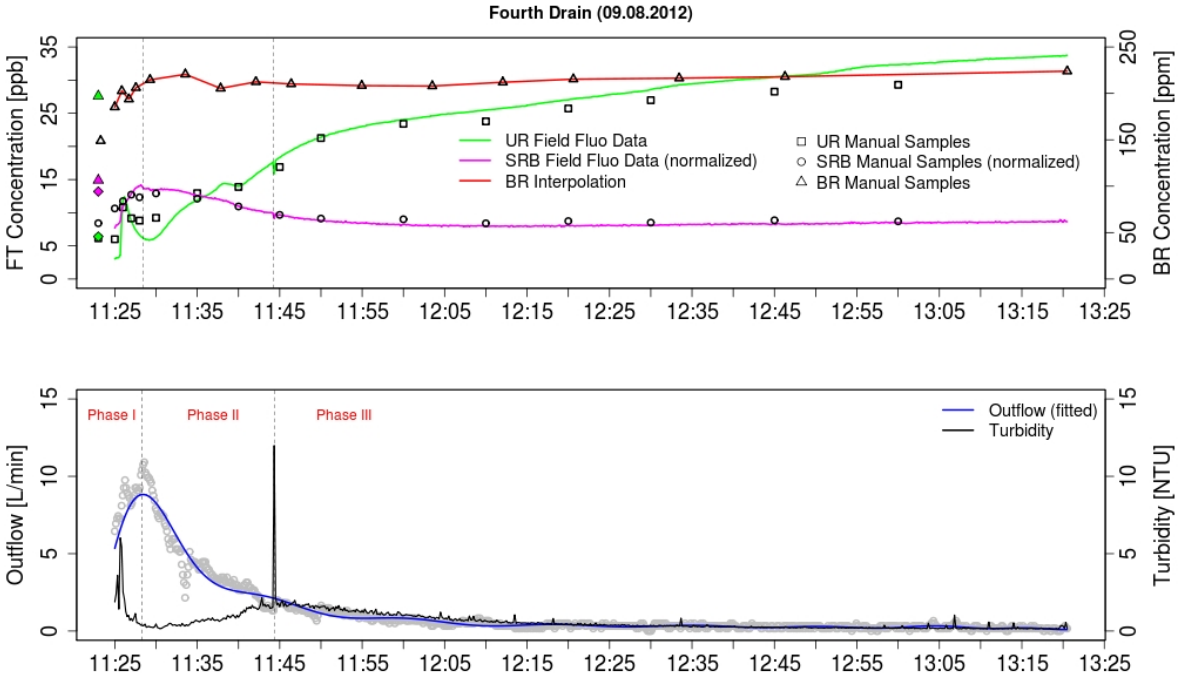

Figure 4.18: Fourth draining of Bed II. The first manual samples were taken before draining from the outlet T-pipe. The inlet (triangle) and outlet (diamond) piezometer tracer concentrations before draining are added (UR = green and SRB = magenta). SRB concentrations were normalized to UR concentrations. The three phases marked in the outflow-turbidity plot roughly correspond to the draining of the immediate outlet zone, the gravel filter and the sand filter, respectively.

Sulphorhodamine B showed a broad concentration spike at the beginning of draining, corresponding to a period of high outflow and low turbidity. The tail-end SRB concentration was always essentially constant. Bromide concentration from the third and fourth draining displayed a broad peak coinciding with the SRB spike, but this was subtle on the fourth draining, and the end-behavior was constant.

4.5.4 Batch Tracer and Metolachlor Recovery

The tracer mass recovered after each Bed II draining was in general low compared to the recovery from the continuous injection bed. The SRB load recovered increased from 1% of the first application to 7% of the third application. The UR recovery data was more ambiguous. Approximately 3% of the UR injection mass were recovered after batch one, two and three. After batch four, more than 5% of the UR injection mass were recovered. The metolachlor mass recovery after each batch draining was also low. Less than 6% of the initially injected metolachlor mass were recovered. Bromide had the highest mass recovery with approximately 50% (data was only available from the last two batches). Table 4.10 lists the recovered tracer

and pesticide mass after each batch experiment in Bed II. It is important to note that after each draining residual tracer and pesticide remained in Bed II. This residual concentration could not be quantified in the successive recoveries and may artificially increase the recovery data.

Table 4.10: Bed II batch tracer and pesticide recovery data: injected mass (M_{inj}), injection concentration (C_{Inj}), concentration measured before draining in the inlet and outlet piezometer (C_{P-In} and C_{P-Out}), maximum tracer concentration measured during draining (C_{max}), final concentration measured during draining (C_{final}), recovered load (R_{Load}) and % recovery (R). Listed values are based on concentrations measured in the manual samples.

Batch	**Chemical**	$\boldsymbol{M_{Inj}}$ [mg]	$\boldsymbol{C_{Inj}}$ $[\mu g/L]$	$\boldsymbol{C_{P-In}}$ $[\mu g/L]$	$\boldsymbol{C_{P-Out}}$ $[\mu g/L]$	$\boldsymbol{C_{max}}$ $[\mu g/L]$	$\boldsymbol{C_{final}}$ $[\mu g/L]$	$\mathbf{R}_{Load}$ $[mg]$	**R** [%]
1	UR	50	83.4	8.3	15.1	19.4	15.5	1.9	3.7
	SRB	100	166.7	11.9	10.9	8.8	5.1	0.9	0.9
	MC	300	-	-	-	-	-	16.6	5.5
2	UR	50	500	10.4	9.7	15.1	11.1	1.5	2.9
	SRB	100	1000	13.4	140.1	145.6	17.9	5.6	5.6
	MC	300	-	-	-	-	-	19.2	6.4
3	UR	50	500	7.7	6.6	7.7	7.6	1.2	2.4
	SRB	100	1000	65.4	61.6	70.0	16.6	7.1	7.1
	MC	300	-	-	-	-	-	13.6	4.3
	BR	62 g	620.6*	203.9*	199.9*	210.9*	147.7*	29.9 g	47.9
4	UR	50	166.7	27.6	6.4	32.1	32.1	2.7	5.4
	SRB	100	333.4	29.8	26.4	25.8	18.6	3.8	3.8
	MC	300	-	-	-	-	-	-	-
	BR	68 g	226.3*	233.3*	203.2*	223.8*	223.8*	36.7 g	54.1

*Bromide concentration in mg/L

4.6 Bed III: Intermittent Flow - Intermittent Contamination

4.6.1 Batch Operation Adjustments

The results of Bed III treatment were compromised due to an improperly sealed bed, which was discovered on June 7^{th} when the bed appeared to be very dry in comparison to Bed II. Upon draining Bed III on June 7^{th}, only 37 L of total outflow were measured compared to 164 L in Bed II. As such, a modified batch treatment was used in order to prevent the contamination of the surrounding soil. In particular, only clean site water was injected during all subsequent batch operations instead of alternating between injection of contaminated and clean water. Bed III was still drained according to the experimental schedule and the outflow water was sampled manually and via the field fluorometer. On all draining occasions the outflow from Bed III was at least 100 L less than from Bed II. Water balance and tracer recovery were not calculated due to the leaking and the resulting uncertainty about the quantity of water residing in Bed III. Manual samples from the piezometers and the draining were still taken and analyzed for UR and SRB, but not for BR, again due to laboratory equipment failure and time constraints. Total outflow and fluorescence tracer data as well as metolachlor results can be found in the Appendix (see Table A.3 and Table A.4).

4.6.2 Tracer and Metolachlor Piezometer Concentrations

The fluorescence tracer and pesticide results from Bed III piezometer samples are illustrated in Figure 4.19. On June 7^{th} and July 26^{th} no samples were taken due to insufficient water level in the piezometers. Uranine concentrations measured in the inlet piezometer were mostly lower than or equal to the outlet piezometer concentrations. After each injection of clean site water, the UR concentration decreased compared to the previous measurement, and by the end of the experiment the UR concentration was 0.16 μg/L. The SRB outlet piezometer concentrations were initially higher than the piezometer inlet concentration, but after June 14^{th}, the piezometer inlet concentration was always slightly higher. Overall, the tail-end SRB piezometer concentrations did not fluctuate and remained near 10 μg/L even ten weeks after tracer injection. Metolachlor behaved similar to SRB and UR.

The linear regression analysis of the averaged UR and SRB inlet and outlet piezometer concentrations with the pooled metolachlor piezometer concentration resulted in R^2 values of 0.94 for SRB and metolachlor, and 0.89 for UR and metolachlor (see Figure 4.20).

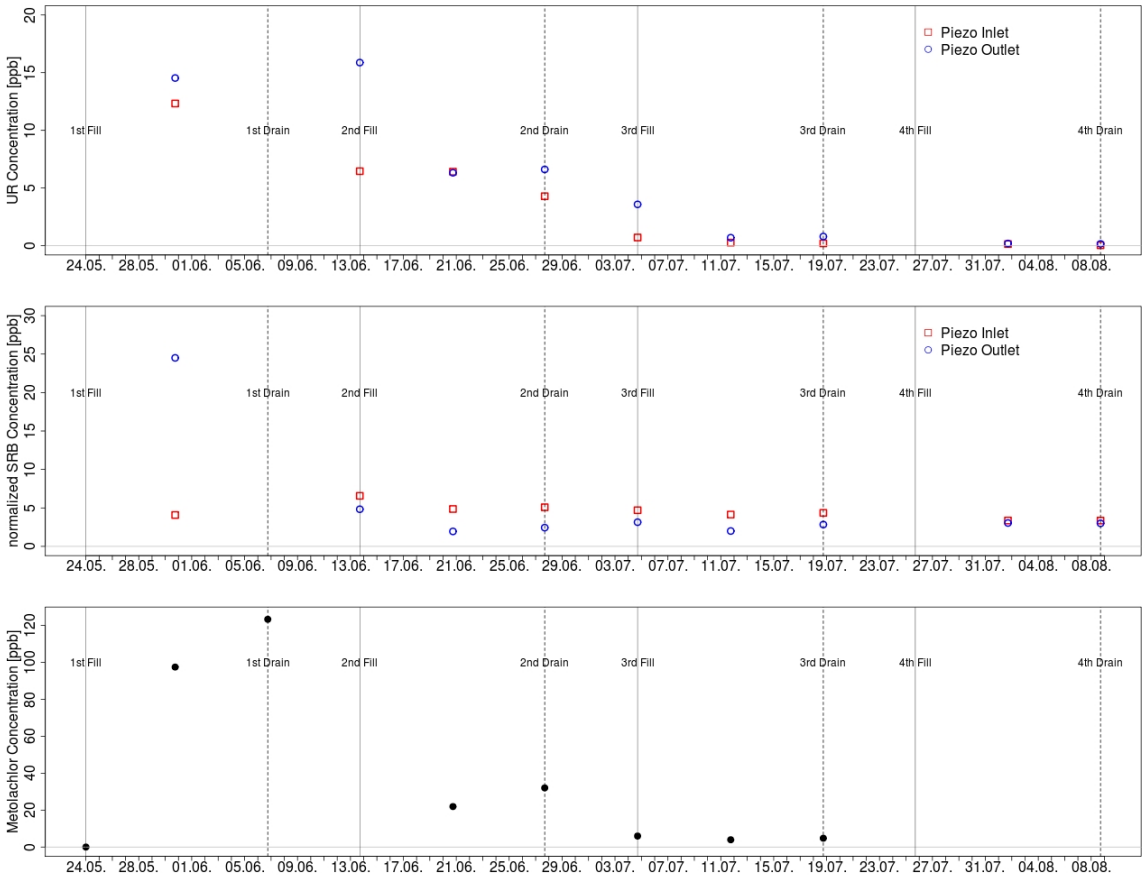

Figure 4.19: Uranine (top), SRB (center) and metolachlor (bottom) concentrations from the Bed III piezometers. Metolachlor samples were taken as pooled samples from all three piezometers. SRB concentrations were normalized to UR. Samples were always taken before filling and draining of Bed III.

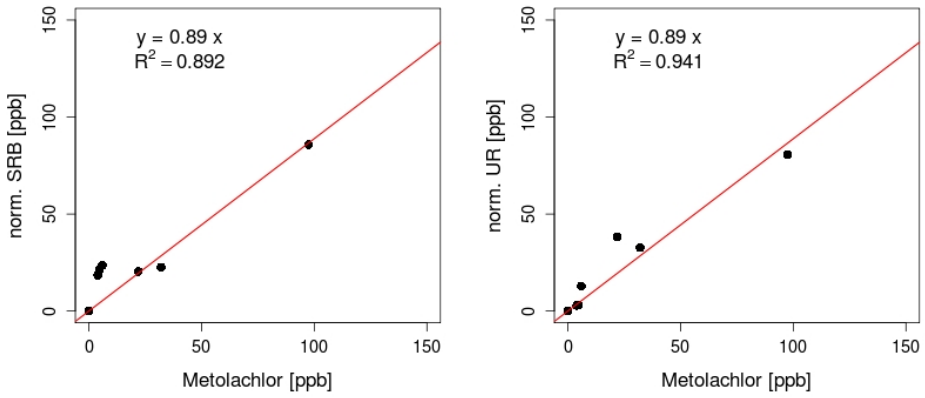

Figure 4.20: Linear regression for SRB (left) and UR (right) concentrations with metolachlor from Bed III piezometer samples. SRB and UR concentrations were normalized to metolachlor and averaged from weekly inlet and outlet piezometer samples in Bed II.

4.7 Vegetation

Plant development in Bed I and Bed II differed significantly. The paired Student's T-Test revealed that the mean plant height in Bed I was significantly greater than the mean plant height in Bed II at a significance level of 0.5 (p-value = 0.004). Figure 4.21 illustrates the evolution of vegetation density and height over time. Additionally, Figure 4.22 shows photographs of the vegetation development and cover in each bed.

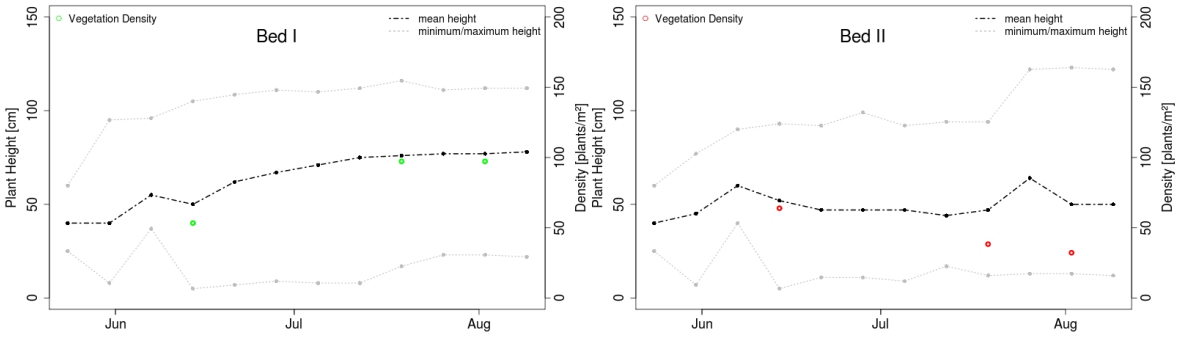

Figure 4.21: Bed I (left) and Bed II (right) plant development throughout the experiment assessed by plant height (minimum, mean and maximum) and plant density.

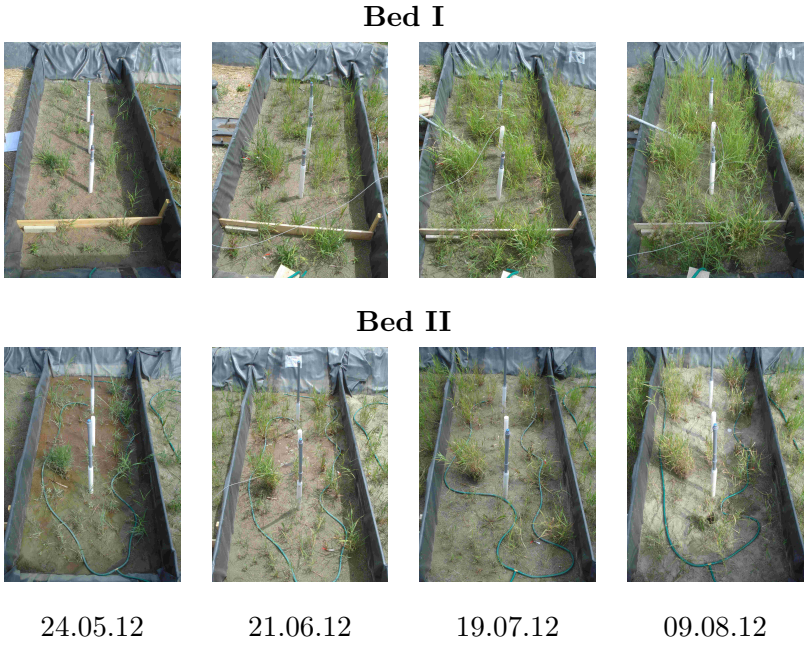

Figure 4.22: Aerial view of plant development in Bed I and Bed II over the course of the 12 week experiment.

5

Discussion

5.1 Bed I Step Injections

5.1.1 Hydrology and Water Balance

The determination of the water balance components for the continuous flow regime in Bed I was crucial in order to obtain a mass balance for the tracers and pesticide applied. The calculated water balance was negative for most of the experimental weeks in Bed I. Uncertainties in the water balance were mainly introduced by inflow irregularities (especially during the second step injection when the inflow pump broke), evapotranspiration overestimation and, to a small extent, by additional outflow from the other beds.

5.1.1.1 Inflow

Inflow quantification depended on the accuracy of the flow meter that was used to fill the inlet tanks and on the inflow pump. While the accuracy of the flow meter introduced a systemic uncertainty, it was the variation of the pump rate that complicated the accurate quantification of the inflow volume. During the first step injection, the pump appeared to work reliably at a 5.9 L/h pump rate, but the pump later failed during the second step injection. In order to estimate injection mix volume that entered the bed during the second step injection, the first inlet tank had to be emptied manually using 10 L beakers. This enabled a calculation of the total inflow volume, but any information on hourly inflow rates

was lost. The installation of a new pump that operated at a higher pump rate resulted in completely different inflow conditions for the second step injection, which complicated direct comparisons between the treatments.

5.1.1.2 Evapotranspiration and Piezometer Water Level:

The effect of evapotranspiration (ET) was best demonstrated by the diurnal fluctuation of the outflow rate and the piezometer water level. As expected, the calculated reference evapotranspiration (ET_0) reached a maximum sometime in the afternoon, depending on wind speed and radiation (see Figure 4.2). Concomitantly, the outflow rate was lowest in the late afternoon. While changing the autosampler sampling bottles at 2 pm on May 27^{th}, a sunny day, an outflow of only 1 L/h was observed. Based on this observation, and taking the average inflow pump rate of 5.9 L/h into account, the actual evapotranspiration (ET_a) in the afternoon can be estimated to be at least 5 L/h. Figure 4.1 shows that the calculated ET_0 lies within the range of 0 to 7 L/h. During the night and in the morning, outflow rates were nearly equal to the average inflow pump rate, implying that saturated horizontal flow occurred during these time periods (see Figure 4.1). The lag time between precipitation input and outflow response was negligibly small ($\leq$ 5 min) attesting good saturated hydraulic conductivity in the sand matrix.

A diurnal fluctuation was also evident in the transient behavior of the piezometer water level measured by the Odyssey probes during the first step injection (see Figure 4.2). These water level fluctuations were likely caused by ET and plant root uptake. The difference between day and night time water level readings was on average 5 mm, which means the ET_a from Bed I under saturated conditions was approximately 36 L per day. Moro et al. (2004) found actual *P. australis* ET rates of 10-30 mm/day in semi-arid Spain. This would mean that 72 to 216 L of water could be lost via ET per day in Bed I. However, this estimation assumes dense reed vegetation, which was not the case here. Since only approximately 20% of Bed I was covered with reeds, it is more likely that 14 to 40 L evaporated per day from Bed I. Chazarenc et al. (2003) measured ET directly on a pilot-scale HSSF wetland plot planted with *P. australis* in France and found that water lost due to ET_a represented up to 40% of the inflow in the summer. The effect of ET on solute transport and flow patterns can be dramatic. Bowmer (1987) stated that during periods of high ET, wetlands operate as a temporary sink and nutrient concentrators. The distribution of water absorbing roots is most influential in determining the pattern of flow during hot weather in the day time, whereas

gravity induced flow will dominate at night and in cooler weather. The effect of ET on the transport of metolachlor and tracers was not investigated in this study, but might be substantial and should be explored in future research.

Limitations of Reference Evapotranspiration The estimation of ET by means of computing reference evapotranspiration has its limitations due to the necessary simplifications inherent to the chosen method of calculation. Evapotranspiration is a complex, dynamic process governed by atmospheric conditions, plant demand for water, and soil properties. The Ref-ET software offers a high level of sophistication by allowing the use of crop factors and site-specific soil parameters for the calculation of reference evapotranspiration, but such detailed information was not available for this experiment. The plants were still growing, so it is likely that the demand for water changed over the course of the experiment. Furthermore, all plants were exposed to pesticides, which might have had an effect on their growth and transpiration rates. Durst (2011) observed inhibited transpiration in *P. australis* during a column experiment with UR, SRB and the pesticides isoproturon and metalaxyl.

5.1.1.3 Outflow

Despite the evident saturation during the first step injection, the weekly water balance recorded in Table 4.1 was mostly negative. Interestingly, this always coincided with weeks where the sum of precipitation surpassed the 50 L mark and single event intensity exceeded 4 mm/h (see Figure 4.1). An explanation for the negative balance during those weeks could be that additional runoff from Bed II and III outlet drains discharged into the man hole outflow tub. The individual bed drains were skirted with heavy rubber mats, which were weighed down by rocks. During high intensity precipitation events, water could have pooled up on the rubber skirt and eventually emptied into the main pipe. Additionally, rainwater could have directly drained into the outlet passing underneath the rubber mat because the outlet drains were level with the surrounding soil. Such rainwater intrusion would have contaminated the pressure probe outflow reading, causing a temporary overestimation of Bed I outflow. During high outflow periods caused by intense precipitation events, no sample dilution was found probably because the sampling interval was too coarse to guarantee a measurement during each fill-flush cycle.

5.1.2 Tracer Step Injections and Recoveries

The tracer breakthrough curves from the two step injections differed greatly due to the inflow irregularities which occurred during the second step injection. The goal of the step injections was to maintain a constant inflow rate in order to enable the comparison of the tracer passage through the bed before and after the vegetation had matured. During the second step injection, the inflow rate was not kept steady and the injection concentration changed between the first and second injection tank. Varying flow regimes are known to impact the hydrochemical conditions and the composition of the plant and microbial communities. Low flow rates may enhance the contact between influent compounds and the soil matrix, whereas high flow rates flush the wetland system and increase mobilization of sorbed components (Bowmer, 1987; Kadlec, 1994; Lange et al., 2011; Maillard et al., 2011). Thus any meaningful comparison between the first and second step injection was not possible because of the inflow anomalies during the second step injection and the resulting ramifications for the tracer transport through the soil matrix.

5.1.2.1 Bromide Breakthrough Curve and Recovery (First Step Injection)

The steeply rising limb of the bromide breakthrough curve (BC) from the first step injection demonstrated the initial conservative transport behavior of the reference tracer through the soil matrix. However, the nominal residence time (t_N = 129 h) was slightly greater than the theoretical hydraulic retention time (HRT = 115 h), which indicated some retardation. Upon flushing with clean site water, the falling limb of the BR breakthrough curve showed some tailing, which was more pronounced than the UR tailing. The overall shape of the BC was asymmetrical, indicating that BR did interact with the soil. Bromide recovery was 77%. Plant uptake and local salt precipitation might account for the missing 23% in the BR mass balance. There have been several studies on the uptake of BR by plants as well as BR losses due to concentration of salt species near the root zone via high transpiration rates (Matamoros et al., 2005; Parsons et al., 2004; Whitmer et al., 2000; Xu et al., 2004). Xu et al. (2004) demonstrated the accumulation of BR in the leaves, stems, and roots of *P. australis* and were able to substantiate the upward translocation of BR in the plant tissue via X-ray spectroscopy. Whitmer et al. (2000) pointed out that plant uptake of BR can be especially high during rapid plant growth, which was the case in Bed I. Another factor contributing to the asymmetrical BC shape might be non-uniform movement of the tracer infiltration front through the bed. Some BR was potentially immobilized near the edges of Bed I in zones that

participated only intermittently in the exchange of water and solutes. However, to obtain more detailed information on the processes involved in BR retention, plant samples and soil samples from the root zone need to be taken and analyzed.

Overall, BR recovery was higher than UR and SRB recovery. Bromide maximum flow velocity (v_{max}) exceeded UR and SRB v_{max} by a factor of two, whereas BR mean flow velocity (v_{mean}) of 0.013 m/h was comparable to the v_{mean} of UR and SRB. A reason could be that in the very beginning of the step injection, the plants were still small and growth was stunted because the wetland was not operating yet. When the injection began, rapid plant growth might have been activated due to the favorable watering conditions, which in turn resulted in BR retention and a small v_{mean}. This phenomenon might also explain why BR tailing was observed and why BR was still detected in the outflow after four weeks of flushing with clean site water. Moreover, on clear and sunny days when ET consumed all the inflow, some BR might have precipitated as salt. The salt crystals might then have adhered to the plant tissue or the sediment until they were remobilized during high rainfall events. Figure 4.3 partially supports this assumption because it shows that BR concentration increased temporarily during big storm events. However, the sampling interval at the end of each step injection was too coarse to make robust statements about the precipitation triggered plug flow.

5.1.2.2 Uranine Breakthrough Curves and Recoveries

First Step Injection It took twice as long for the first detection of BR and the first detection of UR in the outflow during the first step injection. The shape of the UR breakthrough curve was asymmetrical, but the tailing was less pronounced than with BR. The UR tail-end concentration after four weeks of flushing with water was very low compared to BR and SRB. During the decreasing part of the breakthrough curve, UR plug flow was observed when intense precipitation events caused high flow conditions, which facilitated the remobilization of sorbed UR. Overall, UR recovery was lowest among all tracers with only 59% of the injected mass recovered. The UR plateau concentration was only 82% of the UR injection concentration. Some UR might have undergone photolytic decay before it infiltrated the soil near the isolated inlet zone. Uranine recovery is also pH dependent. At pH less than eight, the univalent UR cation form begins to dominate the solution, which has a much lower fluorescence intensity than the UR anion (Käss, 2004; Leibundgut et al., 2009). The switch from the anionic to the cationic form of UR is a reversible process. The pH of the water in Bed I was monitored throughout the experiment and never went below 7 (see Table A.6

in the Appendix). Additionally, random pH dependency checks were performed in the lab during spectrometry. The fluorescence intensities of a sample at in situ pH and at pH 10 were compared. There was never a significant difference in fluorescence intensity. Thus, underestimation of the UR outflow concentration due to fluorescence intensity pH dependency can be excluded. However, the pH also affects the sorption affinity of UR. The sorption affinity increases at lower pH, because the UR cation interacts stronger with the substrate (Leibundgut et al., 2009). Kasnavia et al. (1999) showed that fluorescence tracer sorption was dominated by electrostatic interactions on pure mineral surfaces. Sabatini (2000) extended the findings of Kasnavia et al. (1999) to natural aquifer media and found that tracers with negative functional groups, like UR, adsorb onto positively charged surfaces (for instance alumina, limestone or carbonates at neutral pH). Gerke et al. (2008) found significant UR adsorption in topsoils at neutral pH in Okaya, Japan. Uranine might have been subject to sorption processes in the bed's matrix, which in concert with UR photodegradation could account for the overall UR loss.

Second Step Injection Uranine recovery was much higher from the second step injection experiment. More UR (almost 90%) than SRB (85%) was recovered. The reason for the higher recovery might be that UR sorption was limited due to less available sorption sites. Moreover, Bed I was not saturated for at least five days during tracer injection because of the inlet pump failure, thus the injection mix probably infiltrated more rapidly when the pump started working again and less photolytic decay occurred. Additionally, the inflow pump rate was increased during the second week of the tracer step injection, which might have caused an outwash of previously sorbed UR from the first step injection. Compared to the SRB breakthrough curve, UR concentration increase and decrease was less retarded, indicating less solute-soil matrix interactions. This was also evidenced by the UR plateau concentration, which was near UR injection concentration during the second week of step injection.

5.1.2.3 SRB Breakthrough Curves and Recoveries

First Step Injection The SRB breakthrough curve displayed the highest retardation compared to BR and UR. Sulphorhodamine B has two highly electronegative sulfonic acid groups and a cationic group. Thus, it is expected to have a high sorption potential on mineral surfaces (Kasnavia et al., 1999; Leibundgut et al., 2009; Sabatini, 2000). The overall SRB mass recovery of 67% lies within an expected range of a tracer prone to sorption. It must also be

noted that during the initial stage of Bed I operation, sorption of solutes onto soil substrate would be higher due to the high adsorption capacity of previously unexposed material. This was also observed in other constructed wetland studies performed by Ascuntar Ríos et al. (2009), Bowmer (1987) and George et al. (2003). The SRB tailing was more pronounced than UR and BR, indicating that sorption-desorption mechanisms dominated over convection and dispersion processes affecting the transport of SRB through the matrix. The peak concentration, expressed in percent of injection concentration, was lower for SRB (75%) than for UR (82%), which supports the assumption that SRB losses due to sorption are higher than UR sorption losses. Maximum and mean velocity of SRB were also lower than v_{max} and v_{mean} of UR (see Figure 4.2).

Second Step Injection The SRB recovery was significantly higher for the second step injection experiment. More than 85% of SRB was recovered. Unfortunately, the determination of the first SRB measured in the Bed I outflow was compromised by the inlet pump failure. This failure had more severe impacts on the transport of SRB than the transport of UR. The maximum velocity of SRB was only one third of the v_{max} calculated for the first step injection, and 134 hours passed until SRB was detected in the Bed I outflow, compared to only 44 hours during the first step injection. Consequently, the maximum SRB concentration in the outflow was measured more than 60 hours after the maximum detection of UR. The overall higher SRB recovery from the second step injection indicates that irreversible sorption might have occurred during the first step injection. Thus, most of the potential SRB sorption sites were already occupied when the second step injection started. Kasnavia et al. (1999) and Sabatini (2000) showed that SRB is less likely to adsorb on organic substrates in the presence of mineral surfaces. When the second step injection began, the plants in Bed I had matured for six weeks and the accumulation of soil organic matter had ensued, which might have caused an overall decrease of SRB sorption sites. The quantification of SRB losses due to sorption was beyond the scope of this study. In order to estimate SRB sorption during the first and second step injection, soil samples should have been taken before and after each treatment. However, this would have disturbed the Bed I matrix and possibly introduced heterogeneous flow patterns.

5.1.2.4 Metolachlor Recoveries

The mass recovery of metolachlor for both the step injection was nearly 60%. The analogous metolachlor recoveries from both step injections indicated that a sorption-desorption

equilibrium was potentially reached. Compared to the recovery of SRB from the second step injection, metolachlor retention in Bed I seemed quite high, showing that Bed I acted as a sink for metolachlor. Further details on the fate of metolachlor have to be investigated by analyzing soil samples and plant matter, as well as by identifying possible microbial degradation pathways.

5.1.3 CXTFIT Model Evaluation

Bromide Despite satisfactory indicators of model quality, the shape of the BR breakthrough curve could not be modeled adequately. When the first order degradation coefficient, μ, was fixed at zero, the BC plateau concentration was overestimated, but the tailing was well simulated. When μ was fitted, the plateau shape was simulated well, but the BC tailing was not matched. The overall shape of the BC tail-end resembled that of a non-conservative tracer. Potential BR retardation processes (i.e. plant uptake and salt precipitation) cannot be simulated by the equilibrium CDE model. However, the model results for the pore velocity (v = 0.070 m/s) and the hydrodynamic dispersion coefficient (D = 0.037 m^2/h) were in a realistic range for transport through a sand matrix. Still, compared to the calculated mean solute velocity of BR during the first step injection (v_{mean} = 0.013 m/s), the modeled pore velocity overestimated the BR transport velocity by a factor of seven.

Uranine The two-site nonequilibrium CDE gave the best model results after fitting the hydraulic parameters for mobile (β) and immobile (ω) phase partitioning, the mobile phase degradation coefficient (μ_1) and the retardation factor (Rd). The fitted Rd value was 0.387, which indicates that UR may be subject to anion exclusion processes or that there are zones within the bed containing immobile water that do not contribute to convective transport. However, initial photodegradation losses of UR near the inlet zone could also play a role in the detected retardation of UR transport, but photolysis cannot be modeled using CXTFIT.

Sulphorhodamine B In the case of SRB, the two-site non-equilibrium CDE also resulted in better simulation of the BC. As with modeling UR transport, fitting β, ω, μ_1 and Rd resulted in a high R^2-value. Modeling the SRB breakthrough curve showed good agreement between measured and simulated concentrations with respect to peak concentration and tailing. The fitted Rd value of 2.92 and the mobile phase coefficient of 0.033 indicate that kinetic adsorption processes govern the transport of SRB through the soil matrix, as was expected.

Model Deficiencies Fitting a convection dispersion model to observed BCs is a common way to determine tracer transport parameters. CXTFIT presented a simple approach for obtaining hydraulic transport parameters and for highlighting some of the dominant processes involved in Bed I solute transport. However, the modeling approach employed here was found to be inadequate for reproducing the pronounced tailing in the BCs of BR and UR. Processes causing this tailing might be the slow dissolution of previously precipitated BR and sorption-desorption of UR. The model's shortcomings are due to the assumption of steady flow conditions in homogeneous media, which had to be made in order to apply CXTFIT. Indeed, there were extended periods when the flow rate was not steady due to high ET rates in the daytime, or during high intensity precipitation events. Additionally, the wetland bed media consisted of distinct gravel and sand layers. This heterogeneity in substrate cannot be modeled using CXTFIT.

5.2 Bed II Batch Operations

5.2.1 Hydrology and Water Balance

The water balance calculations in Bed II were negative for almost all batch operations. The contributing factors to Bed II water balance uncertainties are similar to those from Bed I and include inflow irregularities due to varying saturation states of the bed, evapotranspiration overestimation, as well as potential outflow underestimation during draining.

5.2.1.1 Inflow

The tracer-pesticide injection volumes at the beginning of each batch operation varied greatly due to different volumes of residual water in the bed from precipitation input during the preceding week, when batch operation was paused. Shortly after each batch injection, pooling of excess injection mix was observed near the bed's outlet zone. On the one hand, this pooling might have been due to oversaturation because too much mix was injected based on the calculated residual water volume (V_{res}) prior to injection. On the other hand, the conductive properties of the initially unsaturated soil could have caused the pooling. When unsaturated conditions prevail in sandy soils, the unsaturated hydraulic conductivity is much lower than the saturated one (Hillel, 1998; Lal and Shukla, 2004). Under the unsaturated conditions preceding the injection, the relatively big, air-filled pores of the sand in Bed II were non-conductive and impeded infiltration, which could have resulted in the pooling of

water as the injection rate exceeded the infiltration capacity. Regardless, the pooling of tracer-pesticide mix posed a problem, because of the photosensitivity of UR, which likely started to degrade before even entering the bed.

5.2.1.2 Evapotranspiration and Piezometer Water Level:

The diurnal effect of ET on the water level in the Bed II piezometers could barely be discerned compared to Bed I. This might be because the plants in Bed II were less developed and less active or because the bed did not operate under saturated conditions. Thus, water from Bed II did not evaporate at a dependable rate influenced only by meteorological conditions and time of day, as was the case in Bed I during the first step injection. Furthermore, because the plants in Bed II experienced periods of water deficit, they might have reduced transpiration rates and stored water in their roots.

The most salient indicator of the cumulative effects of ET were found in the precipitous declines in the piezometer water level seen in all four batch experiments. Such drops were often preceded by extended periods of negligible change in water level, which taken at face value suggest periods of extremely low ET rates (see Figure 5.1). However, this water level behavior is more convincingly explained by considering the soil properties and the major processes involved in the water transmission at varying stages of soil saturation.

After the batch tracer-pesticide injection, the water level was within the sand zone, the soil was saturated and ET was equal to the atmospheric evaporativity. For the next day, the water level decreased slowly because the bed was saturated. However, in the absence of further soil wetting via precipitation, the soil profile gradually dried from the top. While the water level was still in the sand layer, water was rapidly transmitted to the root and evaporation zone through capillary rise. Literature values for capillary rise range from 25 cm to 75 cm in medium sand material (Hillel, 1998; Lal and Shukla, 2004). Concomitantly, the water level dropped dramatically in accordance with the rate at which the soil could deliver moisture towards the evaporation zone (see Figure 5.1).

Once the water level dropped to the gravel layer zone, the capillary rise diminished to only 2.5 to 5 cm and the upper sand layer was completely desiccated. However, a single but intense precipitation event could recharge the bed and cause the water level to rise (see Figure 5.1). If no such precipitation event occurred, water from the gravel layer could only be transmitted via extremely slow vapor diffusion. The ET rate diminished to almost zero by the time the piezometer water level had dropped to a global minimum (see dashed line in Figure 5.1). Once

the water level had reached the global minimum, only a rainstorm of sufficient magnitude would result in a rise of the water level (compare Figure 4.13 July 1^{st} during the third batch to July 21^{st} during the fourth batch). Otherwise, the water would infiltrate the sand layer, but not saturate it, so no rise in the water level was detected.

Additionally, differences in the porosity between the sand and gravel layer also affect the rate of water level change in the piezometers. The sand layer has a lower porosity than the gravel layer, so the depletion of the water stored in the sand results in a faster water level decrease than a depletion from the gravel layer. Sand and gravel samples from the beds are currently analyzed by the French group for specific pedologic characteristics (pF-curve, porosity, etc.). This additional information will enable a better understanding of the water retention in the beds and the water level dynamics at different moisture contents.

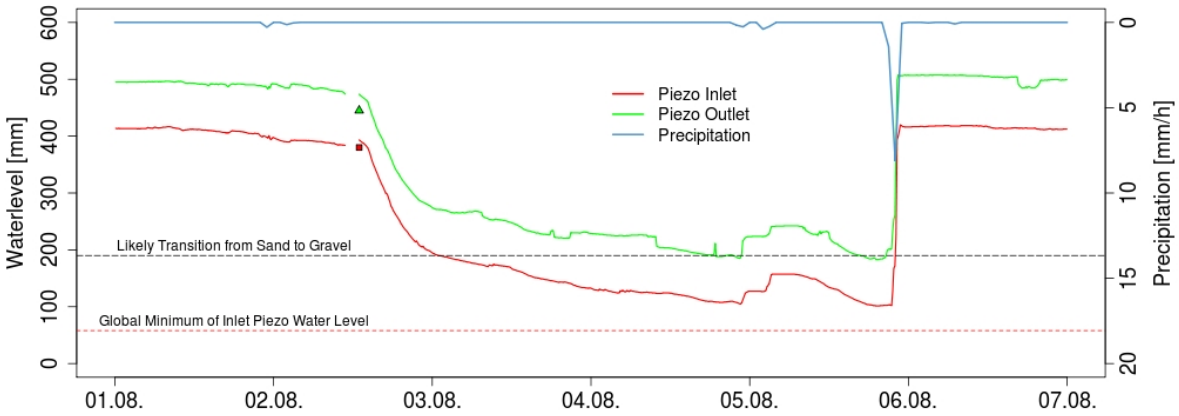

Figure 5.1: Bed II piezometer water level dynamics during the second week of the fourth batch operation. The sand to gravel transition line is shown relative to the inlet piezometer (red line). In particular, a dramatic change in the rate of water level decrease occurs at the intersection.

5.2.1.3 Outflow

The outflow from all batch drains was probably underestimated due to a too coarse logging interval of the pressure probe, especially during the initial draining phase when the outflow rate was near 10 L/h. During that phase the outflow tub would have been filled within 80 seconds, at which point the swimmer triggered pump started to purge the water and some of the water was not quantified due to the interference of the purging pump. The outflow was measured most accurately during the fourth draining, as the pressure probe logging interval was changed from 1 min to 10 sec. Still, uncertainty remains about the outflow volume that was not accounted for during purging. In order to quantify the unaccounted volume,

measurements of the duration of purging would be needed. However, such measurements are not straight forward because the duration of purging is directly related to the (non-constant) outflow rate.

5.2.2 Tracer and Pesticide Concentrations in the Piezometers

The fluctuation patterns of tracer concentrations in the piezometer samples was unique to each tracer. At times, there were big differences in the tracer concentrations between the inlet and the outlet piezometer. Two effects may have contributed to this difference. First of all, tracer convection and dispersion after tracer-pesticide injection was not uniform throughout the bed and sediment layers. Secondly, the inlet and outlet piezometer samples probably had different signatures from the gravel and the sand layer because stratification of tracer-pesticide transport occurred. The bottom of the bed was slanted towards the outlet, so the gravel layer near the inlet piezometer was only half as deep than near the outlet piezometer. Thus, the tracer signature of the gravel layer in the outlet piezometer samples was probably more pronounced than in the inlet piezometer samples.

Uranine The UR concentration in the inlet piezometer was initially higher than in the outlet piezometer, but by the end of the second batch the concentrations had converged. This indicates that despite the high injection concentrations during the second and third batches, UR appeared to mix well within the bed. A general decrease in the UR piezometer concentration from the first to the third batch was noticeable despite fresh injections. Three main processes might be responsible for this decrease. Firstly, some UR was lost due to photolysis when the tracer-pesticide mix pooled up shortly after injection and was exposed to sunlight. Secondly, the residual UR concentration in the bed after draining was diluted by rainwater during the week-long pause between draining and next tracer-pesticide injection. Thirdly, UR sorbed to the soil matrix and thus evaded detection in the water samples. The extreme difference between the UR inlet and outlet piezometer concentrations measured during the fourth batch was puzzling. It might be the case that the sorption sites in the soil near the inlet piezometer zone were occupied and more UR was mobile in the solute phase. Furthermore, the injection of 350 L of tracer-pesticide mix during the fourth batch (three times as much than during batch two and three), possibly triggered some remobilization of formerly sorbed UR.

Sulphorhodamine B The SRB inlet and outlet piezometer concentrations were nearly the same during the first batch, but the outlet piezometer concentration exceeded the inlet piezometer concentration by a factor of four during the second batch experiment. Purging the outlet piezometer before sampling sometimes caused a rapid inflow of water from the gravel layer. Thus, the outlet piezometer samples could have mostly contained the SRB signature from the gravel, which was high because less sorption occurred in the gravel due to diminished solute-solid interactions. The SRB inlet piezometer concentration from the second batch did not deviate much from the concentration measured during the first batch. Samples from the inlet piezometer might have been more representative of the sand layer, where sorption of SRB took place. By the end of the third batch the SRB concentrations of the inlet and outlet piezometer had converged, but were higher than during the second batch. This could indicate that SRB sorption sites were saturated, so more SRB stayed in solution and a concentration equilibrium within the bed was reached.

Metolachlor The metolachlor concentration measured in pooled samples from the inlet and outlet piezometer correlated strongly with the averaged inlet and outlet piezometer SRB concentration ($R^2 = 0.96$) as opposed to a weaker correlation between metolachlor and UR ($R^2 = 0.73$). This suggests that SRB might be an acceptable proxy for metolachlor transport and attenuation in batch operated wetland mesocosms.

5.2.3 Batch Draining Dynamics

The fluorometry samples taken during draining events showed the effects of varying batch injection concentrations, residual batch tracer accumulation, as well as the different signatures of the gravel and sand filters. Three phases of draining were identified using the outflow rate and the turbidity. **Phase I** was characterized by rapidly increasing outflow accompanied by a short-lived turbidity spike probably due to the flushing of a sediment plug that was trapped in the T-pipe) until the maximum outflow rate was reached. Immediately after the plug had been pulled, the outlet T-pipe, which likely contained residual water from the previous drain, mixed with water from the preceding tracer-pesticide mix injection, drained first followed by the fast draining of the gravel layer. The residual tracer concentration was slightly higher in the T-pipe water than in the water draining from the gravel, which likely produced the UR concentration spike and the smaller SRB spike during Phase I.

The beginning of **Phase II** was marked by the maximum outflow rate and the onset of a gradual increase in turbidity. Phase II can be characterized as the draining phase of the

gravel filter, which was often accompanied by a decrease in UR concentration and a broad peak in SRB concentration. The dip in UR concentration sometimes nearly matched the concentration measured in the outlet piezometer shortly before draining (see second and fourth drain in Figures 4.17 and 4.18), but sometimes it was even lower (see first and third drain in Figures 4.16 and 4.17). Samples taken during draining Phase II probably reflected the tracer concentrations in the outlet zone of Bed II, which has a stronger gravel filter signature than the inlet zone. The broad peak in the SRB outflow concentration corresponding to Phase II further supports the assumption of a gravel signature in the outlet piezometer where SRB would be less sorptive.

The beginning of **Phase III** was marked by the broad peak in turbidity at the end of the gravel filter draining, where the outflow rate had slowed to around 2 L/h. During Phase III, both turbidity and outflow rate gradually decreased, which was indicative of the sand filter draining. The SRB concentration decreased compared to Phase II and stabilized near a constant value, demonstrating that SRB was interacting with the sand matrix during batch operation and was less mobile. The UR concentration showed a pronounced increase during Phase III of the fourth drain, where the UR outflow concentration approached the UR concentration measured in the inlet piezometer before draining. The same behavior was observed during Phase III of the first and second draining, but the increase was more subtle. Still, this observation could give a clue about the dynamics of UR sorption, indicating that draining a sand filter potentially remobilizes UR. Overall, the collected draining data includes too many variables (e.g., extreme variation in injection concentration and volumes, climate variations) to conclude that a definitive draining concentration pattern exists for UR and SRB, additional draining experiments under more controlled conditions should be conducted.

5.2.4 Batch Tracer and Pesticide Recoveries

The total tracer masses recovered from each batch were in general low compared to Bed I. Uranine and BR recoveries showed no apparent trend between batches, though the highest UR recovery (5%) occurred during the fourth batch. These low recoveries attest the mitigation capacity via sorption of contaminants in constructed wetland mesocosms, which other authors have reported in their studies (Ascuntar Ríos et al., 2009; Burgoon et al., 1995; George et al., 2003; Page et al., 2010; Stearman et al., 2003). Sulphorhodamine B recovery increased from less than 1% to more than 7% by batch three, indicating that sorption efficiency decreased over time until the equilibrium between sorption and remobilization was reached

under batch flow operation. However, from the fourth batch operation only 4% of the injected SRB mass was recovered, showing that other prevailing environmental conditions (e.g., redox potential, pH and dissolved oxygen) may change the SRB sorption-desorption equilibrium conditions (Garcia et al., 2010). These conditions are known to determine the thermodynamic feasibility of chemical reactions and the activity of indigenous microbial communities (Imfeld et al., 2009). Overall, additional removal processes other than sorption must have contributed to the low recoveries of the tracers, but the identification of these processes require more detailed research in a controlled laboratory setting, such as column experiments. Low recoveries were also observed for metolachlor after batch one and two. Nevertheless, no distinct trend in metolachlor recovery over time was discernible from the data available at this time. Uncertainties in the mass balance due to residual tracer pesticide concentrations after each draining were recognized, but their relative contribution to the next batch recovery could not be quantified because of the lack of means to separate the previous tracer-pesticide load from the current one. However, since the overall recoveries were so low the effect of load propagation from one batch to the next was probably negligible. The recovery results from the Bed II outflow samples have to be put in perspective, regarding results from sediment and plant analysis from samples that were taken at the end of batch four, in order to distinguish other processes involved in contaminant removal (i.e. plant uptake and biodegradation). The analysis of these samples by the French group is still in progress.

5.3 Bed III

The results from the fluorescence tracer and metolachlor concentrations measured in the Bed III piezometers demonstrated the environmental persistence of these compounds. Even after ten weeks of batch flow treatment exclusively with clean site water, the tracer and pesticide concentrations had not returned to zero. The linear regression results between the individual fluorescence tracer and the metolachlor concentrations in the Bed III piezometers are inconclusive. Uranine and SRB displayed high R^2 values with 0.94 and 0.89, respectively. However, the significance of the correlation is impaired because the analysis was based on a six point regression after one tracer-pesticide application followed by clean site water injections, so most data points clustered at low concentrations.

5.4 Comparison of Bed I and Bed II Contaminant Removal Efficiencies

The tracer and pesticide removal efficiency was significantly lower in the continuous flow Bed I than in the batch flow operated Bed II (see Table 5.1). The differences in removal efficiencies can be linked to the differences in the influent contaminant concentration, the hydraulic retention time (HRT), and the water level in the wetland beds. These parameters are known to affect contaminant removal efficiencies in wetlands (Garcia et al., 2010; Lange et al., 2011; Stearman et al., 2003).

Table 5.1: Tracer and pesticide percent removal data from Bed I and Bed II for each treatment.

Bed	**Treatment**	**% Removal**			
		Bromide	UR	SRB	Metolachlor
I	1^{st} Inj.	22	40	33	40
	2^{nd} Inj.	-	10	15	42
II	1^{st} Batch	-	96	99	94
	2^{nd} Batch	-	97	94	94
	3^{rd} Batch	52	98	93	96
	4^{th} Batch	46	95	96	-

When the HRT is high, as was the case in Bed II, slow occurring processes such as sedimentation, biodegradation, and plant uptake potentially dominate the overall contaminant removal Stearman et al. (2003). Additionally, batch operation has been proposed as a suitable method for enhancing oxidizing conditions via intermittent aeration of the wetland matrix pore spaces through controlled draining (Zhang et al., 2012). Chemical and microbial degradation are both coupled to oxygen availability. Mersie et al. (2004) demonstrated that metolachlor can degrade under aerobic as well as anaerobic conditions and is very short-lived in consistently moist and warm conditions. Little information exists on the biochemical degradation pathways of fluorescence tracers and the degradation products of SRB and UR. However, the recovery results from Bed II demonstrate that significant attenuation occurs under batch flow operation.

Under the continuous flow conditions with low HRTs in Bed I, fast occurring sorption processes presumably dominate the removal of tracers and pesticide from the solute phase. The flushing of Bed I sediment with clean site water potentially caused desorption and remobiliza-

tion of tracers and pesticide by disturbing the sorption-desorption equilibrium. The breaking of the pump during the second step injection lead to variations in HRT and influent contaminant concentration, thereby facilitating subsequent contaminant remobilization. Garcia et al. (2010) suggested that the rate of desorption will increase with the time elapsed after sorption. Microbial degradation was less likely in Bed I than in Bed II, due to the low HRTs and the long flushing cycles with pure water, which did not allow microbial communities to adapt to the contaminants and use them for metabolic processes.

5.5 Vegetation in Bed I and Bed II

Figures 4.22 and 4.21 demonstrate that the plant development differed greatly between Bed I and Bed II. The vegetation in Bed I was thriving after the 12 week experiment; plant height and density showed an increasing trend over the experimental period, but no such clear trend was noticeable in Bed II. The plants in Bed II did not look as healthy, and their leaves were yellow and dry probably due to periods of water deficit and long exposures to high concentrations of pesticides. The effects of high metolachlor concentrations on the development of *P. australis*, *P. arundinacea* and *G. maxima* have not been studied yet, but the pesticide may inhibit certain plant-metabolic functions, which leads to stunted growth and poor plant health. Conversely, the exact impact of the maturing vegetation on contaminant removal in Bed I and II could not be discerned because other system variables (e.g. inflow volume fluctuation and influent contaminant concentration variation) were in play. However, some of the observed contaminant removal might be attributable to phytoremediation, despite slow plant development in Bed II, which may in fact be linked to it. Stearman et al. (2003) suggested that planted wetland systems have a higher pesticide removal potential for a number of reasons, including plant uptake, oxygenated rhizosphere zones that enhance aerobic degradation, and increased microbial activity from plant root exudate stimulation.

6

Conclusions

In the presented study, the conservative salt tracer bromide (BR) and the two fluorescence tracers (FT) uranine (UR) and sulphorhodamine B (SRB) were used to investigate the transport and attenuation of the commonly used pesticide metolachlor (MC) in constructed wetland mesocosms operating under different hydraulic regimes and contamination patterns. Bromide served as a reference tracer to evaluate internal system hydraulics, whereas the fluorescence tracers were applied to test whether they could act as proxies for metolachlor transport.

The flow regime had a significant impact on the contaminant removal efficiency in the constructed wetlands. Both flow regimes facilitated contaminant removal, but metolachlor removal efficiencies were significantly higher in the batch flow operated system ($\approx 90\%$) than in the wetland operating under continuous flow conditions ($\approx 40\%$). The impact of different contamination patterns on tracer-pesticide removal efficiencies could not be discerned.

The tracer breakthrough curve (BC) results from each of the two step injections in the continuous flow bed showed tracer retardation for all applied tracers. The retardation in the bromide BC pointed to potential plant uptake and salt precipitation due to high evapotranspiration rates, resulting in an overall bromide loss of 22%. Fluorescence tracer recoveries from the first step injection were similar to the metolachlor recovery (UR = 60%, SRB = 67%, MC = 60%). The high loss of UR was attributed to sorption to organic matter and positively charged mineral surfaces in the soil matrix, as well as possible photodegradation near the inlet zone of the wetland bed. Still, UR has only one negatively charged functional group, thus

sorption should have been more limited compared to SRB, which is known to display sorptive behavior to negatively and positively mineral surfaces (Kasnavia et al., 1999; Sabatini, 2000). This points to other UR removal processes like plant uptake or microbial degradation, which have not been reported in literature so far and need to be investigated. The second step injection FT recoveries were much higher, yet metolachlor recovery remained near first injection levels (UR = 90%, SRB = 85%, MC = 58%). The increase in FT recovery attested that less sorption sites were available and that sorption-desorption processes contributed to additional remobilization of UR and SRB. Metolachlor recovery data indicated that degradation and sorption processes were occurring and that new metolachlor sorption sites became available over time. This could potentially be linked to plant maturation and the increase in organic carbon content near the plant root zone. The divergence in metolachlor and FT recoveries from the second step injection suggest that different processes affect the transport and attenuation of FTs and metolachlor under continuous flow conditions over time. Results regarding the suitability of UR and SRB as proxies for metolachlor behavior under continuous flow conditions were thus inconclusive after two step injections. An extended series of step injection experiments is needed to investigate potential changes in recoveries between the compounds over time.

The FT and metolachlor recoveries from the batch flow bed were below 10% in all four batch treatments. No distinct trend in the removal efficiencies from one batch to the next was recognized. Similar tracer and pesticide recoveries show that UR and SRB might serve as proxies for metolachlor transport under batch flow conditions. In particular, SRB was found to correlate strongly with the metolachlor concentration measured in the wetland bed piezometers. Low tracer and pesticide recoveries were linked to the high hydraulic retention time (HRT) during batch contaminant loading followed by intermittent aeration of the wetland matrix after complete bed draining. Chemical and microbial degradation are both coupled to oxygen availability, and these processes may dominate in the attenuation of metolachlor, UR and SRB. High resolution tracer, outflow and turbidity data from the bed's draining indicated different removal efficiencies in the two sediment layers, which was evidenced by distinct concentration differences between UR and SRB draining from the gravel and the sand filters. Generally, a higher SRB concentration was detected in the water draining from the gravel than from the sand filter. Plant uptake and microbial degradation will most likely occur within the root zone, which resided in the sand layer. Solute interactions with the soil matrix and sorption are also expected to predominate in the sand layer. Using SRB as a proxy, it can

be assumed that metolachlor is degraded in the sand layer, but also that it shows potential to leach and accumulate in the gravel layer. This non-desirable effect could have ramifications for the design of vertical flow wetlands that operate under pipe drain discharge.

Despite the stress of pesticide exposure, the average plant height and density increased over time in Bed I. No such trend was observed in the batch flow bed, where plants experienced periods of water deficit in addition to the contaminant stresses. The effects of plant development on tracer and pesticide transport could not be tested due to varying inflow rates and influent concentrations, which introduced an unintended level of hydraulic and biogeochemical complexities to the wetland system. However, the high metolachlor removal efficiency in the batch flow bed poses the question to which extend phytoremediation, plant uptake and sorption processes contribute to metolachlor removal. Laboratory results for plant uptake in Bed I and II are still pending. Future research might focus on the role of plants in the degradation of FT and metolachlor by contrasting the removal efficiencies of vegetated and nonvegetated wetland systems.

The presented study was suitable to identify the general contaminant mitigation potential of each treatment and illuminated the major factors influencing the contaminant removal efficiencies, such as hydraulic retention time, substrate type, and vegetation. To obtain more detailed information about metolachlor, UR and SRB transformation or biodegradation processes, investigations inside the wetland beds are required. These investigative efforts should include the characterization of site specific pedological properties and phyto- and microbial degradation pathways, as well as the identification of compound specific degradation products. Further emphasis might also be put on comparative studies regarding the feasibility of the use of UR and SRB as reference tracers for metolachlor transport and attenuation in different wetland substrates (gravel, sand, organic matter). These investigations will enhance our knowledge about the complex processes contributing to contaminant removal in constructed wetlands and strengthen the great potential reference tracer hydrology offers in understanding flow pathways and transport mechanisms, thereby enabling better management and protection of our water resources.

References

Accinelli, C., Dinelli, G., Vicari, A., and Catizone, P. (2001). Atrazine and metolachlor degradation in subsoils. *Biology and Fertility of Soils*, 33(6):495–500.

Agritox Online (2012). `http://www.dive.afssa.fr/agritox/php/sa.php?sa=1210` (accessed 23.08.2012).

Allen, R. G. (2011). REF-ET: Reference Evapotranspiration Calculation Software for FAO and ASCE Standardized Equations - Version 3.1.

Allen, R. G., Pereira, L. S., Raes, D., and Smith, M. (2006). FAO Irrigation and Drainage Paper No. 56 - Crop Evpotranspiration. Technical Report 56, United Nations Food and Agricultural Organization.

Ascuntar Ríos, D., Toro Vélez, A., Peña, M., and Madera Parra, C. (2009). Changes of flow patterns in a horizontal subsurface flow constructed wetland treating domestic wastewater in tropical regions. *Ecological Engineering*, 35(2):274–280.

Barra Caracciolo, A., Giuliano, G., Grenni, P., Guzzella, L., Pozzoni, F., Bottoni, P., Fava, L., Crobe, A., Orrù, M., and Funari, E. (2005). Degradation and leaching of the herbicides metolachlor and diuron: a case study in an area of Northern Italy. *Environmental Pollution (Barking, Essex : 1987)*, 134(3):525–34.

Barth, J. A. C., Grathwohl, P., Fowler, H. J., Bellin, A., Gerzabek, M. H., Lair, G. J., Barceló, D., Petrovic, M., Navarro, A., Négrel, P., Petelet-Giraud, E., Darmendrail, D., Rijnaarts, H., Langenhoff, A., Weert, J., Slob, A., Zaan, B. M., Gerritse, J., Frank, E., Gutierrez, A., Kretzschmar, R., Gocht, T., Steidle, D., Garrido, F., Jones, K. C., Meijer,

S., Moeckel, C., Marsman, A., Klaver, G., Vogel, T., Bürger, C., Kolditz, O., Broers, H. P., Baran, N., Joziasse, J., Tümpling, W., Gaans, P., Merly, C., Chapman, A., Brouyère, S., Batlle Aguilar, J., Orban, P., Tas, N., and Smidt, H. (2009). Mobility, turnover and storage of pollutants in soils, sediments and waters: achievements and results of the EU project AquaTerra. A review. *Agronomy for Sustainable Development*, 29(1):161–173.

Bernhard, C., Carbiener, R., Cloots, A. R., Froehlicher, R., Schenck, C., and Zilliox, L. (1992). Nitrate pollution of groundwater in the alsatian plain (France)—A multidisciplinary study of an agricultural area: The Central Ried of the ill river. *Environmental Geology and Water Sciences*, 20(2):125–137.

Bowmer, K. H. (1987). Nutrient removal from effluents by an artificial wetland: Influence of rhizosphere aeration and preferential flow studied using bromide and dye tracers. *Water Research*, 21(5):591–599.

Burgoon, P. S., Reddy, K. R., and Debusk, T. A. (1995). Performance of subsurface flow wetlands with batch-load and continuous-flow conditions. *Water Environment Research*, 67(5):855–862.

Carter, A. (2000). Herbicide movement in soils: principles, pathways and processes. *Weed Research*, 40(1):113–122.

Chazarenc, F., Merlin, G., and Gonthier, Y. (2003). Hydrodynamics of horizontal subsurface flow constructed wetlands. *Ecological Engineering*, 21(2-3):165–173.

Crisanto, T., SanchezCamazano, M., Arienzo, M., and SanchezMartin, M. (1995). Adsorption and mobility of metolachlor in surface horizons of soils with low organic matter content. *Science of the Total Environment*, 166(1-3):69–76.

Dionex (1993). LC20 Chromatography Enclosure Operator's Manual.

Durst, R. (2011). Transfer of Tracers and Pesticides in lab-scale Wetland Systems. Master's thesis, University of Freiburg, Freiburg, Germany.

European Commission (1998). Council Directive 98/83/EC of 3 November 1998 on the quality of water intended for human consumption. *Off. J. Europ. Union*, L 330/32(05/12/1998).

European Commission (2006). Directive 2006/118/EC of the European Parliament and the Council of 12th of December 2006 on the protection of ground water against pollution and deterioration. *Off. J. Europ. Union*, L 372/19(27/12/2006).

Flury, M. (1996). Experimental Evidence of Transport of Pesticides through Field Soils—A Review. *Journal of Environmental Quality*, 25(1):25.

Flury, M. and Wai, N. N. (2003). Dyes as tracers for vadose zone hydrology. *Reviews of Geophysics*, 41(1):1002.

Garcia, J., Rousseau, D. P. L., Morato, J., Lesage, E., Matamoros, V., and Bayona, J. M. (2010). Contaminant Removal Processes in Subsurface-Flow Constructed Wetlands: A Review. *Critical Reviews in Environmental Science and Technology*, 40(5-8):561–661.

George, D., Stearman, G. K., Carlson, K., and Lansford, S. (2003). Simazine and Metolachlor Removal by Subsurface Flow Constructed Wetlands. *Water Environment Research*, 75(2):101–112.

Gerke, K. M., Sidle, R. C., and Tokuda, Y. (2008). Sorption of Uranine on Forest Soils Abstract :. *Hydrological Research Letters - Japan Society of Hydrology and Water Resources*, 35(2):32–35.

Gonçalves, C. M., da Silva, J. C. G. E., and Alpendurada, M. F. (2007). Evaluation of the pesticide contamination of groundwater sampled over two years from a vulnerable zone in Portugal. *Journal of Agricultural and Food Chemistry*, 55(15):6227–35.

Gregoire, C., Elsaesser, D., Huguenot, D., Lange, J., Lebeau, T., Merli, A., Mose, R., Passeport, E., Payraudeau, S., Schütz, T., Schulz, R., Tapia-Padilla, G., Tournebize, J., Trevisan, M., and Wanko, A. (2008). Mitigation of agricultural nonpoint-source pesticide pollution in artificial wetland ecosystems. *Environmental Chemistry Letters*, 7(3):205–231.

Gutierrez, A. and Baran, N. (2009). Long-term transfer of diffuse pollution at catchment scale: Respective roles of soil, and the unsaturated and saturated zones (Brévilles, France). *Journal of Hydrology*, 369(3-4):381–391.

Hanke, I., Singer, H., McArdell-Buergisser, C. Brennwald, M., Traber, D., Muralt, R., Herold, T., Oechslin, R., and Kipfer, R. (2007). Arzneimittel und Pestizide im Grundwasser. *GWA*, 87(3):187–196.

Hench, K. R., Bissonnette, G. K., Sexstone, A. J., Coleman, J. G., Garbutt, K., and Skousen, J. G. (2003). Fate of physical, chemical, and microbial contaminants in domestic wastewater following treatment by small constructed wetlands. *Water Research*, 37(4):921–927.

Herbst, M. and Kappen, L. (1999). The ratio of transpiration versus evaporation in a reed belt as influenced by weather conditions. *Aquatic Botany*, 63(2):113–125.

Hildebrandt, A., Guillamón, M., Lacorte, S., Tauler, R., and Barceló, D. (2008). Impact of pesticides used in agriculture and vineyards to surface and groundwater quality (North Spain). *Water Research*, 42(13):3315–26.

Hillel, D. (1998). *Environmental Soil Physics: Fundamentals, Applications, and Environmental Considerations*. Academic Press.

Imfeld, G., Braeckevelt, M., Kuschk, P., and Richnow, H. H. (2009). Monitoring and assessing processes of organic chemicals removal in constructed wetlands. *Chemosphere*, 74(3):349–62.

Kadlec, R. H. (1992). *Hydrological factors in wetland water treatment. In: Constructed Wetlands for Wastewater Treatment: Municipal, Industrial and Agricultural*. Number 1907. Lewis Publishers Chelsea, MI – USA.

Kadlec, R. H. (1994). Detention and mixing in free water wetlands. *Ecological Engineering*, 3(4):345–380.

Kalkhoff, S. J., Kolpin, D. W., Thurman, E. M., Ferrer, I., and Barcelo, D. (1998). Degradation of Chloroacetanilide Herbicides: The Prevalence of Sulfonic and Oxanilic Acid Metabolites in Iowa Groundwaters and Surface Waters. *Environmental Science & Technology*, 32(11):1738–1740.

Kasnavia, T., Vu, D., and Sabatini, D. A. (1999). Fluorescent Dye and Media Properties Affecting Sorption and Tracer Selection. *Ground Water*, 37(3):376–381.

Käss, W. (2004). *Geohydrologische Markierungstechnik - Volume 9 of Lehrbuch der Hydrogeologie*. Borntraeger, 2nd edition.

Krutz, L. J., Senseman, S. A., McInnes, K. J., Hoffman, D. W., and Tierney, D. P. (2004). Adsorption and Desorption of Metolachlor and Metolachlor Metabolites in Vegetated Filter Strip and Cultivated Soil. *Journal of Environmental Quality*, 33(3):939.

Lal, R. and Shukla, M. K. (2004). *Principles of Soil Physics*, volume 33. CRC Press.

Lange, J., Schuetz, T., Gregoire, C., Elsässer, D., Schulz, R., Passeport, E., and Tournebize, J. (2011). Multi-tracer experiments to characterise contaminant mitigation capacities for

different types of artificial wetlands. *International Journal of Environmental Analytical Chemistry*, 91(7-8):768–785.

Leibundgut, C., Maloszewski, P., and Külls, C. (2009). *Tracers in Hydrology*. Wiley.

Lin, Y. J., Karuppiah, M., Shaw, A., and Gupta, G. (1999). Effect of simulated sunlight on atrazine and metolachlor toxicity of surface waters. *Ecotoxicology and Environmental Safety*, 43(1):35–7.

Loos, R., Locoro, G., Comero, S., Contini, S., Schwesig, D., Werres, F., Balsaa, P., Gans, O., Weiss, S., Blaha, L., Bolchi, M., and Gawlik, B. M. (2010). Pan-European survey on the occurrence of selected polar organic persistent pollutants in ground water. *Water Research*, 44(14):4115–26.

Ma, Y., Liu, W.-P., and Wen, Y.-Z. (2006). Enantioselective Degradation of Rac-Metolachlor and S-Metolachlor in Soil. *Pedosphere*, 16(4):489–494.

Maillard, E., Payraudeau, S., Faivre, E., Grégoire, C., Gangloff, S., and Imfeld, G. (2011). Removal of pesticide mixtures in a stormwater wetland collecting runoff from a vineyard catchment. *Science of the Total Environment*, 409(11):2317–24.

Matamoros, V., García, J., and Bayona, J. M. (2005). Behavior of Selected Pharmaceuticals in Subsurface Flow Constructed Wetlands: A Pilot-Scale Study. *Environmental Science & Technology*, 39(14):5449–5454.

Mersie, W., McNamee, C., Seybold, C., Wu, J., and Tierney, D. (2004). Degradation of Metolachlor in Bare and Vegetated Soils and in Simulated Water-Sediment Systems. *Environmental Toxicology and Chemistry*, 23(11):2627.

Meteo France Online (2012). `http://climat.meteofrance.com/chgt_climat2/climat_france?89461.path=climatstation%252F68205001` (accessed 23.08.2012).

Mitsch, W. J., Gosselink, J. G., Zhang, L., and Anderson, C. J. (2009). *Wetland Ecosystems*.

Moore, M., Rodgers, J., Smith, S., and Cooper, C. (2001). Mitigation of metolachlor-associated agricultural runoff using constructed wetlands in Mississippi, USA. *Agriculture, Ecosystems & Environment*, 84(2):169–176.

Moro, M. J., Domingo, F., and López, G. (2004). Seasonal transpiration pattern of Phragmites australis in a wetland of semi-arid Spain. *Hydrological Processes*, 18(2):213–227.

Page, D., Dillon, P., Mueller, J., and Bartkow, M. (2010). Quantification of herbicide removal in a constructed wetland using passive samplers and composite water quality monitoring. *Chemosphere*, 81(3):394–9.

Parsons, D. F., Hayashi, M., and van der Kamp, G. (2004). Infiltration and solute transport under a seasonal wetland: bromide tracer experiments in Saskatoon, Canada. *Hydrological Processes*, 18(11):2011–2027.

Passeport, E., Tournebize, J., Jankowfsky, S., Prömse, B., Chaumont, C., Coquet, Y., and Lange, J. (2010). Artificial Wetland and Forest Buffer Zone: Hydraulic and Tracer Characterization. *Vadose Zone Journal*, 9(1):73.

Persson, J., Somes, N., and Wong, T. (1999). Hydraulics efficiency of constructed wetlands and ponds. *Water Science and Technology*, 40(3):291–300.

Reichenberger, S., Bach, M., Skitschak, A., and Frede, H.-G. (2007). Mitigation strategies to reduce pesticide inputs into ground- and surface water and their effectiveness; a review. *Science of the Total Environment*, 384(1-3):1–35.

Sabatini, D. A. (2000). Sorption and Intraparticle Diffusion of Fluorescent Dyes with Consolidated Aquifer Media. *Ground Water*, 38(5):651–656.

Schulz, R. (2004). Field Studies on Exposure, Effects, and Risk Mitigation of Aquatic Nonpoint-Source Insecticide Pollution - A Review. *Journal of Environmental Quality*, 33(2):419–448.

Seaman, J., Bertsch, P., and Miller, W. (1995). Ionic tracer movement through highly weathered sediments. *Journal of Contaminant Hydrology*, 20(1-2):127–143.

Seybold, C., Mersie, W., and McNamee, C. (2001). Anaerobic Degradation of Atrazine and Metolachlor and Metabolite Formation in Wetland Soil and Water Microcosms. *Journal of Environmental Quality*, 30(4):1271.

Shaner, D. L., Brunk, G., Belles, D., Westra, P., and Nissen, S. (2006). Soil dissipation and biological activity of metolachlor and S-metolachlor in five soils. *Pest Management Science*, 62(7):617–23.

Si, Y., Tagaki, K., Iwasaki, A., and Zhou, D. (2009). Adsorption, desorption and dissipation of metolachlor in surface and subsurface soils. *Pest Management Science*, 65(9):956–962.

Smart, P. L. and Laidlaw, I. M. S. (1977). An evaluation of some fluorescent dyes for water tracing. *Water Resources Research*, 13(1):15.

Staddon, W. J., Locke, M. A., and Zablotowicz, R. M. (2001). Microbiological Characteristics of a Vegetative Buffer Strip Soil and Degradation and Sorption of Metolachlor. *Soil Science Society of America Journal*, 65(4):1136.

Stearman, G. K., George, D., Carlson, K., and Lansford, S. (2003). Pesticide removal from container nursery runoff in constructed wetland cells. *Journal of Environmental Quality*, 32(4):1548–1556.

Stehle, S., Elsaesser, D., Gregoire, C., Imfeld, G., Niehaus, E., Passeport, E., Payraudeau, S., Schäfer, R. B., Tournebize, J., and Schulz, R. (2011). Pesticide risk mitigation by vegetated treatment systems: a meta-analysis. *Journal of Environmental Quality*, 40(4):1068–80.

Stein, O. R., Hook, P. B., Biederman, J. A., Allen, W. C., and Borden, D. J. (2003). Does batch operation enhance oxidation in subsurface constructed wetlands? *Water Science and Technology*, 48(5):149–156.

Tilman, D., Fargione, J., Wolff, B., D'Antonio, C., Dobson, A., Howarth, R., Schindler, D., Schlesinger, W. H., Simberloff, D., and Swackhamer, D. (2001). Forecasting agriculturally driven global environmental change. *Science (New York, N.Y.)*, 292(5515):281–4.

Toride, N., Leij, F. J., and van Genuchten, M. T. (1995). The CXTFIT Code for Estimating Transport Parameters from Laboratory or Field Tracer Experiments - Version 2.0.

Trang, N. T. D., Konnerup, D., Schierup, H.-H., Chiem, N. H., Tuan, L. A., and Brix, H. (2010). Kinetics of pollutant removal from domestic wastewater in a tropical horizontal subsurface flow constructed wetland system: Effects of hydraulic loading rate. *Ecological Engineering*, 36(4):527–535.

Verhoeven, J. T. and Meuleman, A. F. (1999). Wetlands for wastewater treatment: Opportunities and limitations. *Ecological Engineering*, 12(1-2):5–12.

Vianello, M., Vischetti, C., Scarponi, L., and Zanin, G. (2005). Herbicide losses in runoff events from a field with a low slope: role of a vegetative filter strip. *Chemosphere*, 61(5):717–25.

Wauchope, R. D. (1978). The Pesticide Content of Surface Water Draining from Agricultural Fields—A Review1. *Journal of Environmental Quality*, 7(4):459.

Weber, J. B., Warren, R. L., Swain, L. R., and Yelverton, F. H. (2007). Physicochemical property effects of three herbicides and three soils on herbicide mobility in field lysimeters. *Crop Protection*, 26(3):299–311.

Whitmer, S., Baker, L., and Wass, R. (2000). Loss of Bromide in a Wetland Tracer Experiment. *Journal of Environment Quality*, 29(6):2043.

Xu, S., Leri, A. C., Myneni, S. C. B., and Jaffé, P. R. (2004). Uptake of Bromide by Two Wetland Plants (Typha latifolia L. and Phragmites australis (Cav.) Trin. ex Steud). *Environmental Science & Technology*, 38(21):5642–5648.

Zhang, D. Q., Tan, S. K., Gersberg, R. M., Zhu, J., Sadreddini, S., and Li, Y. (2012). Nutrient removal in tropical subsurface flow constructed wetlands under batch and continuous flow conditions. *Journal of Environmental Management*, 96(1):1–6.

Zhu, H. and Selim, H. (2000). Hysteretic behavior of metolachlor adsorption-desorption in soils. *Soil Science*, 165(8):632–645.

APPENDIX A

Appendix

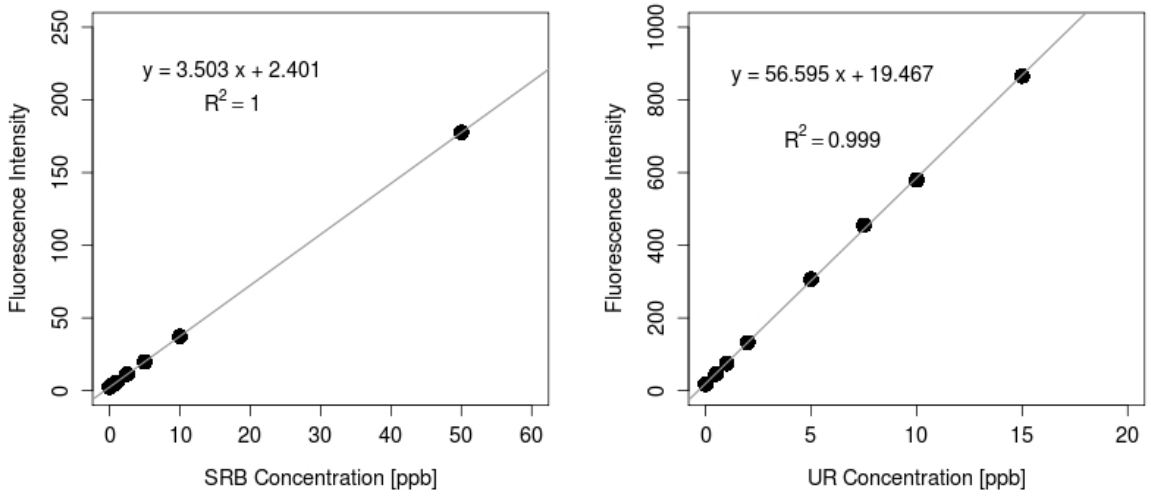

Figure A.1: Fluorometry calibration curve and linear regression equation for sulphorhodamine B (left) and Uranine (right).

Table A.1: Fluorescence tracer and metolachlor concentration data from Bed I piezometer samples.

Date	**Inlet Piezo** $[\mu g/L]$			**Center Piezo** $[\mu g/L]$			**Outlet Piezo** $[\mu g/L]$		
	UR	SRB	MC	UR	SRB	MC	UR	SRB	MC
2012-05-24	0.00	0.00	0.00	0.00	0.00	0.00	0.00	0.00	0.00
2012-05-27	19.11	29.21	-	17.37	24.95	-	17.21	23.45	-
2012-05-31	19.13	38.38	147.96	18.70	37.13	146.67	19.20	35.04	130.47
2012-06-07	28.32	56.39	134.97	26.85	51.50	123.52	26.83	51.85	127.29
2012-06-10	1.08	7.52	-	1.23	10.37	-	1.61	13.09	-
2012-06-14	0.46	3.20	2.72	0.40	3.90	2.76	0.49	4.50	3.23
2012-06-21	0.13	0.90	2.72	0.09	1.66	2.76	0.11	1.86	3.23
2012-06-28	0.07	0.97	1.55	0.02	1.08	3.68	0.08	1.17	1.60
2012-07-05	0.04	0.60	0.63	0.03	0.71	0.79	0.22	1.16	2.45
2012-07-09	14.61	23.80	-	11.03	12.36	-	5.47	1.45	-
2012-07-12	14.09	31.09	67.93	9.77	24.72	53.88	10.74	11.25	40.97
2012-07-16	13.22	24.93	-	12.86	25.18	-	12.59	24.06	-
2012-07-19	12.37	27.33	44.17	12.15	26.20	76.02	11.55	24.99	49.90
2012-07-23	0.16	2.14	-	0.23	3.12	-	0.51	4.38	-
2012-07-26	0.21	2.40	3.80	0.21	2.66	3.55	0.24	2.71	3.49
2012-08-02	0.04	1.34	3.67	0.10	1.82	2.98	0.15	2.33	-
2012-08-09	0.05	1.50	-	0.15	1.68	-	0.23	2.22	-
2012-08-16	0.13	1.28	-	0.12	1.18	-	0.12	1.14	-

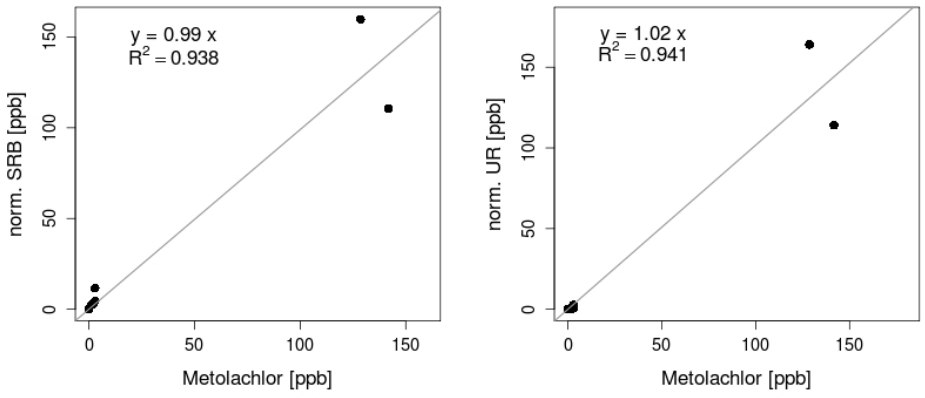

Figure A.2: Linear regression for SRB (left) and UR (right) concentrations with metolachlor concentrations from Bed I first step injection piezometer samples (24.5.12.-05.07.12). All concentrations were averaged from weekly inlet, center and outlet piezometer samples. SRB and UR concentrations were normalized to metolachlor.

Table A.2: Fluorescence tracer and metolachlor data from Bed II piezometer samples.

Date	**Inlet Piezo** $[\mu g/L]$		**Outlet Piezo** $[\mu g/L]$		**Pooled Sample** $[\mu g/L]$
	UR	SRB	UR	SRB	Metolachlor
2012-05-24	0.00	0.00	0.00	0.00	0.00
2012-05-31	11.31	21.46	16.52	15.16	86.31
2012-06-07	8.31	11.99	15.06	10.99	90.14
2012-06-14	6.33	5.38	12.66	7.14	103.28
2012-06-21	12.24	23.16	9.47	178.98	284.54
2012-06-28	10.41	13.43	9.74	140.09	188.90
2012-07-05	6.37	7.19	6.44	36.09	86.19
2012-07-12	7.93	75.52	7.41	92.77	206.25
2012-07-19	7.65	65.38	6.61	61.62	172.35
2012-07-26	-	-	-	-	-
2012-08-02	29.69	43.39	8.37	32.93	-
2012-08-09	27.59	29.84	6.43	26.44	-

Table A.3: Fluorescence tracer and metolachlor data from Bed III piezometer samples.

Date	**Inlet Piezo** $[\mu g/L]$		**Outlet Piezo** $[\mu g/L]$		**Pooled Sample** $[\mu g/L]$
	UR	SRB	UR	SRB	Metolachlor
2012-05-24	0.00	0.00	0.00	0.00	0.00
2012-05-31	12.33	8.16	14.53	49.01	97.50
2012-06-07	-	-	-	-	123.36
2012-06-14	6.46	13.14	15.87	9.65	-
2012-06-21	6.42	9.72	6.32	3.89	21.92
2012-06-28	4.29	10.17	6.61	4.88	32.04
2012-07-05	0.71	9.40	3.58	6.29	5.97
2012-07-12	0.27	8.27	0.69	3.99	3.95
2012-07-19	0.20	8.71	0.79	5.67	4.77
2012-07-26	-	-	-	-	-
2012-08-02	0.14	6.72	0.19	6.08	-
2012-08-09	0.04	6.71	0.16	5.99	-

Table A.4: Bed II and Bed III pressure probe outflow data determined by counting the pumping events during draining and multiplying them by 14L then adding the remaining volume in the tub after the last purging (A), or by using the pressure probe conversion function (B). Dip Stick method data was used for measuring the water level in the wastewater tank.

	Bed 2 Outflow (L)	**Bed 3 Outflow (L)**
1st Drain (7.6.12)	12 pumping events + 6.84	2 pumping events + 8.82
Pressure Probe Data	A: 174.84, B: 156.63	A: 36.82, B: 35.33
Dip Stick Method	265	53
2nd Drain (28.6.12)	14 pumping events + 9.65	7 pumping events + 5.68
Pressure Probe Data	A: 163.65, B: 152.71	A: 86.71, B: 72.35
Dip Stick Method	141	92
3rd Drain (19.7.12)	13 pumping events + 13.12	7 pumping events + 6.18
Pressure Probe Data	A: 195.12, B: 186.00	A: 104.18, B: 99.26
Dip Stick Method	194	106
4th Drain (9.8.12)	16 pumping events + 10.14	7 pumping events + 4.52
Pressure Probe Data	A: 234.14, B: 273.98	A: 102.52, B: 121.20
Dip Stick Method	318	71

Table A.5: Bed II manually measured piezometer waterlevel data, pH data measured in the inlet (P-In), center (P-Cen), and outlet (P-Out) piezometer and plant data. Number of plants correspond to individual stems counted within 25% of the bed's area (i.e. 1.8 m^2).

Date	**Waterlevel [cm]**			**pH**			**Plant Height [cm]**			**No. of plants**
	P-In	P-Cen	P-Out	P-In	P-Cen	P-Out	Min	max	mean	
2012-05-24	-	-	-	7.83	7.82	7.65	25	60	40	-
2012-05-31	40.0	43.4	48.0	7.57	7.60	7.57	7	77	45	-
2012-06-07	16.5	19.5	23.0	7.30	7.33	7.38	40	90	60	115
2012-06-14	22.0	26.0	31.0	7.58	7.56	7.42	5	93	52	-
2012-06-21	38.5	41.5	46.5	7.20	7.37	7.30	11	92	47	-
2012-06-28	6.5	9.5	13.5	7.19	7.17	7.26	11	99	47	-
2012-07-05	19.5	23.0	27.5	7.19	7.22	7.33	9	92	47	-
2012-07-12	41.0	43.5	48.0	7.29	7.38	7.40	17	94	44	69
2012-07-19	13.5	16.5	19.5	7.29	7.27	7.23	12	94	47	-
2012-07-26	0.0	0.0	2.0	-	-	-	13	122	64	58
2012-08-02	38.0	40.5	44.5	7.20	7.19	7.08	13	123	50	-
2012-08-09	3.5	4.0	6.5	7.14	7.15	7.20	12	122	50	-

Table A.6: Bed I manually measured piezometer waterlevel data, pH data measured in the inlet (P - In), center (P - Cen), and outlet (P - Out) piezometer and plant data. Number of plants correspond to individual stems counted within 25% of the bed's area (i.e. 1.8 m^2).

Date	**Waterlevel [cm]**			**pH**			**Plant Height [cm]**			**No. of plants**
	P-In	P-Cen	P-Out	P-In	P-Cen	P-Out	Min	Max	Mean	
2012-05-24	36.0	38.5	41.5	7.80	7.87	7.62	25	60	40	-
2012-05-27	36.0	39.0	42.0	-	-	-	-	-	-	-
2012-05-31	36.0	38.0	42.5	7.64	7.61	7.47	8	95	40	-
2012-06-07	33.0	35.0	38.0	7.52	7.47	7.44	37	96	55	-
2012-06-10	34.0	37.5	40.0	-	-	-	-	-	-	-
2012-06-14	32.0	35.5	39.0	7.56	7.72	7.42	5	105	50	96
2012-06-21	31.5	36.0	39.5	7.43	7.35	7.31	7	108.5	62	-
2012-06-28	24.5	27.0	29.0	7.55	7.46	7.41	9	111	67	-
2012-07-05	32.0	35.0	37.5	7.52	7.48	7.32	8	110	71	-
2012-07-09	10.0	12.5	16.0	-	-	-	-	-	-	-
2012-07-12	28.5	31.0	33.5	7.44	7.26	7.17	8	112	75	-
2012-07-16	34.0	37.0	39.0	-	-	-	-	-	-	-
2012-07-19	33.0	35.0	37.0	7.70	7.61	7.47	17	116	76	175
2012-07-23	33.0	35.0	39.0	-	-	-	-	-	-	-
2012-07-26	20.0	22.0	24.5	7.72	7.56	7.43	23	111	77	-
2012-08-02	33.0	36.0	38.5	7.43	7.25	7.13	23	112	77	175
2012-08-09	7.0	10.0	12.0	7.13	7.01	7.03	22	112	78	-
2012-08-16	33.0	10.0	8.0	7.18	7.24	7.36	24	109	78	-